Stereochemistry of Selenium- or Sulfur-containing

Ligands Coordinated to Cobalt(III) Ion

By

Takumi Konno

The University of Tsukuba

1985

Contents

List of Illustrations

List of Tables

Abbreviation of ligands

en	ethylenediamine	$NH_2CH_2CH_2NH_2$
tn	trimethylenediamine	$NH_2CH_2CH_2CH_2NH_2$
aet	aminoethanethiolate	$NH_2CH_2CH_2S^-$
aes	aminoethaneselenolate	$NH_2CH_2CH_2Se^-$
aese	aminoethanesulfenate	$NH_2CH_2CH_2SO^-$
aesee	aminoethaneselenenate	$NH_2CH_2CH_2SeO^-$
Haese	aminoethanesulfenic acid	$NH_2CH_2CH_2SOH$
Haesee	aminoethaneselenenic acid	$NH_2CH_2CH_2SeOH$
aesi	aminoethanesulfinate	$NH_2CH_2CH_2SO_2^-$
aesei	aminoethaneseleninate	$NH_2CH_2CH_2SeO_2^-$
Haesi	aminoethanesulfinic acid	$NH_2CH_2CH_2SO_2H$
Haesei	aminoethaneseleninic acid	$NH_2CH_2CH_2SeO_2H$
mea	2-(methylthio)ethylamine	$NH_2CH_2CH_2SCH_3$
mseea	2-(methylseleno)ethylamine	$NH_2CH_2CH_2SeCH_3$
eea	2-(ethylthio)ethylamine	$NH_2CH_2CH_2SCH_2CH_3$
eseea	2-(ethylseleno)ethylamine	$NH_2CH_2CH_2SeCH_2CH_3$
bea	2-(benzylthio)ethylamine	$NH_2CH_2CH_2SCH_2C_6H_5$
bseea	2-(benzylseleno)ethylamine	$NH_2CH_2CH_2SeCH_2C_6H_5$

Chapter I. Introduction

Cobalt(III) complexes with sulfur-containing ligands such as 2-aminoethanethiolate, L-cysteinate, D- or L-penicillaminate, and their derivatives have been extensively studied during recent years, especially because of their spectrochemical, stereochemical, and biochemical interests.[1-13] These complexes have shown some unique properties, which have not been observed for cobalt(III) complexes with hard donor atoms such as nitrogen and oxygen. For example, the presence of thiolate donor atoms in the coordination sphere induces a structural trans effect and an extreme specificity concerned with the formation of possible isomers.[1,2]

As a consequence of the great interest in the specific chemical behavior of cobalt(III) complexes with sulfur-containing ligands, it is necessary to extend study of cobalt(III) complexes with sulfur-containing ligands to those with selenium-containing ligands in order to elucidate the causes for the specificity and to increase knowledge of chemical behavior of chalcogen atoms in the complexes. The comparison of properties of cobalt(III) complexes with selenium-containing ligands and those with sulfur-containing ligands will provide valuable information not only for cobalt(III) complexes with selenium-containing ligands but also for those with sulfur-containing ligands. However, no report for cobalt(III) complexes with selenium-containing

ligands except for one[14] has been appeared so far and accordingly, their spectrochemical and stereochemical properties have not been known at all.

In these circumstances, it is worthwhile to prepare new cobalt(III) complexes with selenium-containing ligands and to investigate their properties, especially spectrochemical and stereochemical ones, together with corresponding cobalt(III) complexes with sulfur-containing ligands. In order to elucidate the fundamental chemical behavior of various selenium-containing ligands coordinated to cobalt(III) ion, the $[Co(N)_5(Se)]$ type complexes are best fitted, because this type complexes have not geometrical isomer.

In the present work, therefore, the bis(ethylenediamine) and bis(trimethylenediamine)cobalt(III) complexes with a bidentate 2-aminoethaneselenolato and its derivatives are prepared and optically resolved. These complexes are characterized from their electronic absorption, circular dichroism (CD), and ^1H and ^{13}C NMR spectra. This is the first example of well-defined optically active cobalt(III) complexes with a selenium-containing ligand to be reported. Of these complexes, bis(ethylenediamine)cobalt(III) complex with a 2-aminoethaneseleninato, $(-)_{500}^{CD}-[Co(aesei)(en)_2]^{2+}$, and that with a 2-(methylseleno)ethylamine, $(+)_{500}^{CD}-[Co(mseea)(en)_2]^{3+}$, are established by X-ray diffraction methods, in order to investigate the coordination modes of the bidentate selenium-containing ligands, the absolute configurations of the complexes

and the chiral selenium atoms, and the bond angles and bond
lengths concerning the coordinated selenium-containing ligands,
The spectrochemical and stereochemical properties of the
cobalt(III) complexes with a selenium-containing ligand are
discussed in comparison with those of the corresponding
cobalt(III) complexes with a sulfur-containing ligand, which
are newly prepared in this work, mainly on the basis of their
electronic absorption, CD, and ^{1}H and ^{13}C NMR spectral
behaviors.

Purpose of this work.

    This work was undertaken for the following purposes:
(a)   To prepare new cobalt(III) complexes with a selenium-
containing ligand, together with corresponding complexes with
a sulfur-containing ligand.
(b)   To characterize the complexes on the basis of their
electronic absorption, CD, and ^{1}H and ^{13}C NMR spectra.
(c)   To determine the molecular structures and absolute
configurations of the representative complexes by X-ray
diffraction methods.
(d)   To investigate the electronic absorption and CD spectral
behaviors of the complexes with a selenium-containing ligand
in comparison with those of the corresponding complexes with
a sulfur-containing ligand.
(e)   To explore the stereochemical behaviors of selenium-
containing ligands coordinated to cobalt(III) ion in comparison

- 3 -

with that of anologous sulfur-containing ligands.

(f)　To elucidate the CD contributions from the vicinal effect due to the chiral chalcogen atom and the configurational one due to the skew pair of chelate rings.

Chapter II.   General Background

II-A.   Stereochemistry of Cobalt(III) Complexes.

II-A-1.   Geometrical Isomerism.

Geometrical isomerism arises from the difference in the arrangement of coordinated atoms around the central metal ion. For all of the complexes in this work, which belong to the $[Co(N)_5(X)]$ type, the possible geometrical isomer is only one.

II-A-2.   Linkage Isomerism.

Linkage isomerism occurs when a ligand takes more than two coordination modes. For the complexes containing a bidentate aese, aesee, aesi, or aesei ligand, which can takes two coordination mode, two linkage isomers, S- or Se-bonded and O-bonded, are possible as illustrated representatively for the aesei complex in Fig. 1.

II-A-3.   Optical Isomerism.

Optical isomerism occurs when a complex and its mirror image are not superposable. According to the IUPAC rules,[15] Δ and Λ are used to describe the absolute configuration of a complex due to the skew pair of chelate rings. The pair of optical isomers for the present $[Co(bidentate)(diamine)_2]$ type are shown in Fig. 2.

When a thioether, selenoether, sulfenate, or selenenate ligand employed in this work coordinates to a cobalt(III) ion

Se-bonded   O-bonded
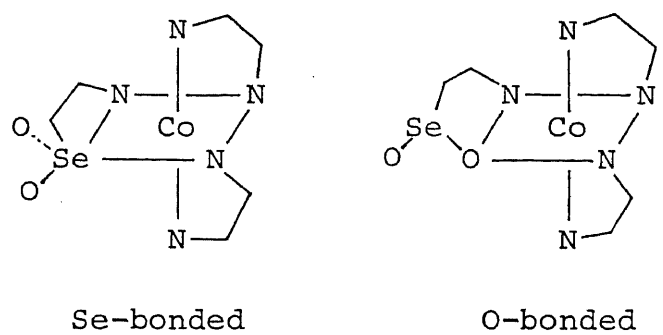
Figure 1. Two linkage isomers of $[Co(aesei)(en)_2]^{2+}$.

Δ   Λ
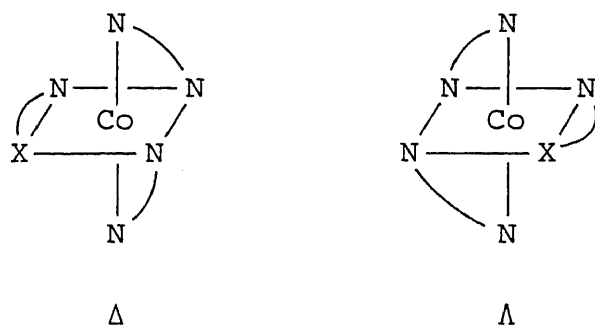
Figure 2. Two optical isomers of the [Co(bidentate)(diamine)$_2$] type complex.

through chalcogen atom and when a sulfinate or seleninate ligand coordinates to cobalt(III) ion through oxygen atom, the chalcogen atoms of these ligands become chiral. The absolute configuration of the chiral chalcogen atom can be designated as (R) or (S) based on the sequence rule[16] as shown in Fig. 3. Therefore, for the [Co(bidentate)(diamine)$_2$] type complexes containing a chiral chalcogen atom, four optical isomers, Δ-(R), Δ-(S), Λ-(R), and Λ-(S), are possible as illustrated representatively for the mseea complex in Fig. 4.

II-B. Electronic Absorption Spectra of Cobalt(III) Complexes.

Electronic absorption spectra of metal complexes are closely related to their structures. All five d-orbitals would be degenerated in a free metal ion, but in an octahedral field, the degeneracy is partially removed to give a set of triply t_{2g} and doubly e_g degenerate orbitals. For most cobalt(III) complexes, the splitting between the t_{2g} and e_g orbitals is great enough so that the six d-electrons are paired in the t_{2g} orbitals.[17] The $(t_{2g})^6$ ground state belongs to A_{1g} configuration in O_h symmetry. When one electron is promoted from the t_{2g} orbital to the e_g one, the $(t_{2g})^5(e_g)^1$ excited state give rise to two triply degenerate electron state, T_{1g} and T_{2g}.[18] Therefore, two visible absorption bands corresponding to the $^1A_{1g} \rightarrow {}^1T_{1g}$ and $^1A_{1g} \rightarrow {}^1T_{2g}$ transitions are generally observed for octahedral cobalt(III) complexes. The lower energy band ($^1A_{1g} \rightarrow {}^1T_{1g}$) is termed the first
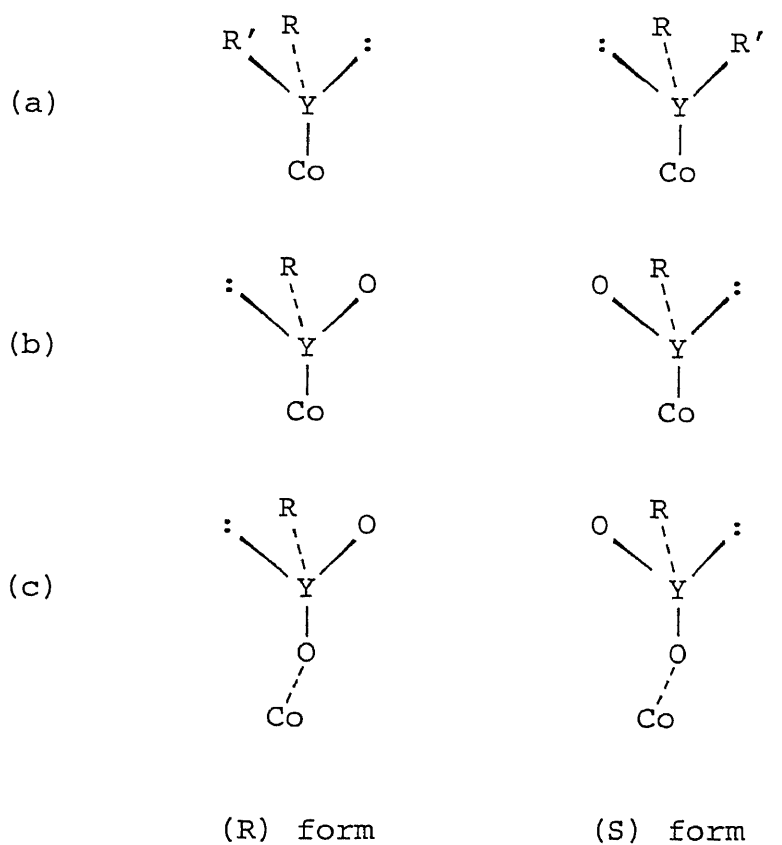
Figure 3. Absolute configuration of the asymmetric chalcogen
atoms; (a) thioether or selenoether, (b) sulfenato
or selenenato, and (C) sulfinato or seleninato.
Y = S or Se, R = $CH_2CH_2NH_2$, R'= CH_3, C_2H_5, or
$CH_2C_6H_5$, and : = lone pair.
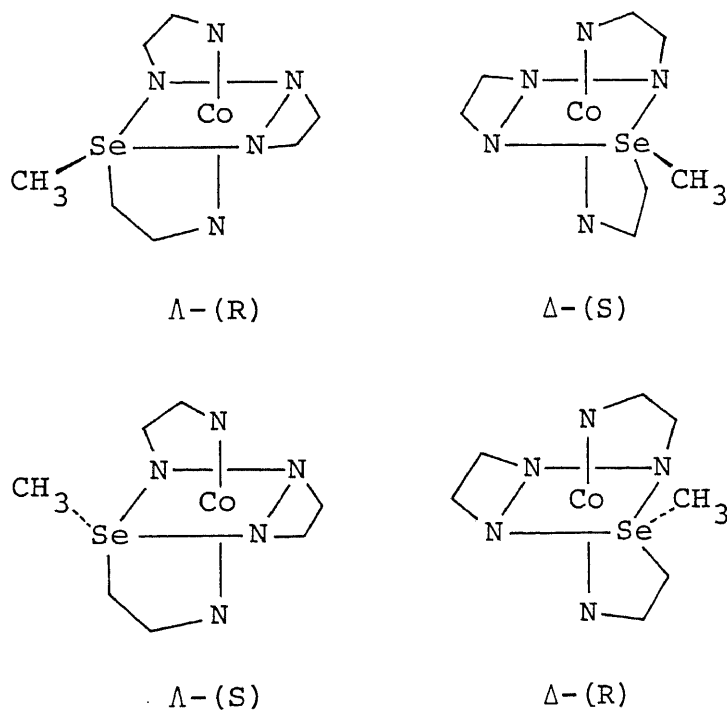
Figure 4. Four optical isomers of $[Co(mseea)(en)_2]^{3+}$.

absorption band and the higher energy one ($^1A_{1g} \rightarrow {}^1T_{2g}$) the second absorption band. When a cobalt(III) complex has a symmetry lower than O_h, the degeneracies of the T_{1g} and T_{2g} levels will be broken and they will be splitted into two or three levels.[19] The positions and shapes of the first and second absorption bands depend on the splitting between the various energy levels. Yamatera has suggested that the position and shape of the first absorption band can be interpreted and predicted from the semiempirical calculation on the basis of the molecular orbital theory.[20]

In the present [Co(N)$_5$(X)] type complexes , which have an approximate C_{4v} symmetry, the T_{1g} level is splitted into two components, A_2 and E_1. According to the Yamatera's treatment, the splitting components of the [Co(N)$_5$(X)] type complex (Fig. 5) is predicted by the calculation as follows:

electron transition	energy of component (cm^{-1})
$d_{xy} \rightarrow d_{x^2-y^2}$	$1/4(\delta N + \delta N + \delta N + \delta N)$
$d_{yz} \rightarrow d_{y^2-z^2}$	$1/4(\delta N + \delta N + \delta N + \delta X)$
$d_{zx} \rightarrow d_{z^2-x^2}$	$1/4(\delta N + \delta N + \delta N + \delta X)$,

where δN and δX are the maxima (cm^{-1}) of the first absorption bands of the [Co(N)$_6$] and [Co(X)$_6$] types complexes, respectively. Therefore, the $^1A_1 \rightarrow {}^1A_2$ transition occurs at δN, that is, at nearly the same energy as the maximum of the first absorption band of the [Co(N)$_6$] type complex, in this case, [Co(en)$_3$]$^{3+}$ (21.4×10^3 cm^{-1}). On the other hand, the $^1A_1 \rightarrow {}^1E_1$ transition, which should correspond to the maximum of the first absorption

band of the $[Co(N)_5(X)]$ type complex, occurs at $1/4(3\delta N + \delta X)$ and the energy of this transition will vary according to the ligand field strength of X. The order of the ligand field strength of the present sulfur- or selenium-containing ligands, therefore, can be known from the maximal position of the first absorption bands of the complexes.

Figure 5. $[Co(N)_5(X)]$ type complex
with coordination system.
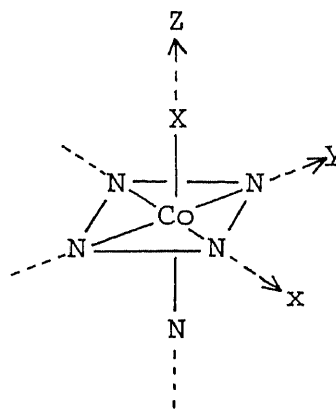
Tsuchida[21] and Fajans[22] were the first to propose that the ligands could be arranged in the order of increasing energy of the first absorption bands: $I^- < Br^- < Cl^- < (RO)_2PS_2^- < F^- < SCN^-, S_2O_3^{2-} < CO_3^{2-}, OH^-, RCO_2^- < SO_4^{2-}, NO_3^- < C_2O_4^{2-} < NCS^-, H_2O, ONO^- < glycinato < pyridine, NH_3 < ethylenediamine < bipyridine < SO_3^{2-}, NO_2^- < C_5H_5 < CN^-$. This list is known as the "spectrochemical series" and corresponds to the order of the ligand field strength. This order is roughly as follows for coordinated atoms: I < Br < Cl < F < S, O < N < C. The ligands with a sulfur donor atom is known to be widly scattered on the spectrochemical series:[23] $SCN^- < (Cl^-) < R_2PS_2^- < (RO)_2PS_2^-, F_2PS_2^- < R_2NCS_2^- < RSCS_2^- < ROCS_2^- < (H_2O) <$

- 11 -

$(NH_2)_2CS < R_2S < (NH_3)$, $SO_3{}^{2-}$. On the other hand, there has not been studied at all concerning the position on the spectrochemical series for the ligands containing a selenium donor atom up to now.

The intensities of the first and second absorption bands of cobalt(III) complexes are rather small (log $\varepsilon \simeq 2$) as compared with that found in the ultraviolet region of the spectrum (log $\varepsilon \simeq 4$), because these transitions are forbidden according to the selection rules.[24] Cobalt(III) complexes with sulfur donor atoms exhibit the intense absorption band (log $\varepsilon \simeq 4$) in the near-ultraviolet region (ca. 33×10^3 cm^{-1}), and the presence of this band is taken to be diagnostic for the existence of a cobalt-sulfur bond. This band is considered to be the sulfur-to-metal charge transfer band from bonding sulfur-centered level to antibonding cobalt-centered level (S(σ) $\rightarrow$ Co(σ^*)). Similarly, the intense bands (selenium-to-metal charge transfer bands) will expected to appear in the near-ultraviolet region in the absorption spectra of cobalt(III) complexes with selenium donor atoms. The position of the ligand-to-metal charge transfer band is related to the reducing power of the ligand. For the halogeno complexes, $[CoX(NH_3)_5]^{2+}$, the order of increasing energy of their ligand-to-metal charge transfer band is as follows: I$^-$ < Br$^-$ < Cl$^-$. For the cobalt(III) complexes with a chalcogen donor atom, there is no systematic study for the position of the chalcogen-to-metal charge transfer band.

II-C. Circular Dichroism (CD) Spectra of Cobalt(III) Complexes.

The CD spectrum is useful for the determination of the absolute configuration of an optically active metal complex. It is now common practice to assign the absolute configuration of a new optically active complex by comparing its CD spectrum with that of other representative complex whose absolute configuration has been known from other kind of methods such as X-ray analysis and stereospecific formation.

Optical   activity of the [Co(bidentate)(diamine)$_2$] type complexes in the present work arises primarily from two sources. One source is the configurational effect which comes from the inherent dissymmetry about the cobalt(III) ion due to the skew pair of chelate rings. The other source is the vicinal effect which is due to an asymmetric donor atom. It has been known that the configurational and vicinal CD effects are separable and additive for many cobalt(III) complexes.[25] The data of the additivities have shown that the configurational CD effect is larger than the vicinal effect due to an asymmetric nitrogen atom in the first absorption band region, and the absolute configuration of the configurational chirality has been assigned from the observed CD spectral behavior in this region. Namely, the complexes showing a positive major CD band in the first absorption band region have been assigned to a Λ configuration and the complexes showing a negative major CD band to a Δ configuration. However, the vicinal CD contribution due to an asymmetric chalcogen atom has little

been clarified up to now. The CD contribution from the configurational effect (Δ or Λ) and the vicinal one due to the asymmetric chalcogen donor atom ((R) or (S)) would be evaluated by applying the following relations to the observed CD curves:

$$\Delta\varepsilon[\Delta] + \Delta\varepsilon[\Lambda] = 0$$

$$\Delta\varepsilon[(R)] + \Delta\varepsilon[(S)] = 0$$

$$\Delta\varepsilon[\Lambda] = 1/2\{\Delta\varepsilon[\Lambda-(S)] + \Delta\varepsilon[\Lambda-(R)]\}$$

$$\Delta\varepsilon[(S)] = 1/2\{\Delta\varepsilon[\Lambda-(S)] - \Delta\varepsilon[\Lambda-(R)]\}$$

Chapter III. Experimental

III-A. Preparation of Reagents.

(1) Ethylenimine.

This compound was prepared by a modified method in the literature.[26] To a solution containing 60 g of NaOH in 90 cm^3 of water was added a solution containing 64.9 g of $NH_2CH_2CH_2Cl \cdot$ HCl in 90 cm^3 of water. The solution temperature was mainteined below 50°C. The mixture was then heated at 50°C for 2 h, after which time it was distilled at slightly reduced pressure (b.p. 30-35°C) until 30 cm^3 of distillate had been collected.

(2) 2-Aminoethaneselenosulfuric Acid: $NH_2CH_2CH_2SeSO_3H$.

This compound was prepared by a modified method of Klayman.[27] Thirty-one point six gram of K_2SO_3 was dissolved in 32 cm^3 of water by heating at the reflux temperature for 20 min under nitrogen atmosphere. To this was added 17.4 g of powdered selenium and ca. 20 mg of sodium lauryl sulfate. The mixture was heated near the reflux temperature with vigorously stirring for 1 h. After cooling to room temperature, the solution was filtered to remove the unreacted selenium. Eight point six gram of ethylenimine was added to the ice-cold filtrate with stirring, followed by the dropwise addition of about 400 cm^3 of 0.5 mol dm^{-3} H_2SO_4 at such a rate that the elemental selenium which separated momentarily redissolved before the succeeding drop was added. When the pH of the solution reached 6, the

addition of H_2SO_4 was stopped and the solution was evaporated

to dryness with a rotary evaporator at about 50°C. The residue

was extracted with two 150 cm^3 portions of boiling 80 % ethanol.

The extract was stood in a refrigerator overnight, and the

resultant white crystals were collected by filtration.

(3) Bis(2-aminoethyl)diselenide Hydrosulfate: $(NH_2CH_2CH_2Se-)_2 \cdot$

   H_2SO_4.

   This compound was prepared by hydrolysis of $NH_2CH_2CH_2-$

$SeSO_3H$.[27] A solution containing 20 g of $NH_2CH_2CH_2SeSO_3H$ in

120 cm^3 of water was heated under reflux for 62 h. The solution

was then evaporated to dryness with a rotary evaporator to give

yellow product. This was recrystallized from water by adding

ethanol.

III-B. Preparation and Optical Resolution of Complexes.

III-B-1. Bis(ethylenediamine)cobalt(III) Complexes.

(4) $(+)_{500}^{CD}$-(2-Aminoethaneselenolato)bis(ethylenediamine)

   cobalt(III) Perchlorate: $(+)_{500}^{CD}$-[Co(aes)(en)$_2$](ClO$_4$)$_2$.

   This complex was prepared by a modified method of Deutsch

et. al.[14] To a deoxygenated solution containing 5.9 g of

Co(NO$_3$)$_2 \cdot$6H$_2$O in 20 cm^3 of water were successively added with

stirring deoxygenated solutions containing 3.5 g of $(NH_2CH_2-$

$CH_2Se-)_2 \cdot H_2SO_4$ in 15 cm^3 of water and 3.75 cm^3 of $NH_2CH_2CH_2NH_2$

in 45 cm^3 of water. The mixture was continuously stirred

under nitrogen atmosphere for 30 min at room temperature.

The dark brown solution was filtered and to the filtrate was added 80 cm^3 of saturated NaNO$_3$. The solution was kept in a refrigerator overnight. The resultant dark brown crystals were collected by filtration and recrystallized from warm water (ca. 50°C).

To a solution containing 2.4 g of [Co(aes)(en)$_2$](NO$_3$)$_2$ in 80 cm^3 of water at 50°C was added a solution containing 2.0 g of K$_2$[Sb$_2$(d-tart)$_2$]·H$_2$O in 20 cm^3 of water. The solution was stirred for 5 min, though fine brown crystals began to appear soon. The crystals were collected by filtration and it was found from the CD measurement that the crystals were the (+)$_{500}^{CD}$ diastereomer with a small amount of the (−)$_{500}^{CD}$ one. After the (−)$_{500}^{CD}$ diastereomer contaminated was removed by grinding in a mortar several times with 10 cm^3 of aqueous solution of NaClO$_4$ (1.5 mol dm^{-3}), the remaining (+)$_{500}^{CD}$ diastereomer was dissolved in an aqueous solution of NaClO$_4$. The solution was concentrated with a rotary evaporator until fine needle crystals appeared. After cooling in a refrigerator, the crystals of the (+)$_{500}^{CD}$-[Co(aes)(en)$_2$](ClO$_4$)$_2$ were collected by filtration, and washed with ethanol and ether.

(5) (+)$_{500}^{CD}$·(−)$_{360}^{CD}$-(2-Aminoethaneselenenato)bis(ethylenediamine) cobalt(III) Perchlorate: (+)$_{500}^{CD}$·(−)$_{360}^{CD}$-[Co(aesee)(en)$_2$] (ClO$_4$)$_2$.

To a solution containing 0.05 g of (+)$_{500}^{CD}$-[Co(aes)(en)$_2$] (ClO$_4$)$_2$ in 1 cm^3 of water was added a calculated amount of 1 % H$_2$O$_2$ (0.31 cm^3) and the solution was stirred for 15 min. The

orange-yellow precipitate was obtained from the reaction

solution by the addition of 2-propanol. This complex was

recrystallized from a small amount of water by adding ethanol.

The selenenato complex obtained showed the identical absorption

and CD spectra with those of the reaction solution, indicating

that the $(+)_{500}^{CD} \cdot (-)_{360}^{CD}$ isomer was selectively formed.

(6)   (2-Aminoethaneseleninato)bis(ethylenediamine)cobalt(III)

   Nitrate: $[Co(aesei)(en)_2](NO_3)_2$.

   To a solution containing 0.4 g of $[Co(aes)(en)_2](NO_3)_2$

in 7 cm^3 of water was added an excess amount of 5% aqueous

H_2O_2 (5 cm^3), followed by the addition of 2 cm^3 of 15% HNO_3.

The solution was stirred for 20 min and stood in a refrigerator

for a day. The solution was then adjusted to pH 7 by the

addition of an aqueous solution of NaOH (2 mol dm^{-3}) and

concentrated with a rotary evaporator. The resultant crystals

were collected by filtration. The spontanious resolution of

the nitrate salt was observed for the needle crystals as

follows; the racemic nitrate was dissolved in a small amount

of water at room temperature and when the solution was kept

in a refrigerator overnight, the spontaniously resolved red

complex was obtained as fairly large needle crystals. A piece

of these crystals was used for the X-ray diffraction study.

(7) $(+)_{500}^{CD}$-(2-Aminoethaneseleninato)bis(ethylenediamine)

   cobalt(III) Perchlorate: $(+)_{500}^{CD}$-$[Co(aesei)(en)_2](ClO_4)_2$.

   This complex was prepared by the same procedure as that

used for $[Co(aesei)(en)_2](NO_3)_2$ described in (6), using

$(+)_{500}^{CD}$-[Co(aes)(en)$_2$](ClO$_4$)$_2$ instead of [Co(aes)(en)$_2$](NO$_3$)$_2$.

(8) $(+)_{500}^{CD}$-(2-(Methylseleno)ethylamine)bis(ethylenediamine) cobalt(III) Perchlorate: $(+)_{500}^{CD}$-[Co(mseea)(en)$_2$](ClO$_4$)$_3$.

To a solution containing 0.05 g of $(+)_{500}^{CD}$-[Co(aes)(en)$_2$] (ClO$_4$)$_2$ in 1 cm^3 of water was added 1 cm^3 of dimethyl sulfate. The mixture was allowed to stand in a refrigerator overnight and separated into two layers. The orange-red upper layer was poured onto a column of QAE-Sephadex A-25 (ClO$_4^-$ form, 2 cm x 20 cm), and the adsorbed band was eluted with water. The eluate was concentrated with a rotary evaporator until red crystals appeared. The resultant red complex was recrystallized from a small amount of water and obtained as fairly large plate crystals. A piece of the crystals was used for the X-ray diffraction study.

(9) $(+)_{500}^{CD}$-(2-(Ethylseleno)ethylamine)bis(ethylenediamine) cobalt(III) Perchlorate: $(+)_{500}^{CD}$-[Co(eseea)(en)$_2$](ClO$_4$)$_3$.

To a solution containing 0.05 g of $(+)_{500}^{CD}$-[Co(aes)(en)$_2$] (ClO$_4$)$_2$ in 2 cm^3 of N,N-dimethylformamide was added 0.25 g of ethyl iodide. The mixture was allowed to stand in a refrigerator for two days, whereupon the color of the solution turned from dark brown to dark red. N,N-dimethylformamide and unreacted ethyl iodide were extracted into ether and to the remaining dark red oil was added a small amount of water. This solution was poured onto a column of QAE-Sephadex A-25 (ClO$_4^-$ form, 2 cm x 20 cm) and the adsorbed band was eluted

with water. The eluate was concentrated almost to dryness

with a rotary evaporator and to this was added a small amount

of ethanol. After cooling in a refrigerator, the resultant

crystals were collected by filtration and washed with ethanol-

ether (1 : 1) and ether.

(10) $(+)^{CD}_{500}$-(2-(Benzylseleno)ethylamine)bis(ethylenediamine)

cobalt(III) Perchlorate: $(+)^{CD}_{500}$-[Co(bseea)(en)$_2$](ClO$_4$)$_3$.
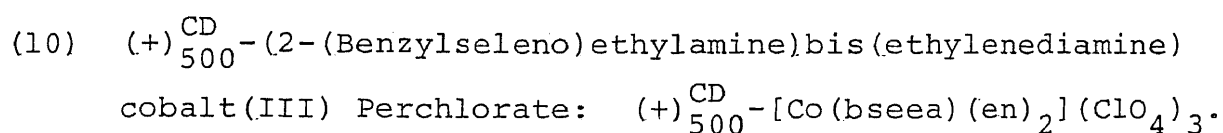
This complex was prepared by a procedure similar to that

used for $(+)^{CD}_{500}$-[Co(eseea)(en)$_2$](ClO$_4$)$_3$ described in (9), using

benzyl chloride instead of ethyl iodide.

(11) $(+)^{CD}_{500}$-(2-Aminoethanethiolato)bis(ethylenediamine)

cobalt(III) Perchlorate: $(+)^{CD}_{500}$-[Co(aet)(en)$_2$](ClO$_4$)$_2$.
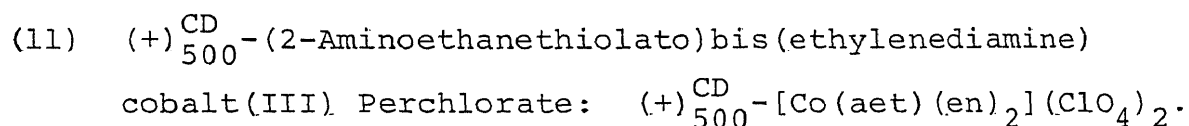
This complex was prepared by a procedure similar to that

used for $(+)^{CD}_{500}$-[Co(aes)(en)$_2$](ClO$_4$)$_2$ described in (4), using

(NH$_2$CH$_2$CH$_2$S-)$_2$·2HCl instead of (NH$_2$CH$_2$CH$_2$Se-)$_2$·H$_2$SO$_4$. $(+)^{CD}_{500}$-

[Co(aet)(en)$_2$](ClO$_4$)$_2$ showed the same CD pattern as that of

Λ-[Co(aet)(en)$_2$]$^{2+}$ reported by Yamanari et al,[4] but the CD

intensity of the former ($\Delta\varepsilon_{522}$ = +1.37) are much higher than

that of the latter ($\Delta\varepsilon_{522}$ = +0.54).

(12) $(+)^{CD}_{500}·(+)^{CD}_{360}$- and $(+)^{CD}_{500}·(-)^{CD}_{360}$-(2-Aminoethanesulfenato)

bis(ethylenediamine)cobalt(III) Perchlorate:

$(+)^{CD}_{500}·(+)^{CD}_{360}$- and $(+)^{CD}_{500}·(-)^{CD}_{360}$-[Co(aese)(en)$_2$](ClO$_4$)$_2$.
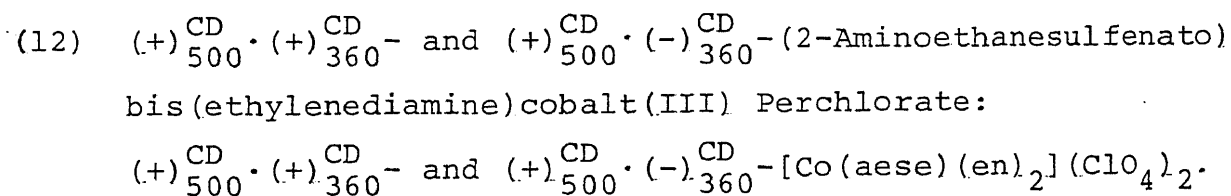
To a solution containing 0.2 g of $(+)^{CD}_{500}$-[Co(aet)(en)$_2$]

(ClO$_4$)$_2$ in 4 cm^3 of water was added a calculated amount of

1% aqueous H$_2$O$_2$ (1.24 cm^3) and the mixture was stirred for

15 min. The orange precipitate was obtained from the reaction solution by adding a large amount of 2-propanol. This complex was dissolved in a small amount of water and then 2-propanol was added until fine orange crystals began to appear. After cooling in a refrigerator overnight, the crystals of $(+)_{500}^{CD} \cdot$ $(+)_{360}^{CD}$-[Co(aese)(en)$_2$](ClO$_4$)$_2$ was collected by filtration. $(+)_{500}^{CD} \cdot (-)_{360}^{CD}$-[Co(aese)(en)$_2$](ClO$_4$)$_2$ was obtained from the filtrate by the addition of 2-propanol. These two isomers were recrystallized twice from water by adding 2-propanol. $(+)_{500}^{CD} \cdot (+)_{360}^{CD}$ and $(+)_{500}^{CD} \cdot (-)_{360}^{CD}$ aese isomers showed the same CD spectra as Λ-(S)- and Λ-(R)-[Co(aese)(en)$_2$]$^{2+}$, respectively, reported by Kita et al.[10] The formation ratio of the two isomers, Λ-(S) : Λ-(R), was about 1 : 3, which was evaluated from the CD spectra of the reaction solution.

(13)   (2-Aminoethanesulfinato)bis(ethylenediamine)cobalt(III)
        Nitrate: [Co(aesi)(en)$_2$](NO$_3$)$_2$.

    This complex was prepared by a procedure similar to that used for [Co(aesei)(en)$_2$](NO$_3$)$_2$ described in (6), using [Co(aet)(en)$_2$](NO$_3$)$_2$ instead of [Co(aes)(en)$_2$](NO$_3$)$_2$.

(14) $(+)_{500}^{CD}$-(2-Aminoethanesulfinato)bis(ethylenediamine)
        cobalt(III) Perchlorate: $(+)_{500}^{CD}$-[Co(aesi)(en)$_2$](ClO$_4$)$_2$.

    This complex was prepared by the same procedure as that used for [Co(aesi)(en)$_2$](NO$_3$)$_2$ described in (13), using $(+)_{500}^{CD}$-[Co(aet)(en)$_2$](ClO$_4$)$_2$ instead of [Co(aet)(en)$_2$](NO$_3$)$_2$. The concentration of this isomer was evaluated from the extinction coefficient of the racemic nitrate salt.

(15) $(+)_{500}^{CD}$-(2-(Methylthio, Ethylthio, or Benzylthio)-

ethylamine)bis(ethylenediamine)cobalt(III) Nitrate:

$(+)_{500}^{CD}$-[Co(mea, eea, or bea)(en)$_2$](NO$_3$)$_3$.

These thioether complexes were prepared by procedures

similar to those used for selenoether complexes described in

(8)-(10), using $(+)_{500}^{CD}$-[Co(aet)(en)$_2$](ClO$_4$)$_2$ instead of $(+)_{500}^{CD}$-

[Co(aes)(en)$_2$](ClO$_4$)$_2$. The nitrate salts were obtained by use

of an anion exchange resin (QAE-Sephadex A-25, NO$_3^-$ form).

$(+)_{500}^{CD}$-[Co(mea or eea)(en)$_2$](NO$_3$)$_3$ showed the same CD spectra

as Λ-(R)-[Co(mea or eea)(en)$_2$]$^{3+}$, reported by Yamanari et al.[4]

III-B-2. Bis(trimethylenediamine)cobalt(III) Complexes.

(16) $(+)_{600}^{CD}$-(2-Aminoethanethiolato)bis(trimethylenediamine)

cobalt(III) Perchlorate: $(+)_{600}^{CD}$-[Co(aet)(tn)$_2$](ClO$_4$)$_2$.

To a deoxygenated solution containing 4.0 g of CoCl$_2$·6H$_2$O

in 15 cm^3 of water were successively added with stirring

deoxygenated solutions containing 1.9 g of (NH$_2$CH$_2$CH$_2$S-)$_2$·2HCl

in 15 cm^3 of water and 4.0 g of NH$_2$(CH$_2$)$_3$NH$_2$ in 40 cm^3 of water.

The mixture was continuously stirred under nitrogen atmosphere

for 40 min in an ice bath. The dark brown solution was

filtered and to the filtrate was added a solution containing

15 g of NaI in 50 cm^3 of ice-cold water. The solution was kept

in a refrigerator overnight. The resultant dark brown crystals

were collected by filtration and washed with ice-cold ethanol

and ether.

One point five gram of [Co(aet)(tn)$_2$]I$_2$ was dissolved in

70 cm^3 of ice-cold water. To this were added with stirring a solution containing 1.0 g of $K_2[Sb_2(d-tart)_2]\cdot H_2O$ in 20 cm^3 of water and 20 cm^3 of ethanol. The solution was stirred for 20 min in an ice bath, though fine reddish brown crystals began to appear after a few minutes. The crystals were collected by filtration and washed with ethanol and ether.

Zero point seven gram of $(+)^{CD}_{600}$-[Co(aet)(tn)$_2$][Sb$_2$(d-tart)$_2$]·1.5H$_2$O was dissolved in 20 cm^3 of aqueous solution containing 4.0 g of $NaClO_4$ with stirring in an ice bath. When the solution was continuously stirred for 10 min, fine dark brown crystals appeared. The resultant crystals were collected by filtration and washed with ice-cold ethanol and ether. The concentration of this isomer was evaluated from the extinction coefficient of the racemic iodide salt.

(17) $(+)^{CD}_{550}\cdot(+)^{CD}_{370}$-(2-Aminoethanesulfenato)bis(trimethylene-
diamine)cobalt(III) Perchlorate and $(+)^{CD}_{550}\cdot(-)^{CD}_{370}$-(2-
Aminoethanesulfenato)bis(trimethylenediamine)cobalt(III)
Iodide: $(+)^{CD}_{550}\cdot(+)^{CD}_{370}$-[Co(aese)(tn)$_2$](ClO$_4$)$_2$ and $(+)^{CD}_{550}\cdot$
$(-)^{CD}_{370}$-[Co(aese)(tn)$_2$]I$_2$.

The preparation procedure was operated without light. To a solution containing 0.2 g of $(+)^{CD}_{600}$-[Co(aet)(tn)$_2$](ClO$_4$)$_2$ in 2 cm^3 of ice-cold water was added a calculated amount of 2% H_2O_2 (0.6 cm^3). The mixture was stirred for 20 min in an ice bath and the resultant precipitate of the $(+)^{CD}_{550}\cdot(+)^{CD}_{370}$ aese isomer was collected by filtration. When the filtrate was kept in a refrigerator for 2 h, the $(+)^{CD}_{550}\cdot(+)^{CD}_{370}$ aese

- 23 -

isomer was obtained as fairly large needle crystals. A piece of these crystals was used for the X-ray diffraction study.

After the crystals of the $(+)_{550}^{CD} \cdot (+)_{370}^{CD}$ isomer were filtered off, to the filtrate was soon added 0.5 g of NaI and the solution was stirred for 10 min in an ice bath. The resultant precipitate, which was found from the CD measurement to be the $(+)_{550}^{CD} \cdot (-)_{370}^{CD}$ aese isomer containing a small amount of the $(+)_{550}^{CD} \cdot (+)_{370}^{CD}$ one, was filtered off. To the filtrate were added 1.0 g of NaI and a large amount of 2-propanol-ether (2 : 1), and then the solution was allowed to stand in a refrigerator overnight. The resultant orange-red precipitate of the $(+)_{550}^{CD} \cdot (-)_{370}^{CD}$ aese isomer was collected by filtration. The formation ratio of the two isomers, $(+)_{550}^{CD} \cdot (+)_{370}^{CD}$: $(+)_{550}^{CD} \cdot (-)_{370}^{CD}$, was about 6 : 5, which was evaluated from the CD spectra of the reaction solution.

(18) $(+)_{500}^{CD}$-(2-Aminoethanesulfinato)bis(trimethylenediamine)
       cobalt(III) Perchlorate: $(+)_{500}^{CD}$-[Co(aesi)(tn)$_2$](ClO$_4$)$_2$.

To a solution containing 0.1 g of $(+)_{600}^{CD}$-[Co(aet)(tn)$_2$] (ClO$_4$)$_2$ in 2 cm^3 of ice-cold water was added an excess amount of 10% H$_2$O$_2$ (0.6 cm^3), followed by the addition of 0.3 cm^3 of 60% HClO$_4$. The solution was stirred for 20 min in an ice bath and allowed to stand in a refrigerator for two days. The solution was poured onto a column of QAE-Sephadex A-25 (ClO$_4^-$ form, 2 cm x 20 cm) and the adsorbed band was eluted with water. The eluate was concentrated to a small volume with a rotary evaporator and to this was added an appropriate amount

of ethanol. The solution was kept in a refrigerator for several days and the resultant crystals were collected by filtration.

(19) $(+)^{CD}_{550}$-(2-(Methylthio)ethylamine)bis(trimethylenediamine) cobalt(III) Nitrate: $(+)^{CD}_{550}$-[Co(mea)(tn)$_2$](NO$_3$)$_3$.

To a solution containing 0.1 g of $(+)^{CD}_{600}$-[Co(aet)(tn)$_2$] (ClO$_4$)$_2$ in 2 cm^3 of ice-cold water was added 2 cm^3 of ice-cold dimethyl sulfate. When the mixture was allowed to stand in a refrigerator overnight, it was separated into two layers. The red upper layer was poured onto a column of QAE-Sephadex A-25 (NO$_3^-$ form, 2 x 20 cm) and the adsorbed band was eluted with water. The eluate was concentrated to a small volume with a rotary evaporator and to this was added a small amount of ethanol. After cooling in a refrigerator overnight, the resultant crystals were collected by filtration and washed with ethanol and ether.

(20) $(+)^{CD}_{600}$-(2-Aminoethaneselenolato)bis(trimethylenediamine) cobalt(III) Perchlorate: $(+)^{CD}_{600}$-[Co(aes)(tn)$_2$](ClO$_4$)$_2$.

This complex was prepared by a procedure similar to that used for $(+)^{CD}_{600}$-[Co(aet)(tn)$_2$](ClO$_4$)$_2$ described in (16), using (NH$_2$CH$_2$CH$_2$Se-)$_2$·H$_2$SO$_4$ instead of (NH$_2$CH$_2$CH$_2$S-)$_2$·2HCl. The concentration of this isomer was evaluated from the extinction coefficient of the racemic iodide salt.

(21)   (2-Aminoethaneselenenato)bis(trimethylenediamine) cobalt(III) Ion: [Co(aesee)(tn)$_2$]$^{2+}$.

This complex was prepared by the same procedure as that used for $(+)_{550}^{CD} \cdot (+)_{370}^{CD} -$ and $(+)_{550}^{CD} \cdot (-)_{370}^{CD} - [\text{Co(aese)(tn)}_2]^{2+}$ described in (17), using $(+)_{600}^{CD} - [\text{Co(aes)(tn)}_2](\text{ClO}_4)_2$ instead of $(+)_{600}^{CD} - [\text{Co(aet)(tn)}_2](\text{ClO}_4)_2$, but could not be isolated because of its hygroscopic and unstable properties.

(22) $(+)_{550}^{CD} - (2-\text{Aminoethaneseleninato})\text{bis(trimethylenediamine)}$ cobalt(III) Perchlorate: $(+)_{550}^{CD} - [\text{Co(aesei)(tn)}_2](\text{ClO}_4)_2$.
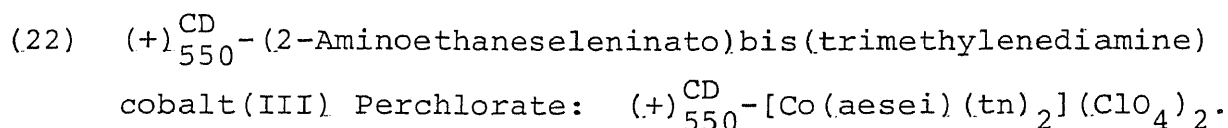
This complex was prepared by a procedure similar to that used for $(+)_{500}^{CD} - [\text{Co(aesi)(tn)}_2](\text{ClO}_4)_2$ described in (18), using $(+)_{600}^{CD} - [\text{Co(aes)(tn)}_2](\text{ClO}_4)_2$ instead of $(+)_{600}^{CD} - [\text{Co(aet)(tn)}_2]$ $(\text{ClO}_4)_2$.

(23) $(+)_{550}^{CD} - (2-(\text{Methylseleno})\text{ethylamine})\text{bis(trimethylenediamine)}$ cobalt(III) Nitrate: $(+)_{550}^{CD} - [\text{Co(mseea)(tn)}_2](\text{NO}_3)_3$.
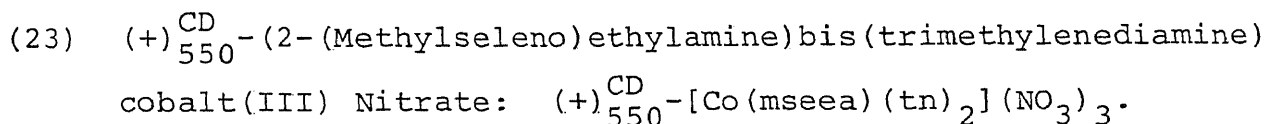
This complex was prepared by a procedure similar to that used for $(+)_{550}^{CD} - [\text{Co(mea)(tn)}_2](\text{NO}_3)_3$ described in (19), using $(+)_{600}^{CD} - [\text{Co(aes)(tn)}_2](\text{ClO}_4)_2$ instead of $(+)_{600}^{CD} - [\text{Co(aet)(tn)}_2]$ $(\text{ClO}_4)_2$.

III-B-3. Elemental Analytical Data.

The elemental analytical data of the complexes are summarized in Table 1.

III-C. General Data.

The electronic absorption spectra were measured with a JASCO UVIDEC-1 spectrophotometer. The CD spectra were recorded

Table 1. Elemental analytical data.

Complex	Found (%)			Calcd (%)		
	C	H	N	C	H	N
$[Co(aes)(en)_2](NO_3)_2$	16.94	5.18	22.99	16.90	5.20	23.00
$(+)_{500}^{CD}-[Co(aes)(en)_2][Sb_2(d-tart)_2]\cdot2H_2O$	19.36	3.36	7.93	19.24	3.46	8.01
$(+)_{500}^{CD}-[Co(aes)(en)_2](ClO_4)_2$	14.81	4.32	13.96	14.38	4.42	13.97
$(+)_{500}^{CD}-[Co(aesee)(en)_2](ClO_4)_2$	13.96	4.04	13.35	13.93	4.28	13.54
$[Co(aesei)(en)_2](NO_3)_2$	15.76	4.85	21.36	15.72	4.84	21.39
$(+)_{500}^{CD}-[Co(aesei)(en)_2](ClO_4)_2\cdot0.5H_2O$	13.21	4.27	12.94	13.29	4.28	12.92
$(+)_{500}^{CD}-[Co(mseea)(en)_2](ClO_4)_3$	13.89	3.94	11.39	13.65	4.09	11.37
$(+)_{500}^{CD}-[Co(eseea)(en)_2](ClO_4)_3$	15.15	4.19	10.98	15.26	4.32	11.12
$(+)_{500}^{CD}-[Co(bseea)(en)_2](ClO_4)_3\cdot1.5H_2O$	21.57	4.11	9.88	21.73	4.49	9.74
$[Co(aet)(en)_2](NO_3)_2$	18.82	5.89	25.89	19.00	5.84	25.85
$(+)_{500}^{CD}-[Co(aet)(en)_2](ClO_4)_2$	15.86	4.90	15.51	15.86	4.88	15.42
$(+)_{500}^{CD}\cdot(+)_{360}^{CD}-[Co(aese)(en)_2](ClO_4)_2$	15.52	4.52	14.68	15.32	4.71	14.89
$(+)_{500}^{CD}\cdot(-)_{360}^{CD}-[Co(aese)(en)_2](ClO_4)_2$	15.45	4.47	14.77	15.32	4.71	14.89
$[Co(aesi)(en)_2](NO_3)_2\cdot H_2O$	16.71	5.62	22.91	16.79	5.63	22.84

Table 1. Continued

Complex	Found (%)			Calcd (%)		
	C	H	N	C	H	N
$(+)^{CD}_{500}$ -[Co(mea)(en)$_2$](NO$_3$)$_3$	18.68	5.53	24.45	18.42	5.52	24.55
$(+)^{CD}_{500}$ -[Co(eea)(en)$_2$](NO$_3$)$_3$·0.25C$_2$H$_5$OH	21.00	5.92	22.97	21.19	5.96	23.25
$(+)^{CD}_{500}$ -[Co(bea)(en)$_2$](NO$_3$)$_3$·H$_2$O	28.23	5.66	20.23	28.37	5.68	20.36
[Co(aet)(tn)$_2$]I$_2$	17.86	4.89	13.03	17.88	4.87	13.03
$(+)^{CD}_{600}$ -[Co(aet)(tn)$_2$][Sb$_2$(d-tart)$_2$]$_2$·1.5H$_2$O	22.60	3.88	8.26	22.72	3.93	8.28
$(+)^{CD}_{550}$ ·$(+)^{CD}_{370}$ -[Co(aese)(tn)$_2$](ClO$_4$)$_2$	19.31	5.23	14.03	19.28	5.26	14.05
$(+)^{CD}_{550}$ ·$(-)^{CD}_{370}$ -[Co(aese)(tn)$_2$]I$_2$·H$_2$O	16.61	4.60	12.04	16.83	4.94	12.26
$(+)^{CD}_{500}$ -[Co(aesi)(tn)$_2$](ClO$_4$)$_2$	18.59	5.12	13,51	18.68	5.09	13.61
$(+)^{CD}_{550}$ -[Co(mea)(tn)$_2$](NO$_3$)$_3$·0.5H$_2$O	22.01	6.09	22.77	21.19	6.13	22.71
[Co(aes)(tn)$_2$]I$_2$·H$_2$O	15.69	4.91	11.86	15.96	4.69	11.63
$(+)^{CD}_{550}$ -[Co(aes)(tn)$_2$][Sb$_2$(d-trat)$_2$]$_2$·2H$_2$O	21.19	3.73	7.72	21.31	3.80	7.77
$(+)^{CD}_{550}$ -[Co(aesei)(tn)$_2$](ClO$_4$)$_2$·0.5H$_2$O	16.70	4.70	12.11	16.85	4.77	12.28
$(+)^{CD}_{550}$ -[Co(mseea)(tn)$_2$](NO$_3$)$_3$·2H$_2$O	19.10	5.74	19.61	19.05	5.86	19.75

with a JASCO J-20 spectropolarimeter. All measurements were carried out in an aqueous solution (ca. 10^{-3} mol dm^{-3}) using a 1 cm quartz cell for the absorption spectra and 1.0 or 2.0 cm quartz cell for the CD spectra at room temperature. The hydrogen ion concentration was measured with a Horiba pH meter (F7-SS), equipped with a glass and a saturated calomel electrodes.

The ^1H and ^{13}C NMR spectra of the complexes were recorded on a JEOL JNM-FX-100 of JNM-FX-90-Q NMR spectrometer operating at 100 MHz, in D_2O or $HClO_4$-D_2O solution at the probe temperature. Sodium 2,2-dimethyl-2-silapentane-5-sulfonate (DSS) was used as the initial reference.

The caluculations were carried out on a FACOM M-200 computer at the university of Tsukuba.

III-D. X-Ray Characterization.

The unit cell parameters and intensity data were measured on a Rigaku-denki automated four-circle diffractometer (AFC-5) with a graphitemonochromatized Mo $K\alpha$ radiation (λ = 0.710690 Å). The unit cell parameters were determined by least-squares refinement based on 24, 20, and 48 reflections for $(+)_{500}^{CD}$-[Co(mseea)(en)$_2$](ClO$_4$)$_3$, $(-)_{500}^{CD}$-[Co(aesei)(en)$_2$](NO$_3$)$_2$, and $(+)_{550}^{CD} \cdot (+)_{370}^{CD}$-[Co(aese)(tn)$_2$](ClO$_4$)$_2$, respectively. The systematic absences led to the space group P2$_1$2$_1$2$_1$ for $(+)_{500}^{CD}$-[Co(mseea)(en)$_2$](ClO$_4$)$_3$, P2$_1$ for $(-)_{500}^{CD}$-[Co(aesei)(en)$_2$](NO$_3$)$_2$, and P6$_5$ for $(+)_{550}^{CD} \cdot (+)_{370}^{CD}$-[Co(aese)(tn)$_2$](ClO$_4$)$_2$. The crystal

data for these complexes are listed in Tables 2-4.

The intensity data were collected by the $\omega-2\theta$ scan technique with a scan rate of $4°$ min^{-1} for $(+)_{500}^{CD}$-[Co(mseea) (en)$_2$](ClO$_4$)$_3$ and $3°$ min^{-1} for $(-)_{500}^{CD}$-[Co(aesei)(en)$_2$](NO$_3$)$_2$ and $(+)_{550}^{CD} \cdot (+)_{370}^{CD}$-[Co(aese)(tn)$_2$](ClO$_4$)$_2$, respectively. The intensity data were converted to the Fo data in the usual manner. Absorption corrections were not applied. A total of 2176, 2358, and 1090 independent reflections for $(+)_{500}^{CD}$-[Co (mseea) (en)$_2$](ClO$_4$)$_3$, $(-)_{500}^{CD}$-[Co(aesei)(en)$_2$](NO$_3$)$_2$, and $(+)_{550}^{CD} \cdot (+)_{370}^{CD}$-[Co(aese)(tn)$_2$](ClO$_4$)$_2$, respectively, with $|Fo| > 3\sigma(|Fo|)$ were considered as 'observed' and used for the structural analyses.

Table 2. Crystal data of $(-)_{500}^{CD}$-[Co(aesei)(en)$_2$](NO$_3$)$_2$.

C$_6$H$_{22}$N$_7$O$_8$SeCo	M. W. = 458.2
Monoclinic	P2$_1$
a = 9.572(4) Å	b = 10.410(3) Å c = 8.838 Å
β = 115.35(3)°	V = 795.9(6) Å^3
Dm = 1.90 g cm^{-3}	Dc = 1.91 g cm^{-3} Z = 2

Table 3. Crystal data of $(+)_{500}^{CD}$-[Co(mseea)(en)$_2$](ClO$_4$)$_3$.

C$_7$H$_{25}$N$_5$O$_{12}$Cl$_3$SeCo	M. W. = 615.6
Orthorhombic	P2$_1$2$_1$2$_1$
a = 12.220(15) Å	b = 19.224(7) Å c = 8.977(11) Å
V = 2108.9(11) Å^3	
Dm = 1.91 g cm^{-3}	Dc = 1.92 g cm^{-3} Z = 4

Table 4. Crystal data of $(+)_{550}^{CD} \cdot (+)_{370}^{CD}$-[Co(aese)(tn)$_2$](ClO$_4$)$_2$.

C$_8$H$_{26}$N$_5$O$_9$SCl$_2$Co	M. W. = 498.2
Hexagonal	P6$_5$
a = 9.367(1) Å	b = 37.878(15) Å V = 2878.5(13) Å^3
Dm = 1.73 g cm^{-3}	Dc = 1.72 g cm^{-3} Z = 6

Chapter IV.   Determination of Crystal Structures.

IV-A.   Solution and Refinement of Structures.

The positions of the cobalt and selenium atoms were obtained from the three dimensional Patterson function. The difference-Fourier maps based on the cobalt and selenium positions revealed all non-hydrogen atoms. The structures were refined by a full-matrix least-squares refinement of the positional and anisotropic thermal parameters of all the non-hydrogen atoms (program RFINE by L. W. Finger, as modified by H. Horiuchi, was used). The neutral atomic scattering factors for all the non-hydrogen atoms were taken from literature.[28] The final residual values were $R = 0.090$ and $Rw = 0.119$ for $(+)^{CD}_{500}$-[Co(mseea)(en)$_2$](ClO$_4$)$_3$, $R = 0.036$ and $Rw = 0.049$ for $(-)^{CD}_{500}$-[Co(aesei)(en)$_2$](NO$_3$)$_2$, and $R = 0.072$ and $Rw = 0.083$ for $(+)^{CD}_{550} \cdot (+)^{CD}_{370}$-[Co(aese)(tn)$_2$] (ClO$_4$)$_2$, respectively. The final parameters are listed in Tables 5-10.

IV-B.   Determination of Absolute Configurations.

The absolute configurations of $(+)^{CD}_{500}$-[Co(mseea)(en)$_2$] (ClO$_4$)$_3$ and $(-)^{CD}_{500}$-[Co(aesei)(en)$_2$](NO$_3$)$_2$ were determined by the anomalous scattering technique. The anomalous dispersion corrections, $\Delta f'$ and $\Delta f''$, for all the non-hydrogen atoms were taken from the literature.[28] When the refinements were carried out by the use of a set of the atomic parameters containing

Table 5. Positional and thermal parameters of $(-)_{500}^{CD}$-[Co-(aesei)(en)$_2$](NO$_3$)$_2$.

Atom	X	Y	Z	$B_{eq}/Å^2$ a)
Co	0.25167(6)	0.0	0.11267(7)	1.81
Se	-0.06427(5)	0.04554(8)	0.15590(6)	2.39
O1	0.0520(4)	-0.0458(4)	0.0985(4)	2.29
O2	-0.0878(5)	0.1826(4)	0.0473(5)	3.04
N1	0.1851(5)	0.1665(4)	-0.0006(5)	2.54
N2	0.1715(5)	-0.0733(4)	-0.1139(5)	2.47
N3	0.3147(5)	-0.1705(5)	0.2097(5)	2.60
N4	0.3256(5)	0.0842(5)	0.3356(5)	2.92
N5	0.4619(5)	0.0146(5)	0.1258(6)	3.03
C1	0.0851(7)	0.1023(7)	0.3766(6)	2.99
C2	0.2217(7)	0.1724(6)	0.3701(7)	3.15
C3	0.1390(8)	0.1502(6)	-0.1835(7)	3.47
C4	0.0607(7)	0.0220(6)	-0.2290(6)	3.23
C5	0.4603(7)	-0.2055(7)	0.1979(9)	3.63
C6	0.5582(7)	-0.0888(8)	0.2409(9)	3.99
N11	0.4785(7)	-0.5686(6)	0.2448(8)	3.84
N21	0.7421(6)	-0.7714(6)	0.4177(7)	3.42
O11	0.5894(6)	-0.5020(6)	0.2682(7)	4.72
O12	0.4169(8)	-0.6259(9)	0.1023(8)	7.22
O13	0.4301(13)	-0.5822(13)	0.3464(12)	11.39
O21	0.7180(6)	-0.8041(7)	0.2720(7)	5.14

Table 5. Continued

O22	0.6499(9)	-0.8119(11)	0.4731(8)	9.27
O23	0.8529(6)	-0.7038(6)	0.5012(7)	5.33

a) B_{eq} is the equivalent isotropic temperature factors defined by Hamilton.[29]

Table 6. Anisotropic thermal parameters (with e.s.d.'s) of $(-)_{500}^{CD}-[Co(aesei)(en)_2](NO_3)_2$.

Atom	$B_{11} \times 10^4$	$B_{22} \times 10^4$	$B_{33} \times 10^4$	$B_{12} \times 10^4$	$B_{13} \times 10^4$	$B_{23} \times 10^4$
Co	61(1)	40(0)	71(1)	-1(0)	27(1)	0(1)
Se	77(1)	52(0)	114(1)	6(0)	52(1)	6(0)
O1	75(4)	49(3)	105(5)	-0(3)	44(4)	3(3)
O2	110(5)	60(4)	126(6)	28(4)	50(5)	25(4)
N1	117(6)	40(3)	99(6)	7(4)	51(5)	14(4)
N2	100(6)	51(4)	93(6)	4(4)	46(5)	3(4)
N3	83(5)	56(4)	103(6)	9(4)	30(5)	11(4)
N4	82(5)	86(5)	86(6)	1(4)	22(4)	-18(4)
N5	76(5)	75(5)	149(7)	-6(4)	55(5)	-8(5)
C1	117(7)	81(5)	85(7)	20(5)	52(6)	3(5)
C2	113(7)	73(6)	101(8)	9(5)	34(6)	-21(5)
C3	177(11)	62(5)	108(9)	12(6)	73(8)	26(6)
C4	133(8)	73(8)	81(7)	4(5)	31(6)	8(5)
C5	96(7)	71(6)	168(11)	35(5)	33(7)	9(6)
C6	70(6)	101(7)	197(13)	21(5)	39(8)	6(8)
N11	116(7)	88(6)	172(10)	-8(5)	66(7)	-5(6)
N21	106(6)	71(5)	138(8)	-2(4)	36(6)	-10(5)
O11	132(6)	71(4)	260(11)	-19(5)	64(7)	-16(6)
O12	237(12)	190(11)	167(10)	-96(10)	17(9)	-13(9)
O13	465(25)	330(21)	409(22)	-147(20)	344(21)	-63(19)
O21	172(8)	133(7)	203(10)	-45(7)	103(7)	-56(7)

Table 6. Continued

O22	337(16)	322(18)	245(14)	-196(15)	213(13)	-138(13)
O23	145(7)	98(6)	209(10)	-22(6)	4(7)	-35(7)

Temperature factor $= \exp[-(B_{11} \times h^2 + B_{22} \times k^2 + B_{33} \times l^2 + B_{12}$

$\times hk + B_{13} \times hl + B_{23} \times kl)]$

Table 7. Positional and thermal parameters of $(+)_{500}^{CD}$-[Co-(mseea)(en)$_2$](ClO$_4$)$_3$.

Atom	X	Y	Z	B_{eq}/$\overset{\circ}{A}^2$ [a]
Co	0.038(2)	-0.1444(1)	0.3033(2)	3.02
Se	-0.1078(1)	-0.0720(1)	0.2191(3)	5.22
N1	0.0308(12)	-0.0951(7)	0.4976(16)	4.18
N2	-0.0741(10)	-0.2122(8)	0.3687(17)	3.77
N3	0.0402(12)	-0.1953(9)	0.1192(16)	4.90
N4	0.1552(10)	-0.0840(7)	0.2349(19)	4.60
N5	0.1569(10)	-0.2016(8)	0.3859(18)	4.11
C1	-0.0400(24)	0.0092(13)	0.1150(33)	8.69
C2	-0.1316(19)	-0.0357(13)	0.4196(26)	7.06
C3	-0.0253(20)	-0.0257(12)	0.4917(28)	6.69
C4	-0.1130(28)	-0.2463(22)	0.2291(44)	16.71
C5	-0.0166(23)	-0.2645(12)	0.1284(27)	7.43
C6	0.2663(14)	-0.1210(11)	0.2548(29)	6.42
C7	-0.2664(14)	-0.1606(13)	0.3903(29)	6.95
CL1	0.3085(4)	-0.3489(3)	0.2018(5)	4.63
CL2	0.7182(5)	-0.4203(3)	0.1679(7)	5.74
CL3	0.5909(4)	-0.1714(3)	0.3222(7)	5.86
O11	0.3504(15)	-0.3295(9)	0.3385(20)	8.29[b]
O12	0.3859(26)	-0.3664(16)	0.1078(36)	16.08[b]
O13	0.2657(22)	-0.2884(14)	0.1209(31)	13.74[b]
O14	0.2218(33)	-0.3944(19)	0.2235(45)	21.41[b]

Table 7. Continued

O21	0.8232(35)	−0.4252(23)	0.1180(49)	22.83[b]
O22	0.7268(21)	−0.4373(13)	0.3151(30)	13.04[b]
O23	0.6918(27)	−0.3592(18)	0.1146(40)	17.93[b]
O24	0.6404(30)	−0.4566(20)	0.1096(43)	20.41[b]
O31	0.6914(22)	−0.1624(13)	0.3681(30)	13.27[b]
O32	0.5252(24)	−0.1708(16)	0.4616(33)	14.55[b]
O33	0.5692(270	−0.2453(20)	0.3186(38)	18.25[b]
O34	0.5343(38)	−0.1474(24)	0.2063(51)	25.84[b]

a) B_{eq} is the equivalent isotropic temperature factors defined by Hamilton.[29]   b) Isotropic temperature factor.

Table 8. Anisotropic thermal parameters (with e.s.d.'s) of $(+)_{500}^{CD}-[Co(mseea)(en)_2](ClO_4)_3$.
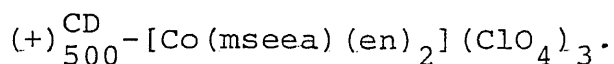
Atom	$B_{11}x10^4$	$B_{22}x10^4$	$B_{33}x10^4$	$B_{12}x10^4$	$B_{13}x10^4$	$B_{23}x10^4$
Co	37(1)	22(1)	112(3)	-2(1)	-3(2)	3(1)
Se	50(1)	42(1)	199(4)	12(1)	1(2)	30(1)
N1	68(11)	26(4)	142(21)	-1(7)	-21(15)	19(9)
N2	48(9)	28(5)	135(22)	-15(5)	7(12)	5(9)
N3	59(10)	50(7)	118(21)	-16(8)	-1(15)	3(10)
N4	35(8)	29(5)	230(30)	-2(5)	22(13)	-0(10)
N5	46(9)	28(5)	168(25)	3(6)	-8(13)	24(9)
C1	155(26)	39(8)	343(59)	31(14)	32(37)	75(19)
C2	114(21)	58(10)	181(35)	55(13)	59(24)	23(16)
C3	112(22)	39(8)	237(43)	10(11)	48(27)	-44(15)
C4	233(41)	131(22)	523(95)	-143(27)	281(54)	-177(40)
C5	165(28)	37(8)	219(40)	-43(13)	26(30)	-15(15)
C6	41(11)	45(8)	312(49)	-1(8)	-8(20)	75(17)
C7	35(11)	60(10)	310(49)	-14(9)	-32(20)	55(20)
CL1	72(3)	38(2)	124(6)	-2(2)	15(4)	-12(3)
CL2	109(5)	34(2)	179(9)	4(2)	-17(5)	-5(3)
CL3	61(3)	42(2)	240(11)	-6(2)	-35(5)	17(4)

Temperature factor = $\exp[-(B_{11} \times h^2 + B_{22} \times k^2 + B_{33} \times l^2 + B_{12} \times hk + B_{13} \times hl + B_{23} \times kl)]$

Table 9.   Positional and thermal parameters of $(+)^{CD}_{550} \cdot (+)^{CD}_{370}-$
[Co(aese)(tn)$_2$](ClO$_4$)$_2$.

Atom	X	Y	Z	$B_{eq}/Å^2$ [a)
Co	0.3506(4)	0.1855(3)	0.1500	2.47
S	0.1971(8)	0.1128(8)	0.1021(2)	3.80
N1	0.1408(24)	0.0688(28)	0.1793(6)	5.14
N2	0.3426(31)	0.3969(28)	0.1533(8)	5.36
N3	0.5566(26)	0.2983(24)	0.1225(7)	4.44
N4	0.3684(26)	-0.0185(21)	0.1454(7)	4.37
N5	0.4831(27)	0.2571(27)	0.1968(7)	5.20
C1	0.0082(41)	-0.0463(33)	0.1250(11)	6.53
C2	-0.0070(41)	0.0233(41)	0.1565(10)	7.21
C3	0.3844(47)	0.5068(37)	0.1251(11)	7.17
C4	0.5675(44)	0.5706(38)	0.1195(12)	7.86
C5	0.5813(36)	0.4247(35)	0.0963(11)	6.44
C6	0.4845(49)	-0.0397(45)	0.1679(9)	7.38
C7	0.4913(66)	-0.0018(44)	0.2036(11)	9.30
C8	0.5550(46)	0.1697(49)	0.2167(12)	8.35
CL1	0.0030(9)	0.5436(10)	0.1646(2)	5.23
CL2	0.6555(9)	0.6914(8)	0.2332(3)	5.55
O11	0.0565(65)	0.5804(81)	0.1318(17)	28.80
O12	0.0886(36)	0.6837(32)	0.1854(10)	10.03
O13	-0.1582(33)	0.4986(36)	0.1645(12)	13.46
O14	0.0220(38)	0.4181(32)	0.1781(7)	9.44
O21	0.5382(47)	0.6463(30)	0.2055(9)	12.57

Table 9. Continued

O22	0.8319(51)	0.7926(52)	0.2229(15)	19.00
O23	0.6199(56)	0.7722(44)	0.2622(10)	15.25
O24	0.6422(40)	0.5510(30)	0.2488(9)	10.40
O31	0.2283(24)	0.2521(24)	0.2422(5)	5.36

a) B_{eq} is the equivalent isotropic temperature factors defined by Hamilton.[29]

Table 10. Anisotropic thermal parameters (with e.s.d.'s) of
$(+)_{550}^{CD} \cdot (+)_{370}^{CD}$-[Co(aese)(tn)$_2$](ClO$_4$)$_2$.

Atom	$B_{11}\times 10^4$	$B_{22}\times 10^4$	$B_{33}\times 10^4$	$B_{12}\times 10^4$	$B_{13}\times 10^4$	$B_{23}\times 10^4$
Co	100(5)	93(5)	4(0)	39(4)	-1(1)	-4(1)
S	171(12)	158(11)	5(1)	87(10)	-10(2)	-7(2)
N1	124(36)	241(47)	4(2)	-8(33)	-2(6)	-9(7)
N2	281(53)	196(41)	8(2)	148(38)	10(9)	-1(8)
N3	183(40)	136(38)	6(2)	43(33)	-1(7)	0(7)
N4	232(45)	95(30)	7(2)	75(30)	-0(8)	-5(7)
N5	173(42)	179(43)	12(3)	96(35)	-3(8)	-3(8)
C1	230(61)	100(43)	17(5)	53(43)	-9(13)	-8(11)
C2	220(62)	260(68)	11(5)	42(52)	38(14)	-3(12)
C3	382(89)	184(57)	16(4)	222(63)	-31(16)	-15(13)
C4	289(82)	195(66)	18(5)	108(60)	2(16)	28(14)
C5	182(57)	163(53)	16(4)	51(47)	7(12)	5(12)
C6	419(94)	393(90)	9(3)	320(82)	-38(15)	-36(15)
C7	578(138)	217(72)	14(5)	233(85)	-43(20)	-13(14)
C8	243(75)	313(93)	18(6)	123(70)	-19(16)	-5(17)
CL1	145(12)	194(14)	10(1)	59(11)	-4(2)	-0(3)
CL2	163(13)	138(12)	12(1)	25(10)	4(3)	2(3)
O11	953(200)	1220(255)	42(10)	394(184)	62(37)	209(45)
O12	344(66)	257(59)	21(5)	82(48)	-25(14)	19(12)
O13	249(61)	415(76)	37(8)	112(58)	-16(15)	-35(18)
O14	616(97)	312(59)	12(3)	323(67)	22(14)	23(11)
O21	753(117)	258(55)	17(4)	207(65)	-75(17)	-14(11)

Table 10. Continued

O22	493(112)	636(130)	49(11)	308(102)	92(26)	80(30)
O23	1073(165)	648(113)	17(4)	691(126)	-50(21)	-54(18)
O24	620(98)	241(52)	15(4)	220(60)	-13(14)	18(10)
O31	203(39)	268(42)	5(2)	102(33)	5(6)	2(7)

Temperature factor $= \exp[-(B_{11} \times h^2 + B_{22} \times k^2 + B_{33} \times l^2 + B_{12} \times hk + B_{13} \times hl + B_{23} \, xkl)]$

the Δ configuration of the complex cation, the residual values

converged to R = 0.095 and Rw = 0.124 for $(+)^{CD}_{500}$-[Co(mseea)

(en)$_2$](ClO$_4$)$_3$ and R = 0.035 and Rw = 0.046 for $(-)^{CD}_{500}$-[Co

(aesei)(en)$_2$](NO$_3$)$_2$, respectively. On the contrary, the

refinements in the enantiometric atomic parameters (the Λ

configuration) resulted in the residual values of R = 0.090

and Rw = 0.119 for $(+)^{CD}_{500}$-[Co(mseea)(en)$_2$](ClO$_4$)$_3$ and R =

0.041 and Rw = 0.055 for $(-)^{CD}_{500}$-[Co(aesei)(en)$_2$](NO$_3$)$_2$,

respectively. These facts indicate that $(+)^{CD}_{500}$-[Co(mseea)

(en)$_2$]$^{3+}$ has the Λ configuration and $(-)^{CD}_{500}$-[Co(aesei)(en)$_2$]$^{2+}$

has the Δ one. These absolute configurations are supported

by the CD spectral behavior of these complexes (vide infra).

Chapter V. Results and Discussion

V-A. X-Ray Diffraction Studies.

V-A-1. Crystal Structure of Δ-(-)$_{500}^{CD}$-[Co(aesei)(en)$_2$](NO$_3$)$_2$.

Perspective drawing of the complex cation is given in Fig. 6 and its packing mode is illustrated in Fig. 7. The bond lengths and angles with their estimated standard deviations in the complex are summarized in Table 11.

The coordination geometry around the cobalt atom is approximately octahedral. The aesei ligand coordinates to cobalt atom with the nitrogen and oxygen atoms instead of the nitrogen and selenium ones in the starting complex, [Co(aes)-(en)$_2$]$^{2+}$,[14] in contrast to the case of the analogous aesi ligand whose coordinated atoms remain intact during the oxidation process.[3] This suggests that the treatment of the selenolato complex with excess hydrogen peroxide is accompanied by linkage isomerization and the O-bonded seleninato complex is obtained. The asymmetric selenium atom in the Δ-(-)$_{500}^{CD}$-[Co(aesei-N,O)(en)$_2$]$^{2+}$ takes the (S) configuration and the pendant oxygen atom, O2, have the axial orientation (Fig. 14). This configuration seems to be stabilized by the intramolecular hydrogen bond between the pendant oxygen atom, O2, and the adjacent amino group, N1, because the distance between O2 and N1 is 2.824 Å.

The bond lengths and angles are similar to those for the
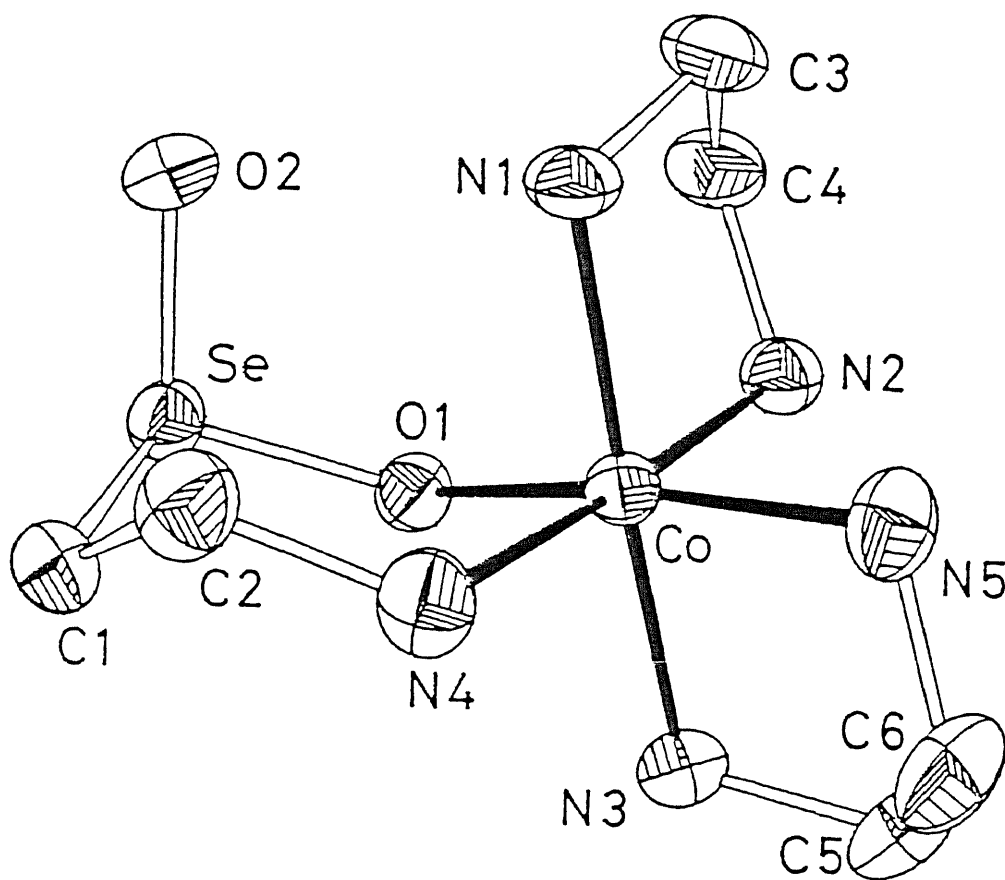
Figure 6. A perspective drawing of $\Delta\text{-}(-)_{500}^{CD}\text{-}[Co(aesei\text{-}N,O)\text{-}(en)_2]^{2+}$ with the numbering scheme of atoms.
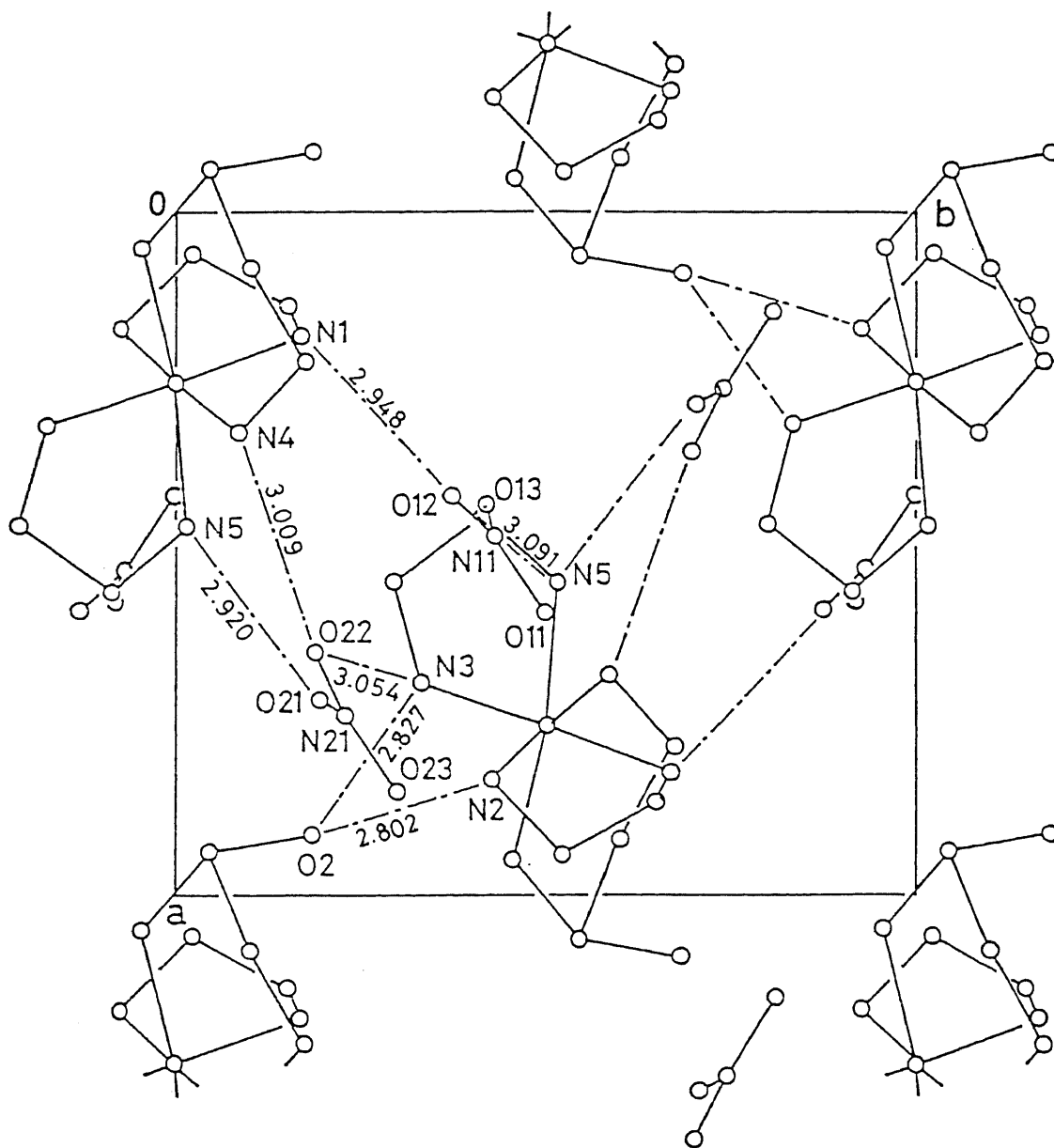
Figure. 7. A projection of the crystal packing of $\Delta\text{-}(-)_{500}^{CD}$- $[Co(aesei\text{-}N,O)(en)_2](NO_3)_2$ viewed along the c axis. The hydrogen bonds are represented by the lines $(-\cdot-\cdot-)$.

Table 11. Intermolecular distances and bond angles (with e.s.d.'s) of $(-)_{500}^{CD}$-[Co(aesei)(en)$_2$](NO$_3$)$_2$.

(a) Bond Distances (l/Å)

Co-O1	1.922(4)	Co-N1	1.966(4)
Co-N2	1.967(5)	Co-N3	1.950(5)
Co-N4	1.988(5)	Co-N5	1.972(5)
Se-O1	1.698(4)	Se-O2	1.680(4)
N1-C3	1.491(8)	N2-C4	1.490(7)
N3-C5	1.487(9)	N4-C2	1.479(9)
N5-C6	1.497(8)	C1-Se	1.952(5)
C1-C2	1.520(10)	C3-C4	1.500(9)
C5-C6	1.481(10)	N11-O11	1.209(8)
N11-O12	1.286(9)	N11-O13	1.183(16)
N21-O21	1.255(9)	N21-O22	1.251(12)
N21-O23	1.223(7)		

(b) Bond Angles ($\phi/°$)

O1-Co-N1	95.1(2)	O1-Co-N2	83.9(2)
O1-Co-N3	85.1(2)	O1-Co-N4	95.6(2)
O1-Co-N5	170.0(2)	N1-Co-N2	85.6(2)
N1-Co-N3	175.9(2)	N1-Co-N4	90.9(2)
N1-Co-N5	93.5(2)	N2-Co-N3	90.4(2)
N2-Co-N4	176.4(2)	N2-Co-N5	91.9(2)
N3-Co-N4	93.1(2)	N3-Co-N5	85.9(2)
N4-Co-N5	89.2(2)	O1-Se-O2	104.5(2)

Table 11. Continued

O1-Se-C1	100.1(2)	O2-Se-C1	100.1(2)
Co-O1-Se	127.0(2)	Co-N1-C3	109.5(4)
Co-N2-C4	106.9(3)	Co-N3-C5	108.4(4)
Co-N4-C2	119.5(3)	Co-N5-C6	107.5(4)
Se-C1-C2	112.4(4)	N4-C2-C1	112.0(5)
N1-C3-C4	105.9(5)	N2-C4-C3	106.4(4)
N3-C5-C6	106.8(6)	N5-C6-C5	106.1(4)
O11-N11-O12	115.8(8)	O11-N11-O13	122.6(8)
O12-N11-O13	121.6(8)	O21-N21-O22	117.4(6)
O21-N21-O23	120.4(7)	O22-N21-O23	122.2(7)

[Co(L)(en)$_2$] type complexes, where L denotes a selenium- or sulfur-containing ligand such as 2-aminoethaneseleninate[14] and 2-aminoethanesulfinate.[3] The selenium-oxygen bond lengths, Se-O1 and Se-O2, are 1.698 and 1.680 Å, respectively. They are longer than those of the sulfur-oxygen one (1.456 and 1.476 Å) in [Co(aesi-N,S)(en)$_2$](ClO$_4$)·(NO$_3$).[3] The bond angle of O1-Co-N4 for the six-membered chelate ring is 95.6°, which is consistent with that of the cobalt(III) complexes containing amino carboxylate.[25,30] The bond angles around the selenium atom are about 100°, and this value seems to be reasonable for the selenium atom whose tetragonal positions are occupied by the three bonding pairs and a lone pair.[31]

In the present complex cation, two gauche conformations, δ and λ, are possible for each of the two ethylenediamine chelate rings.[25] As shown in Fig. 6 and Table 12, both of the ethylenediamine chelate rings in Δ-(-)$_{500}^{CD}$-[Co(aesei-N,O)-(en)$_2$]$^{2+}$ take up the reasonable λ gauche conformation. The six-membered chelate ring (O1-Se-C1-C2-N4) of the coordinated aesei ligand takes up a chair conformation (Table 12) and dihedral angle for the two planes, O1-Co-N4 and Se-C1-C2, is 24.5°. This suggests that the six-membered chelate ring is distorted from the normal chair conformation, because the bond lengths and angles around the selenium atom are larger than those around the carbon atom (Table 11).

The crystal structure consists of the complex cations and nitrate anions, and the distance between the two nitrate

Table 12. Displacements of atoms from the least-squares
plane ($d/Å$) of $(-)_{500}^{CD}$-[Co(aesei)(en)$_2$](NO$_3$)$_2$.

2-Aminoethaneseleninato chelate ring

Plane 1; $0.1970X - 0.8736Y + 0.4451Z - 0.7914 = 0$

| Co | 0.0000 | O1 | 0.0000 | N4 | 0.0000 | Se | 0.8888 |
| C1 | 0.5029 | C2 | 0.9017 | | | | |

Ethlenediamine chelate ring

Plane 2; $0.9929X + 0.1190Y - 0.0007Z - 1.9677 = 0$

| Co | 0.0000 | N1 | 0.0000 | N2 | 0.0000 | C3 | -0.2292 |
| C4 | 0.5024 | | | | | | |

Plane 3; $0.0791X - 0.3879Y - 0.9175Z + 0.6695 = 0$

| Co | 0.0000 | N4 | 0.0000 | N5 | 0.0000 | C5 | 0.3421 |
| C6 | -0.3855 | | | | | | |

The X, Y, and Z coordinates in $Å$ are referred to the
crystallographic axes.

anions is 3.140 Å. The O2-N2 and O2-N3 distances between

adjacent complex cations are 2.802 and 2.827 Å, respectively.

In addition, the distances between the nitrogen atoms of the

complex cation and the oxygen atoms of the nitrate anions are

from 2.948 Å to 3.091 Å, as shown in Fig. 7. These distances

suggest that they are hydrogen bonds.

V-A-2. Crystal structure of $\Lambda-(+)_{500}^{CD}-[Co(mseea)(en)_2](ClO_4)_3$.

Perspective drawing of the complex cation obtained is

given in Fig. 8 and its packing mode is illustrated in Fig. 9.

The bond lengths and angles with their estimated standard

deviations in the complex are summarized in Table 13.

The coordination geometry around the cobalt atom is

approximately octahedral. The selenium atom coordinates to

the cobalt atom and the mseea ligand acts as a bidentate.

The asymmetric selenium atom in $\Lambda-(+)_{500}^{CD}-[Co(mseea)(en)_2]^{3+}$

takes the (R) configuration. This result supports the

prediction that a steric interaction occurs between the methyl

group, C1, and the ethylenediamine chelate ring, N2-C4-C5-N3,

if the asymmetric selenium atom takes the (S) configuration.

The methyl group of this isomer takes the axial orientation,

which causes the chelate ring of 2-(methylseleno)ethylamine,

Se-C2-C3-N1, to have the gauche form with λ conformation

(Fig. 8 and Table 14), though the methyl group is expected to

take the equatorial orientation in general.[25,32] This fact

seems to point out that the methyl group and the amino groups
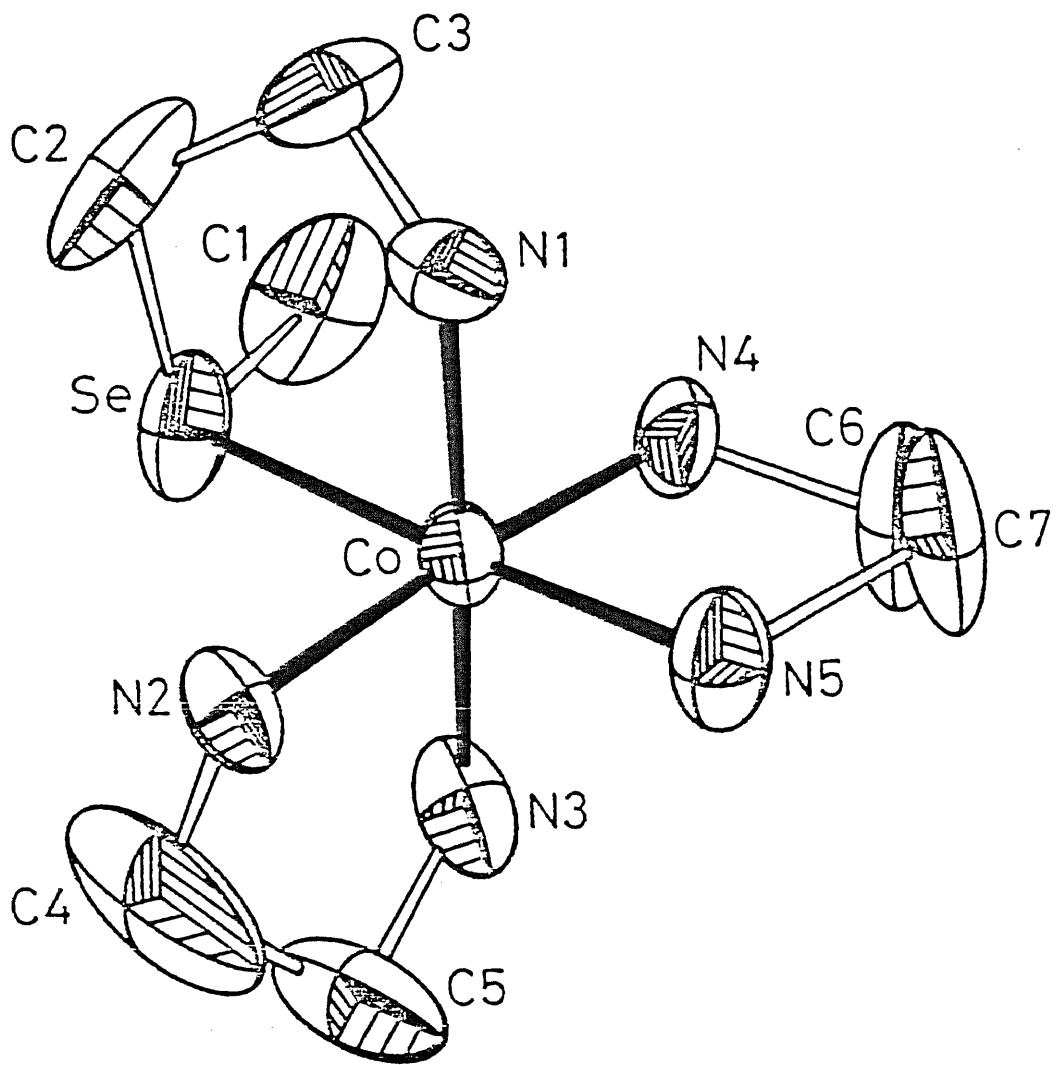
Figure 8. A perspective drawing of Λ-(+)$_{500}^{CD}$-[Co(mseea)-
(en)$_2$]$^{3+}$ with the numbering scheme of atoms.
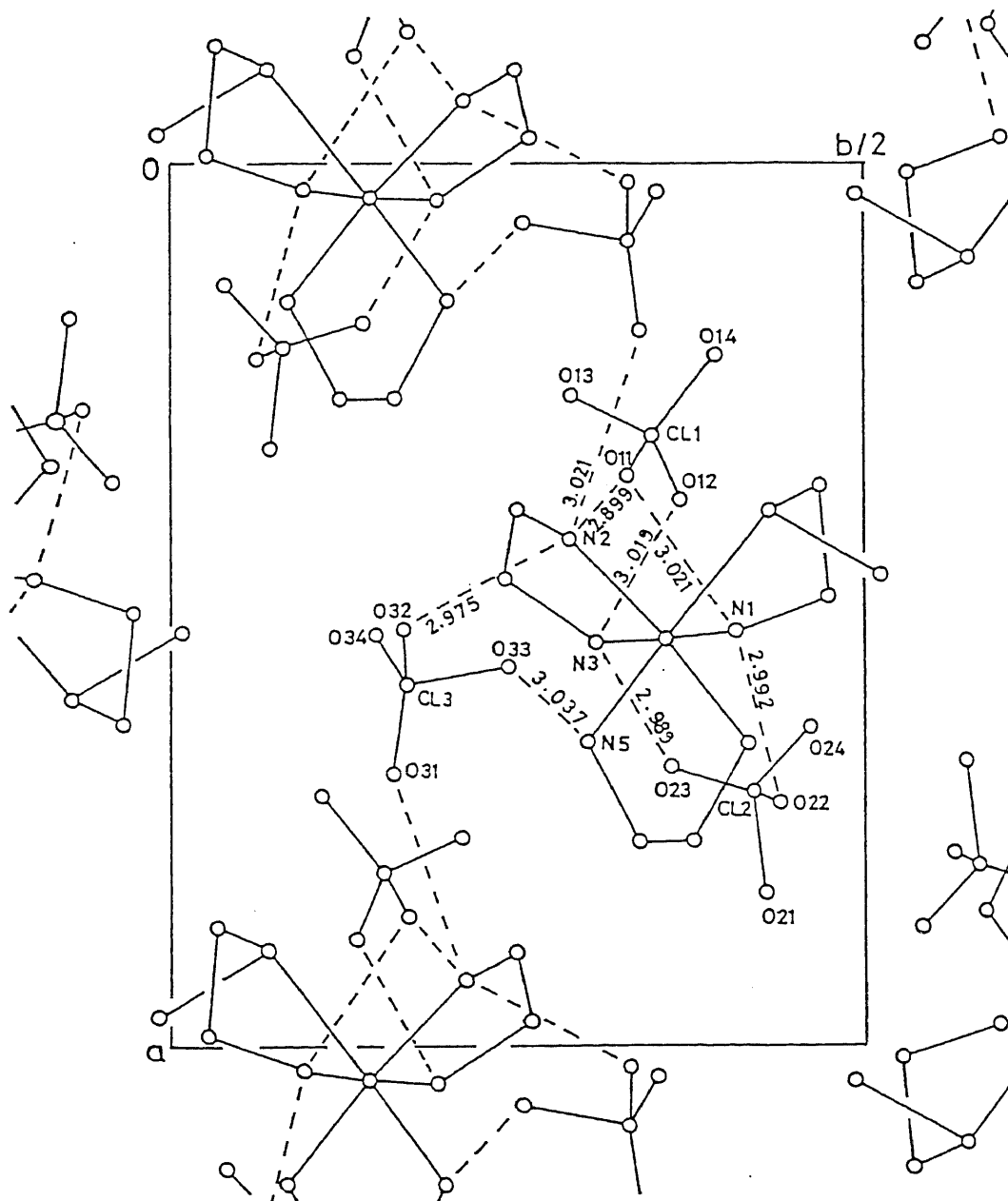
Figure 9. A projection of the crystal packing of $\Lambda-(+)_{500}^{CD}-$ [Co(mseea)(en)$_2$](ClO$_4$)$_3$ viewed along the c axis. The hydrogen bonds are represented by the lines (-----).

Table 13. Intermolecular distances and bond angles (with e.s.d.'s) of (+)$_{500}^{CD}$-[Co(mseea)(en)$_2$](ClO$_4$)$_3$.

(a) Bond Distances (1/Å)

Co-Se	2.386(3)	Co-N1	1.987(15)
Co-N2	1.983(14)	Co-N3	1.921(15)
Co-N4	1.940(14)	Co-N5	1.964(14)
Se-C1	1.999(26)	Se-C2	1.952(24)
N1-C3	1.501(27)	N2-C4	1.492(42)
N3-C5	1.503(29)	N4-C6	1.543(22)
N5-C7	1.554(23)	C2-C3	1.464(34)
C4-C5	1.525(45)	C6-C7	1.435(36)
CL1-O11	1.381(19)	CL1-O12	1.311(35)
CL1-O13	1.467(28)	CL1-O14	1.388(39)
CL2-O21	1.362(43)	CL2-O22	1.366(27)
CL2-O23	1.308(35)	CL2-O24	1.291(38)
CL3-O31	1.307(27)	CL3-O32	1.487(30)
CL3-O33	1.446(38)	CL3-O34	1.331(47)

(b) Bond Angles (φ/Å)

Se-Co-N1	88.0(4)	Se-Co-N2	87.7(4)
Se-Co-N3	91.9(5)	Se-Co-N4	95.8(4)
Se-Co-N5	176.2(5)	N1-Co-N2	91.2(6)
N1-Co-N3	177.1(6)	N1-Co-N4	91.5(7)
N1-Co-N5	88.2(6)	N2-Co-N3	85.9(7)
N2-Co-N4	175.6(6)	N2-Co-N5	91.7(6)

Table 13. Continued

N3-Co-N4	91.4(7)	N3-Co-N5	91.8(7)
N4-Co-N5	84.9(6)	Co-Se-Cl	107.1(8)
Co-Se-C2	91.6(7)	Cl-Se-C2	102.3(11)
Co-N1-C3	114.4(13)	Co-N2-C4	105.1(17)
Co-N3-C5	113.5(13)	Co-N4-C6	109.6(11)
Co-N5-C7	111.1(12)	Se-C2-C3	108.7(16)
N1-C3-C2	107.8(18)	N2-C4-C5	110.6(25)
N3-C5-C4	100.8(21)	N4-C6-C7	110.1(16)
N5-C7-C6	104.3(16)		
O11-CL1-O12	112.0(16)	O11-CL1-O13	111.0(13)
O11-CL1-O14	109.2(19)	O12-CL1-O13	98.2(18)
O12-CL1-O14	118.6(21)	O13-CL1-O14	107.2(20)
O21-CL2-O22	103.3(22)	O21-CL2-O23	100.1(24)
O21-CL2-O24	121.5(25)	O22-CL2-O23	126.1(19)
O22-CL2-O24	108.6(21)	O23-CL2-O24	98.9(23)
O31-CL3-O32	10.4(17)	O31-CL3-O33	108.0(17)
O31-CL3-O34	133.5(24)	o32-CL3-O33	85.8(18)
O32-CL3-O34	112.0(23)	O33-CL3-O34	103.1(24)

N3 and N4, repel each other, if the methyl group takes the equatorial orientation. The ethylenediamine chelate ring, N4-C6-C7-N5, takes the reasonable gauche form with δ conformation, while the other ethylenediamine chelate ring, N2-C4-C5-N3, takes the unusual gauche form with λ conformation (Fig. 8 and Table 14).

The bond lengths and angles are similar to those for the [Co(L)(en)$_2$] type complexes, where L denotes a selenium- or sulfur-containing ligand such as 2-aminoethaneselenolate[14] and 2-(methylthio)ethylamine.[5] The average Co-N bond length is 1.959 Å and no significant trans effect is observed, as well as the cobalt(III) complexes with a coordinated thioether sulfur atom.[2j,5] The bond lengths of Co-Se, Se-C1, and Se-C2 (2.386, 1.999, and 1.952 Å) are longer than the bond lengths of Co-S (2.267 Å) and S-C (1.817 and 1.834 Å) in the corresponding [Co(mea)(en)$_2$]$^{3+}$,[5] and this results in a smaller bond angle of Co-Se-C2 (91.6°) than the angle of the corresponding Co-S-C (97.9°).[5] The other two bond angles around the selenium donor atom (Co-Se-C1 = 107.1° and C1-Se-C2 = 102.3°) are reasonable for the tetrahedral geometry in contrast to those around the sulfur donor atom in [Co(mea)(en)$_2$]$^{3+}$ (Co-S-C = 114.2° and C-S-C = 99.4°).[5] This fact seems to depend on the longer bond lengths of Co-Se and Se-C1.

The crystal structure consists of the complex cations and perchlorate anions. The distances of the nitrogen atoms of the complex cation and the oxygen atoms of the perchlorate

Table 14. Displacements of atoms from the least-squares plane ($d/\text{Å}$) of $(+)_{500}^{CD}$-[Co(mseea)(en)$_2$](ClO$_4$)$_3$.

2-(Methylseleno)ethylamine chelate ring

Plane 1; $0.66326X - 0.67175Y - 0.32990Z + 2.45197 = 0$

Co	0.0000	Se	-0.0000	N1	-0.0000	Cl	1.9064
C2	-0.3179	C3	0.4590				

Etylenediamine chelate ring

Plane 2; $-0.71865X - 0.59399Y - 0.36156Z + 2.96969 = 0$

Co	0.0000	N2	0.0000	N3	0.0000	C4	0.4060
C5	-0.3208						

Plane 3, $0.04888X + 0.51340Y - 0.85676Z + 0.88497 = 0$

Co	-0.0001	N4	0.0001	N5	0.0001	C6	0.2782
C7	-0.3723						

The X, Y, and Z coordinates in Å are referred to the crystallographic axes.

anions are from 2.90 Å to 3.04 Å. The distances suggest that they are hydrogen bonds.

V-A-3. Crystal Structure of $(+)_{550}^{CD} \cdot (+)_{370}^{CD}$-[Co(aese)(tn)$_2$]-(ClO$_4$)$_2$.

The perspective drawing of $(+)_{550}^{CD} \cdot (+)_{370}^{CD}$-[Co(aese)(tn)$_2$]$^{2+}$ ion is shown in Fig. 10. The bond lengths and angles are summarized in Table 12. The coordination geometry around the cobalt atom is approximately octahedral. The 2-aminoethane-sulfenate coordinates to cobalt atom with the nitrogen and sulfur atom. The asymmetric sulfur atom in $(+)_{550}^{CD} \cdot (+)_{370}^{CD}$-[Co(aese)(tn)$_2$]$^{2+}$ takes the (S) configuration for the Λ configuration. The five membered chelate ring of the coordinated aese ligand, S-C1-C2-N1, takes the reasonable gauche form with δ conformation (Fig. 10 and Table 13). The six-membered trimethylenediamine chelate ring, N2-C3-C4-C5-N3, takes the reasonable chair conformation. The other trimethylenediamine chelate ring, N4-C5-C6-C7-N5, however, has the distorted gauche form with δ conformation (Fig. 10 and Table 13). The irregular conformation seems to be caused by the intramolecular hydrogen bond between the sulfenato oxygen atom, O, and the amino group, N4, because the distance between the oxygen atom and nitrogen one, N4, is 2.963 Å.

The coordination angles in the diamine chelate rings, N2-Co-N3 and N4-Co-N5, are 90.8° and 93.4°, respectively, which are slightly smaller than those found in $(-)_{589}$-[Co(tn)$_3$]$^{3+}$
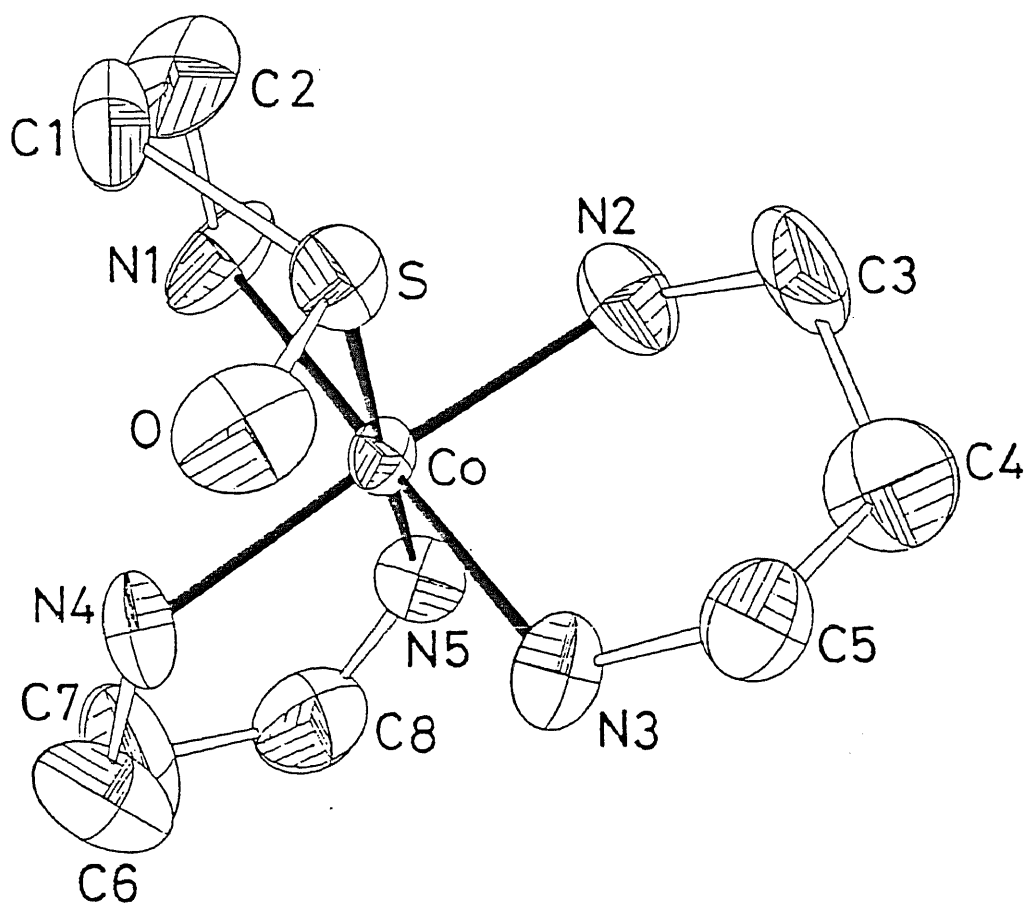
Figure. 10. A perspective drawing of $(+)^{CD}_{550} \cdot (+)^{CD}_{370}$-[Co(aese)-(en)$_2$]$^{2+}$ with the numbering scheme of atoms.

Table 15. Intermolecular distances and bond angles (with e.s.d.'s) of $(+)^{CD}_{550} \cdot (+)^{CD}_{370}$-[Co(aese)(tn)$_2$](ClO$_4$)$_2$.

(a) Bond Distances (1/Å)

Co-S	2.202(7)	Co-N1	2.036(20)
Co-N2	2.023(30)	Co-N3	1.972(22)
Co-N4	2.007(24)	Co-N5	2.075(26)
S-C1	1.863(31)	S-O	1.548(26)
N1-C2	1.503(44)	N2-C3	1.396(47)
N3-C5	1.471(45)	N4-C6	1.472(54)
N5-C8	1.497(60)	C1-C2	1.400(58)
C3-C4	1.523(58)	C4-C5	1.684(58)
C6-C7	1.392(56)	C7-C8	1.491(59)
CL1-O11	1.319(63)	CL1-O12	1.391(30)
CL1-O13	1.349(32)	CL1-O14	1.374(37)
CL2-O21	1.421(38)	CL2-O22	1.488(41)
CL2-O23	1.464(48)	CL2-O24	1.391(34)

(b) Bond Angles (ϕ/°)

S-Co-N1	88.8(7)	S-Co-N2	90.9(9)
S-Co-N3	92.4(7)	S-Co-N4	89.2(7)
S-Co-N5	176.0(9)	N1-Co-N2	89.6(11)
N1-Co-N3	178.8(10)	N1-Co-N4	93.0(10)
N1-Co-N5	88.1(9)	N2-Co-N3	90.8(10)
N2-Co-N4	177.3(10)	N2-Co-N5	86.6(12)
N3-Co-N4	86.5(10)	N3-Co-N5	90.7(10)

Table 15. Continued

N4-Co-N5	93.4(11)	Co-S-Cl	94.3(13)
Co-S-O	111.1(9)	Co-N1-C2	110.0(19)
Co-N2-C3	122.7(26)	Co-N3-C5	120.4(22)
Co-N4-C6	119.8(19)	Co-N5-C8	127.9(23)
S-Cl-C2	107.5(19)	N1-C2-Cl	109.2(35)
N2-C3-C4	104.0(36)	N3-C4-C5	106.5(24)
N3-C5-C4	104.8(30)	C6-C7-C8	122.7(37)
N4-C6-C7	118.1(46)	N5-C8-C7	112.0(35)
O11-CL1-O12	108.8(29)	O11-CL1-O13	107.5(34)
O11-CL1-O14	112.4(40)	O12-CL1-O13	108.8(23)
O12-CL1-O14	109.6(20)	O13-CL1-O14	109.6(20)
O21-CL2-O22	116.4(27)	O21-CL2-O23	111.4(27)
O21-CL2-O24	110.1(17)	O22-CL2-O23	109.6(26)
O22-CL2-O24	105.0(27)	O23-CL2-O24	103.5(23)

Table 16. Displacements of atoms from the least-squares plane $(d/\overset{\circ}{A})$ of $(+)^{CD}_{550} \cdot (+)^{CD}_{370} - [Co(aese)(tn)_2](ClO_4)_2$.

2-Aminoethanesulfenato chelate ring

Plane 1; $0.53006X + -0.84676Y + 0.04509Z + 0.25083 = 0$

Co 0.0003	S 0.0002	N1 0.0004	C1 0.5116
C2 -0.2695	O 1.1509		

Trimethylenediamine chelate ring

Plane 2; $-0.47727X + -0.23462Y + 0.84686Z + 6.31756 = 0$

Co 0.0000	N2 0.0001	N3 0.0000	C3 0.7531
C4 0.1369	C5 0.7711		

Plane 3; $0.68212X + 0.51670Y + 0.51744Z + 0.51519 = 0$

Co 0.0004	N4 -0.0000	N5 0.0002	C6 0.2801
C7 -0.3388	C8 -0.0173		

The X, Y, and Z coordinates in $\overset{\circ}{A}$ are referred to the crystallographic axes.

(mean 94.5°)[32a] and $(-)_{589}$-[Co(acac)(tn)$_2$]$^{2+}$ (mean 96°).[32c]

The average bond lengths of Co-N2, Co-N3, and Co-N4, where the diamine nitrogen atoms are cis position to the sulfur donor atom, is 2.001 Å, and this value is in consistent with that of Co-N in other (trimethylenediamine)cobalt(III) complexes.[32]

On the other hand, the trans Co-N5 bond length (2.075 Å) is longer than the average cis Co-N one. A similar trans effect is observed in the bis(ethylenediamine)cobalt(III) complexes with a coordinated sulfenato sulfur atom, [Co(aese)(en)$_2$]$^{2+}$ [6] and [Co(L-cysteinesulfenato-N,S)(en)$_2$]$^{2+}$.[2b] The bond lengths and angles associated with the aese ligand are similar to those of the corresponding bis(ethylenediamine) complex, [Co(aese)(en)$_2$]$^{2+}$,[6] though the Co-S bond length (2.202 Å) is somewhat shorter and the Co-N1 one (2.036) somewhat longer than those in [Co(aese)(en)$_2$]$^{2+}$ (Co-S = 2.253 Å, Co-N = 1.987 Å).

V-B. Electronic Absorption Spectra.

V-B-1. Bis(ethylenediamine)cobalt(III) Complexes.

The electronic absorption spectra of the bis(ethylene-diamine)cobalt(III) complexes with a selenium- or sulfur-containing ligand are shown in Figs. 11-16 and their data are summarized in Table 17.

The absorption spectral behavior of the cobalt(III) complexes which belong to the $[Co(N)_5(Se)]$ type is quite similar to that of the corresponding $[Co(N)_5(S)]$ type complexes (Figs. 11-15). The intense bands at around 32-36 x 10^3 cm^{-1} of the former complexes correspond well to the so-called sulfur-to-metal charge transfer bands of the latter ones,[4-6] and then these bands can be assigned to the selenium-to-metal charge transfer bands. The chalcogen-to-metal charge transfer bands of the selenolato, selenenato, and selenoether complexes commonly shift to lower energy than those of the corresponding thiolato, sulfenato, and thioether complexes, respectively (Fig. 11-15). This suggests that the coordinated selenium is better reductant than the analogous coordinated sulfur in these systems. Of these complexes, $[Co(aesee)(en)_2]^{2+}$ shows another intense band at 27.55 x 10^3 cm^{-1} (Fig. 12). This band corresponds to the characteristic band (ca. 27.0 x 10^3 cm^{-1}) of the sulfenato complex, $[Co(aese)(en)_2]^{2+}$.[6] Therefore, the band at 27.55 x 10^3 cm^{-1} seems to be characteristic for the selenenato complex as well as the sulfenato complex.
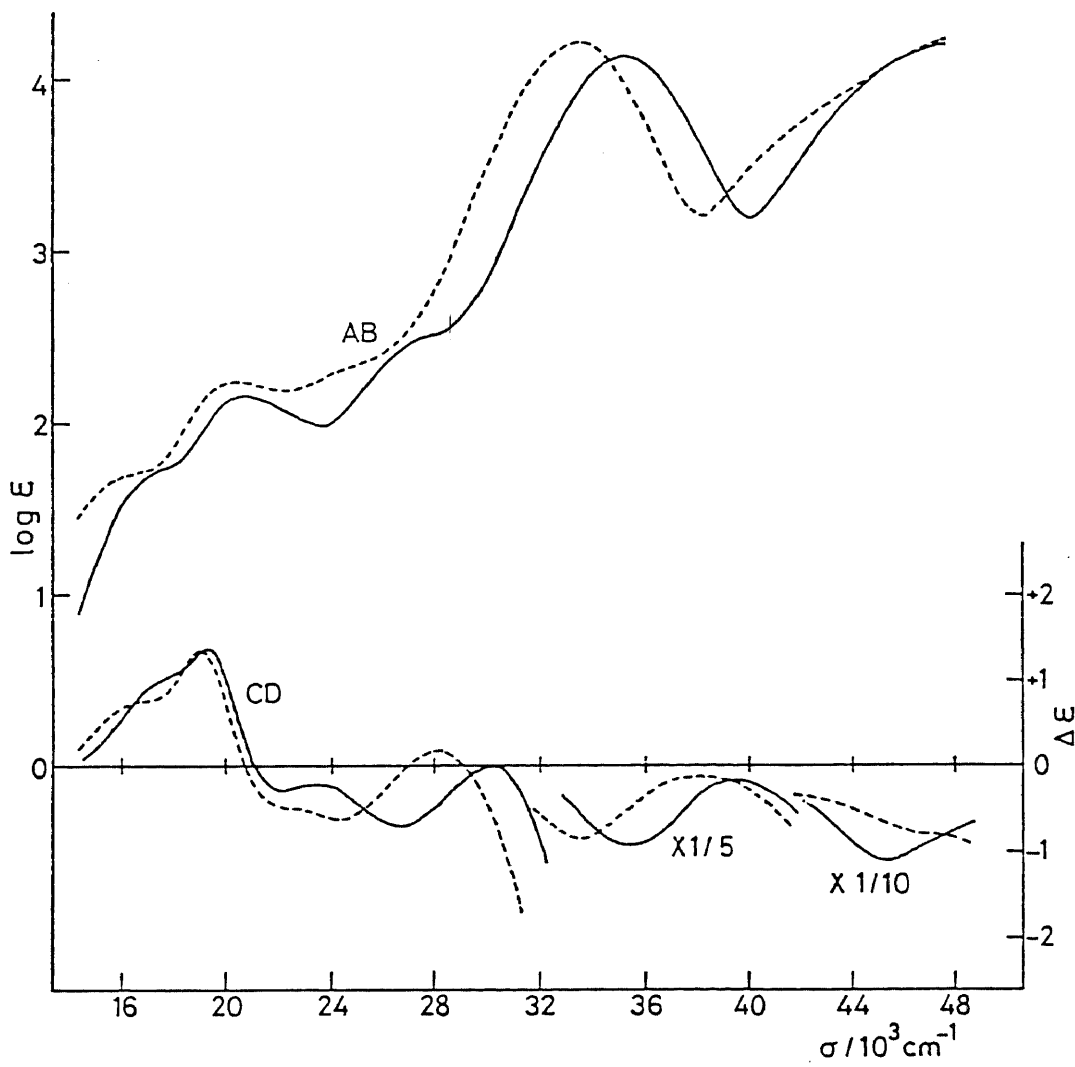
Figure 11. Absorption and CD spectra of $(+)^{CD}_{500}$-[Co(aes)-(en)$_2$]$^{2+}$ (-----) and $(+)^{CD}_{500}$-[Co(aet)(en)$_2$]$^{2+}$ (————).
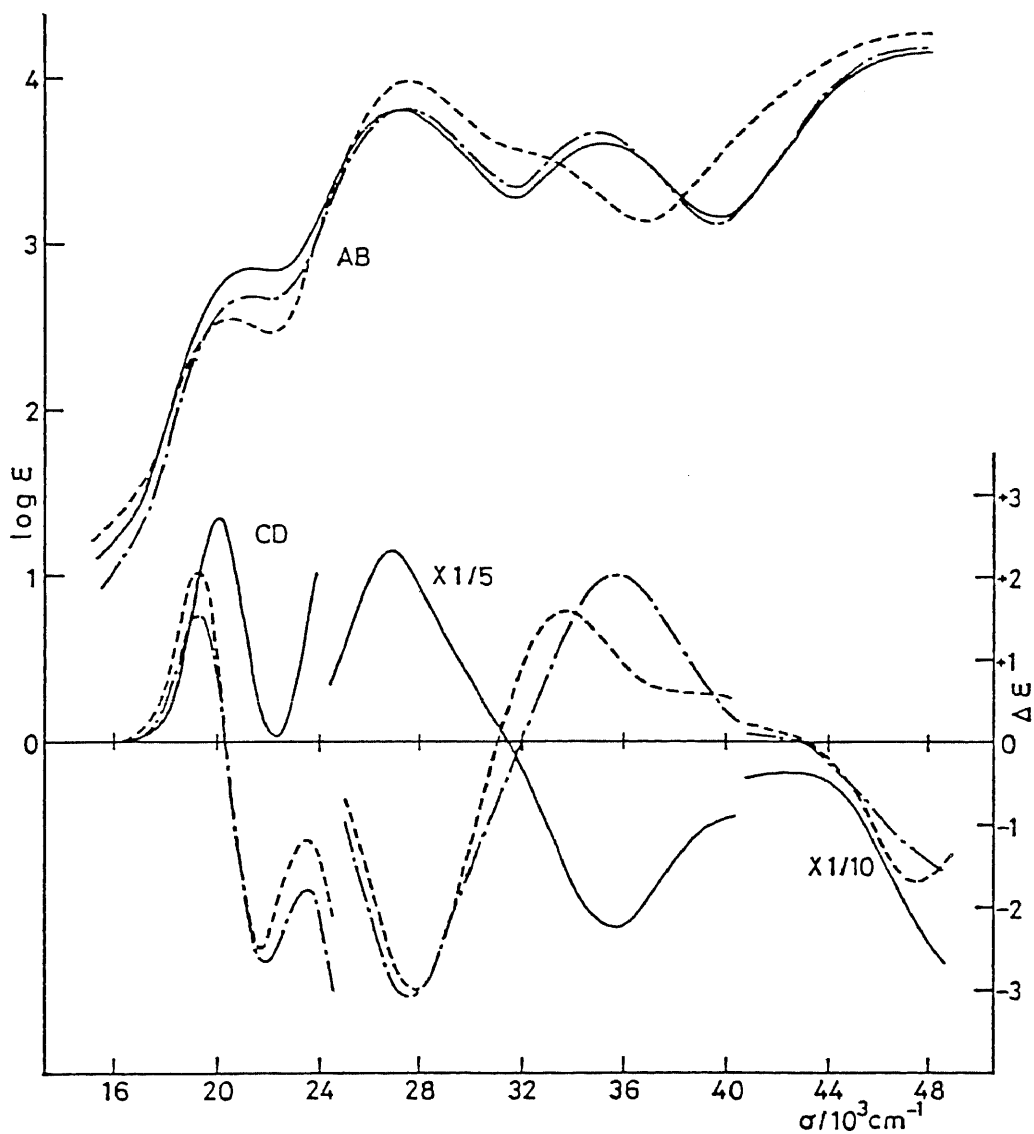
Figure 12. Absorption and CD spectra of $(+)^{CD}_{500} \cdot (-)^{CD}_{360}$-[Co-(aesee)(en)$_2$]$^{2+}$ (— — —), $(+)^{CD}_{500} \cdot (-)^{CD}_{360}$-[Co(aese)-(en)$_2$]$^{2+}$ (—·—·—), and $(+)^{CD}_{500} \cdot (+)^{CD}_{360}$-[Co(aese)-(en)$_2$]$^{2+}$ (———).
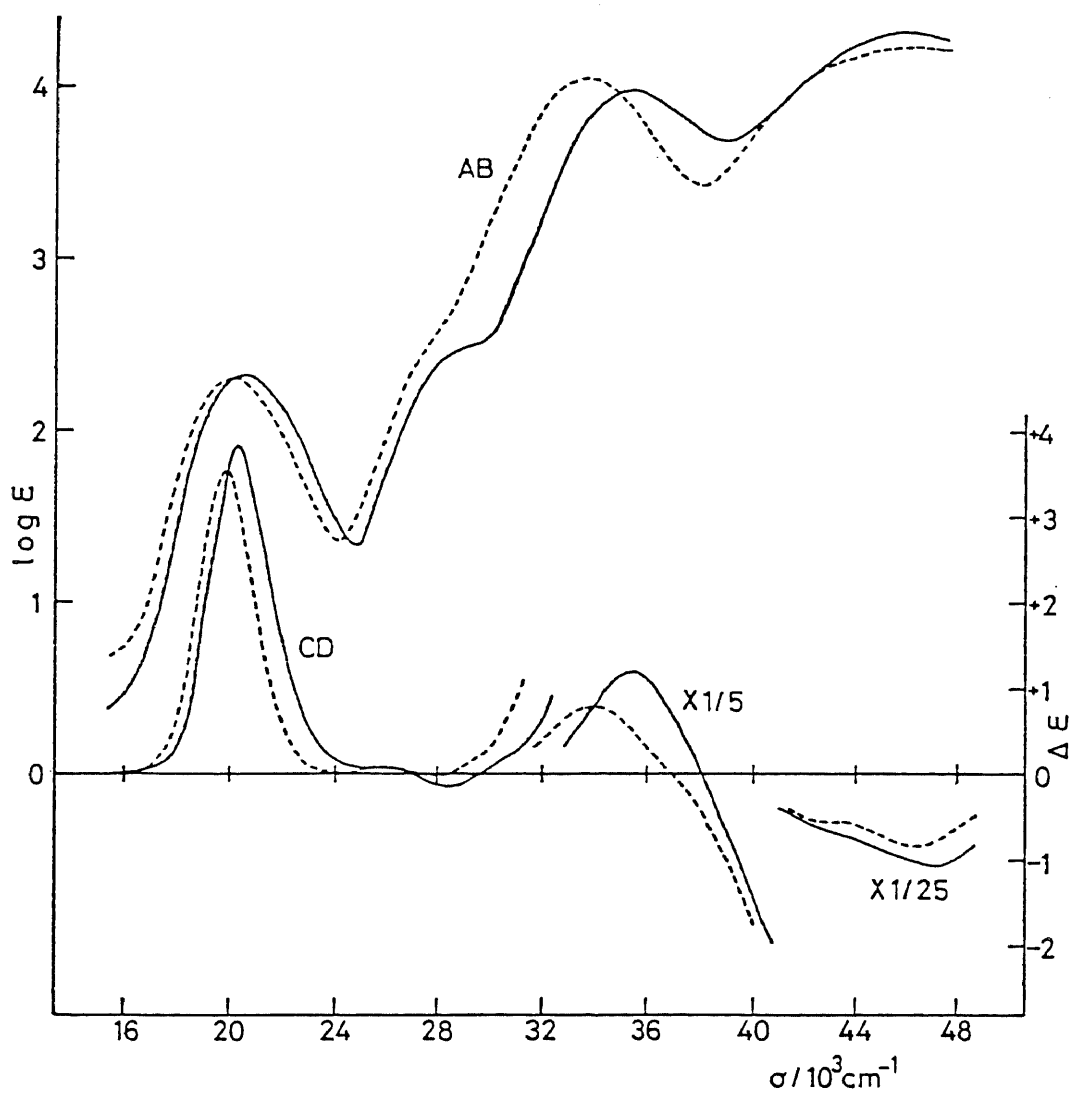
Figure 13. Absorption and CD spectra of $(+)_{500}^{CD}$-[Co(mseea)-(en)$_2$]$^{3+}$ (-----) and $(+)_{500}^{CD}$-[Co(mea)(en)$_2$]$^{3+}$ (————).
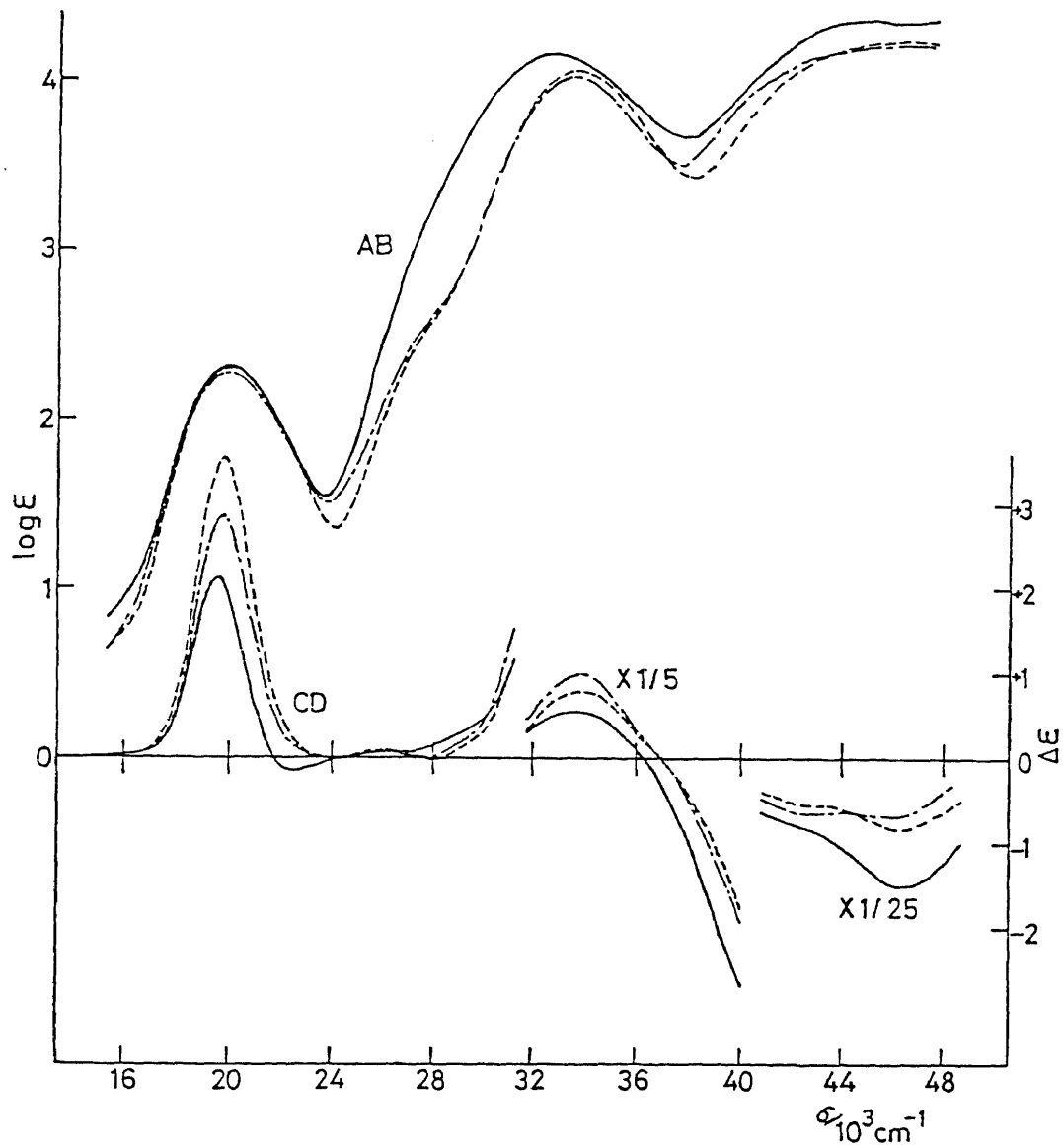
Figure 14. Absorption and CD spectra of $(+)_{500}^{CD}$-[Co(mseea)-$(en)_2]^{3+}$ (------), $(+)_{500}^{CD}$-[Co(eseea)(en)$_2]^{3+}$ (---·--·---), and $(+)_{500}^{CD}$-[Co(bseea)(en)$_2]^{3+}$ (———).
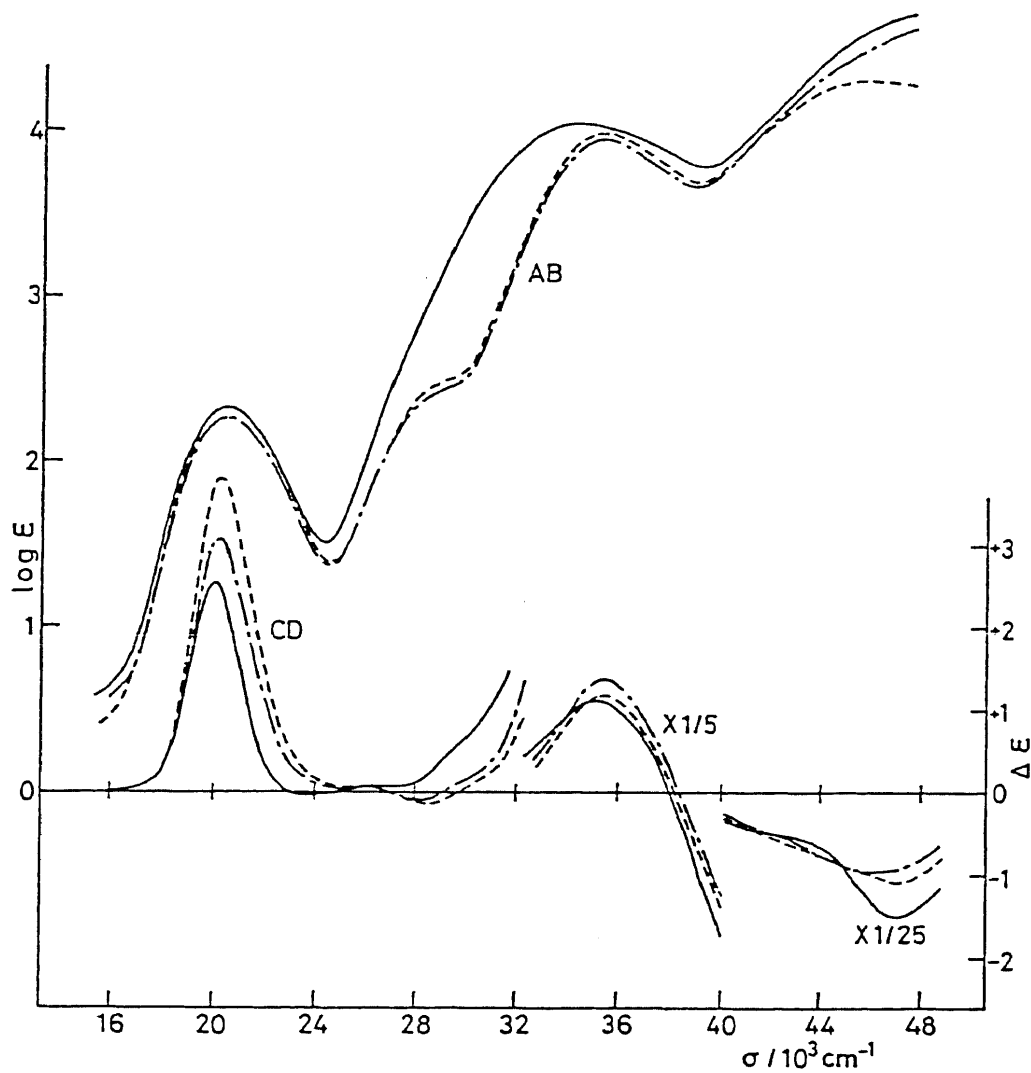
Figure 15. Absorption and CD spectra of $(+)^{CD}_{500}$-[Co(mea)-
(en)$_2$]$^{3+}$ (-----), $(+)^{CD}_{500}$-[Co(eea)(en)$_2$]$^{3+}$ (—·—·—),
and $(+)^{CD}_{500}$-[Co(bea)(en)$_2$]$^{3+}$ (———).
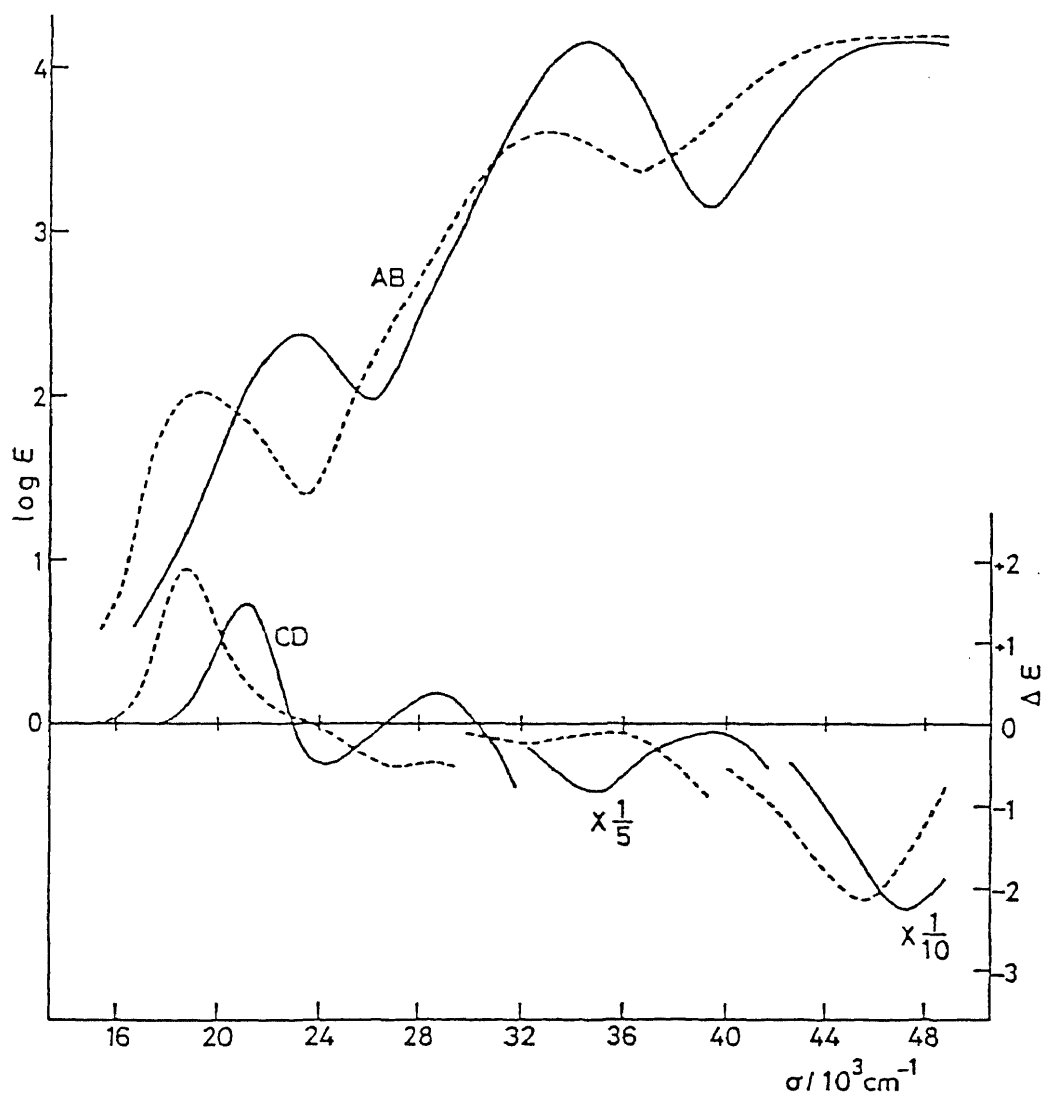
Figure 16. Absorption and CD spectra of $(+)^{CD}_{500}$-[Co(aesei-N,O)(en)$_2$]$^{2+}$ (-----) and $(+)^{CD}_{500}$-[Co(aesi-N,S)-(en)$_2$]$^{2+}$ (———).

Table 17. Absorption data of bis(ethylenediamine)cobalt(III) complexes.

Complex	First band	Second band	Charge transfer band
$(+)_{500}^{CD}$-[Co(aet)(en)$_2$]$^{2+}$	17.5 (1.72sh) 20.66 (2.16)	28.2 (2.52sh)	35.21 (4.13) 48.78 (4.22)
$(+)_{500}^{CD}$-[Co(aes)(en)$_2$]$^{2+}$	16.5 (1.71sh) 20.35 (2.24)	24.7 (2.33sh)	33.44 (4.22)
$(+)_{500}^{CD}\cdot(+)_{360}^{CD}$-[Co(aese)(tn)$_2$]$^{2+}$	21.12 (2.85)		26.99 (3.81) 35.03 (3.61) 49.26 (4.18)
$(+)_{500}^{CD}\cdot(-)_{360}^{CD}$-[Co(aese)(en)$_2$]$^{2+}$	21.12 (2.68)		27.32 (3.82) 34.84 (3.68) 49.26 (4.21)
$(+)_{500}^{CD}\cdot(-)_{360}^{CD}$-[Co(aesee)(en)$_2$]$^{2+}$	20.45 (2.55)		27.55 (3.99) 32.0 (3.55sh) 47.85 (4.30)
$(+)_{500}^{CD}$-[Co(aesi-N,S)(en)$_2$]$^{2+}$	23.07 (2.37)		34.48 (4.16) 47.06 (4.18)
$(+)_{500}^{CD}$-[Co(aesei-N,O)(en)$_2$]$^{2+}$	19.23 (2.02)		33.00 (3.61) 47.17 (4.19)
$(+)_{500}^{CD}$-[Co(mea)(en)$_2$]$^{3+}$	20.47 (2.32)	29.3 (2.50sh)	35.34 (3.99) 45.66 (4.32)

Table 17. Continued

$(+)^{CD}_{500}$-[Co(eea)(en)$_2$]$^{3+}$	20.45 (2.26)	29.4 (2.45sh)	35.34 (3.95)	48.90 (4.63)
$(+)^{CD}_{500}$-[Co(bea)(en)$_2$]$^{3+}$	20.45 (2.33)		34.31 (4.05)	49.0 (4.75sh)
$(+)^{CD}_{500}$-[Co(mseea)(en)$_2$]$^{3+}$	20.00 (2.30)		33.56 (4.06)	46.30 (4.24)
$(+)^{CD}_{500}$-[Co(eseea)(en)$_2$]$^{3+}$	19.96 (2.27)		33.44 (4.03)	46.51 (4.22)
$(+)^{CD}_{500}$-[Co(bseea)(en)$_2$]$^{3+}$	19.92 (2.31)		32.57 (4.16)	44.84 (4.36)

Wave numbers and log ε values (in parentheses) are given 10^3 cm^{-1} and mol^{-1} dm^3 cm^{-1}, respectively. Sh denotes a shoulder.

In the first absorption band region, $[Co(aes)(en)_2]^{2+}$
shows an explicit shoulder on the lower energy side of the
major peak (ca. 16.6×10^3 cm^{-1}) as well as $[Co(aet)(en)_2]^{2+}$
(Fig. 11). This kind of shoulder was also observed in the
absorption spectra of cobalt(III) complexes with a thiolato
type ligand such as L-cysteinate[2c,d] and D- or L-penicillami-
nate,[2d,h] and this band seems to be also characteristic for
the selenolato coordination. Adamson et al. pointed out that
the $^1A_1 \rightarrow {}^1E_1$ transition of the thiolato or selenolato complex
would be splitted into two nondegenerate ones, because of the
perturbation of Co d(π) orbitals by a p-like lone pair on the
chalcogen atom.[8] Therefore, the maximum and shoulder of the
first absorption band of the selenolato or thiolato complex
can be assigned to the two nondegenerate components generated
from the $^1A_1 \rightarrow {}^1E_1$ transition in C_{4v} symmetry, considering
that the component generated from $^1A_1 \rightarrow {}^1A_2$ should occur at
nearly the same energy as the maximum of the first absorption
band of $[Co(en)_2]^{3+}$ (21.4×10^3 cm^{-1}) as mentioned in Chapter
II-B. For the selenoether complexes, $[Co(mseea)(en)_2]^{3+}$,
$[Co(eseea)(en)_2]^{3+}$, and $[Co(bseea)(en)_2]^{3+}$, the first absorption
bands are rather sharp and no shoulder is observed as in the
case for the thioether complexes (Figs. 13-15). Similarly,
no clear shoulder appears in the first absorption bands of the
selenenato and sulfenato complexes, though the molar absorption
coefficients of these bands is larger as compared with those of
other complexes (Fig. 12). The absence of the shoulder in the

- 74 -

first absorption bands of these complexes may be due to the absence of a p-like lone pair on the chalcogen atom for selenoether, thioether, selenenate, or sulfenate type ligand. The maxima of the first absorption bands of the selenolato, selenenato, and selenoether complexes shift to lower energy than those of the corresponding thiolato, sulfenato, and thioether complexes, respectively (Fig. 11-15), indicating that the order of the ligand field strength is S > Se.

As shown in Fig. 16, the O-bonded seleninato complex, $[Co(aesei-N,O)(en)_2]^{2+}$, whose molecular structure was determined by X-ray analytical study (Chapter V-A-1), exhibits a broad band at 19.23×10^3 cm^{-1} with a vague shoulder on higher energy in the first absorption band region. This absorption behavior agrees well with that of the $[Co(aminocarboxylato)(en)_2]$ type complexes.[34] On the other hand, the S-bonded sulfinato complex, $[Co(aesi-N,S)(en)_2]^{2+}$, shows a first absorption band at 23.07×10^3 cm^{-1} with a vague shoulder on the lower energy side, indicating that the S-bonded sulfinato provide a ligand field stronger than ethylenediamine. The intense absorption band at 33.00×10^3 cm^{-1} of the O-bonded aesei complex is weaker than that of the S-bonded aesi complex (Fig. 16). Since the seleninato moiety can still interact with a cobalt center (Fig. 8), this absorption band seems to be a new charge transfer band from the seleninato chromophore to the cobalt atom. A similar absorption spectral trend was also observed for the photoproduct of $[Co(aesi-N,S)(en)_2]^{2+}$.[7,13]

V-B-2. Bis(trimethylenediamine)cobalt(III) Complexes.

The electronic absorption spectra of the bis(trimethylene-diamine)cobalt(III) complexes with a selenium- or sulfur-containing ligand are shown in Figs. 17-21, together with those of the corresponding bis(ethylenediamine)cobalt(III) complexes and their data are summarized in Table 18.

The absorption spectral behavior of the bis(trimethylene-diamine)cobalt(III) complexes with a selenium or sulfur donor atom is quite similar to that of the corresponding [Co-(bidentate-N,Se or -N,S)(en)$_2$] type complexes. These complexes show the chalcogen-to-metal charge transfer bands at 32-35 x 10^3 cm^{-1}, which shift to lower energy than those of the corresponding bis(ethylenediamine) complexes. As for [Co(aese)-(tn)$_2$]$^{2+}$, another characteristic charge transfer band appears at ca. 27 x 10^3 cm^{-1}, as in the case for [Co(aese)(en)$_2$]$^{2+}$ (Fig. 19).

The first absorption bands of the [Co(bidentate-N,Se or -N,S)(tn)$_2$] type complexes shift to lower energy than those of the corresponding [Co(bidentate-N,Se or -N,S)(en)$_2$] type ones (Figs. 17-20), in analogous with the fact that the [Co(L)(tn)$_2$] type complexes show the first absorption bands at lower energy as compared with those of the corresponding [Co(L)(en)$_2$] ones; L denotes a bidentate ligand such as glycinate and oxalate.[35] In the bis(trimethylenediamine)cobalt(III) complexes, the selenolato and selenoether complexes, [Co(aes)(tn)$_2$]$^{2+}$ and [Co(mseea)(tn)$_2$]$^{3+}$, show the first absorption bands at lower
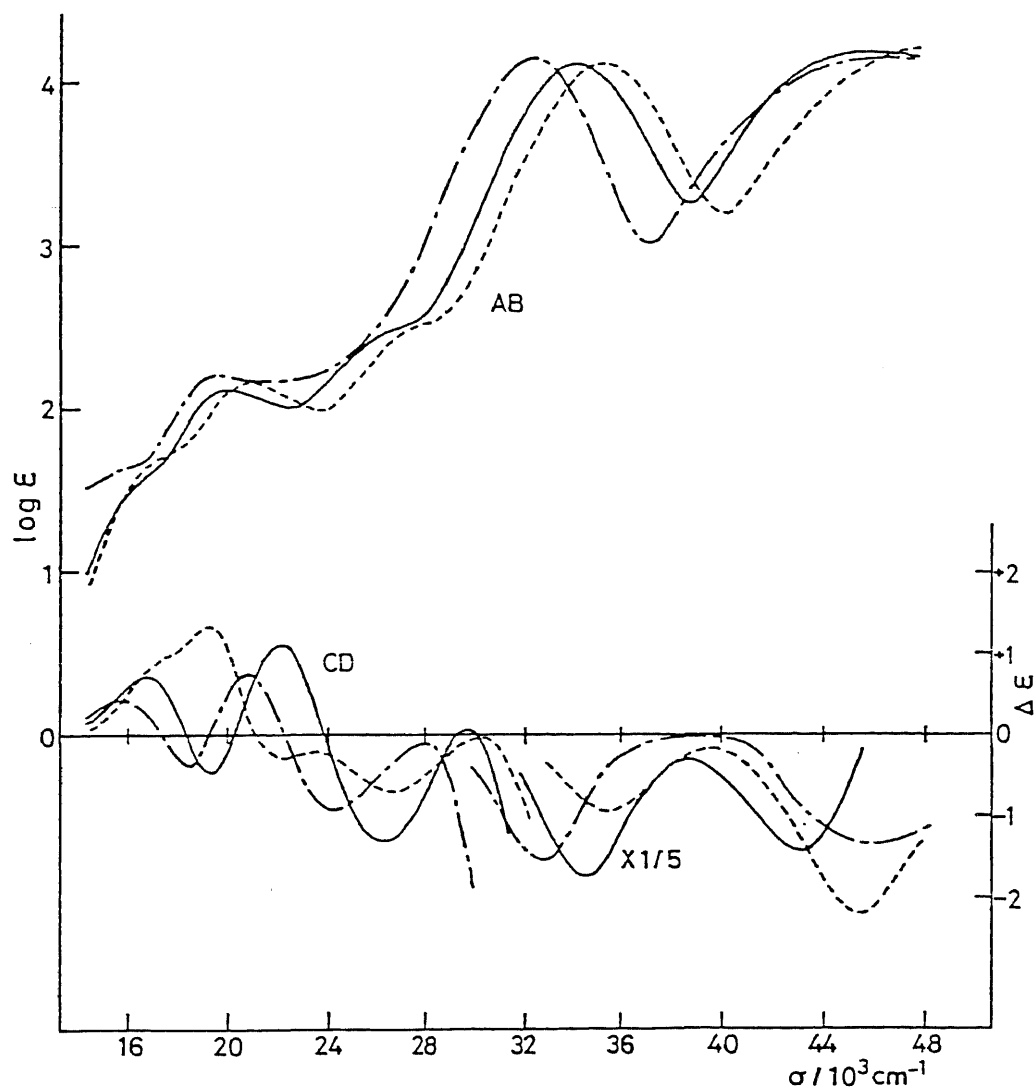
Figure 17. Absorption and CD spectra of $(+)^{CD}_{600}$-[Co(aet)(tn)$_2$]$^{2+}$ (———), $(+)^{CD}_{600}$-[Co(aes)(tn)$_2$]$^{2+}$ (—·—·—), and Λ-[Co(aet)(en)$_2$]$^{2+}$ (-----).

- 77 -
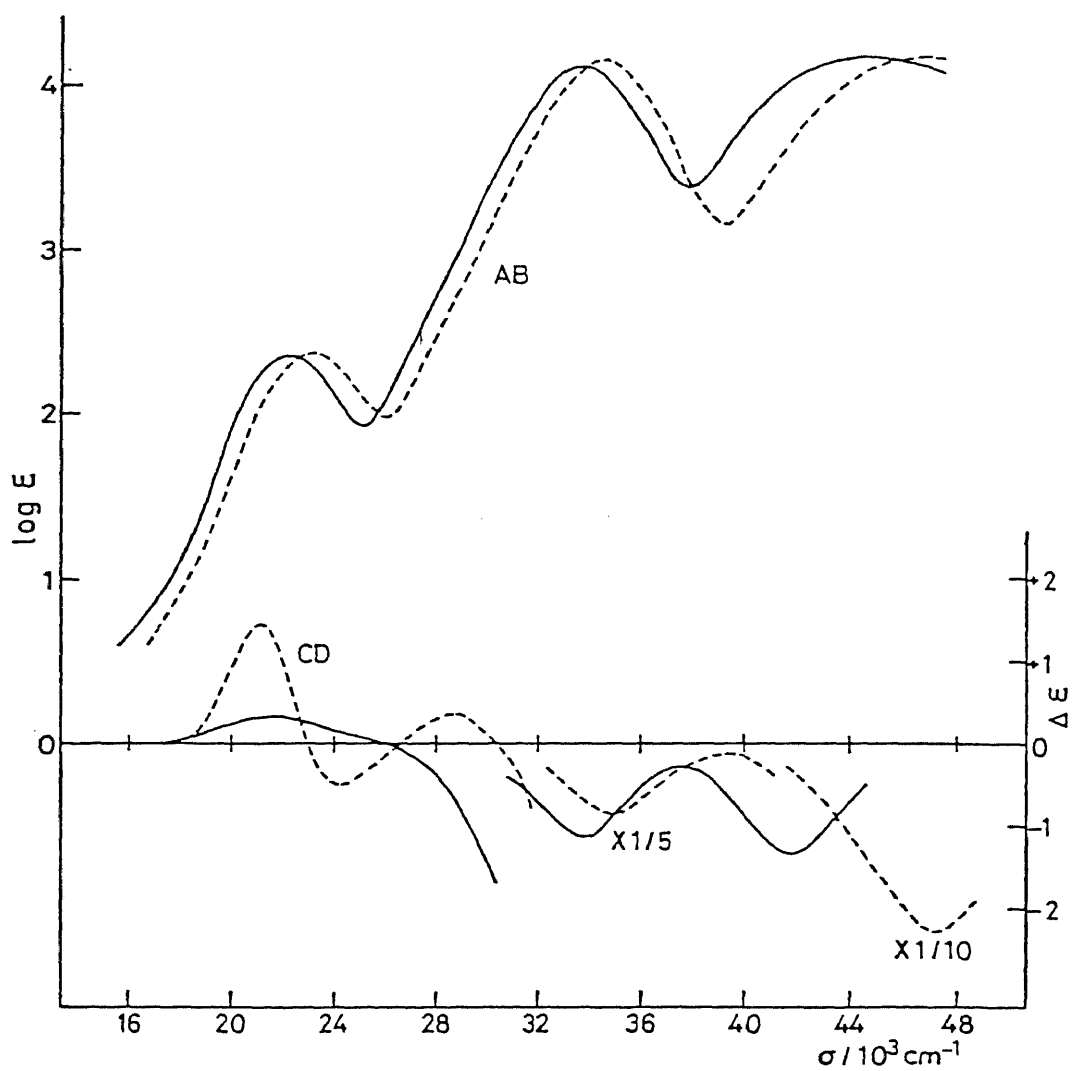
Figure 18. Absorption and CD spectra of $(+)^{CD}_{500}$-[Co(aesi)-
(tn)$_2$]$^{2+}$ (————) and Λ-[Co(aesi-N,S)(en)$_2$]$^{2+}$ (-----).
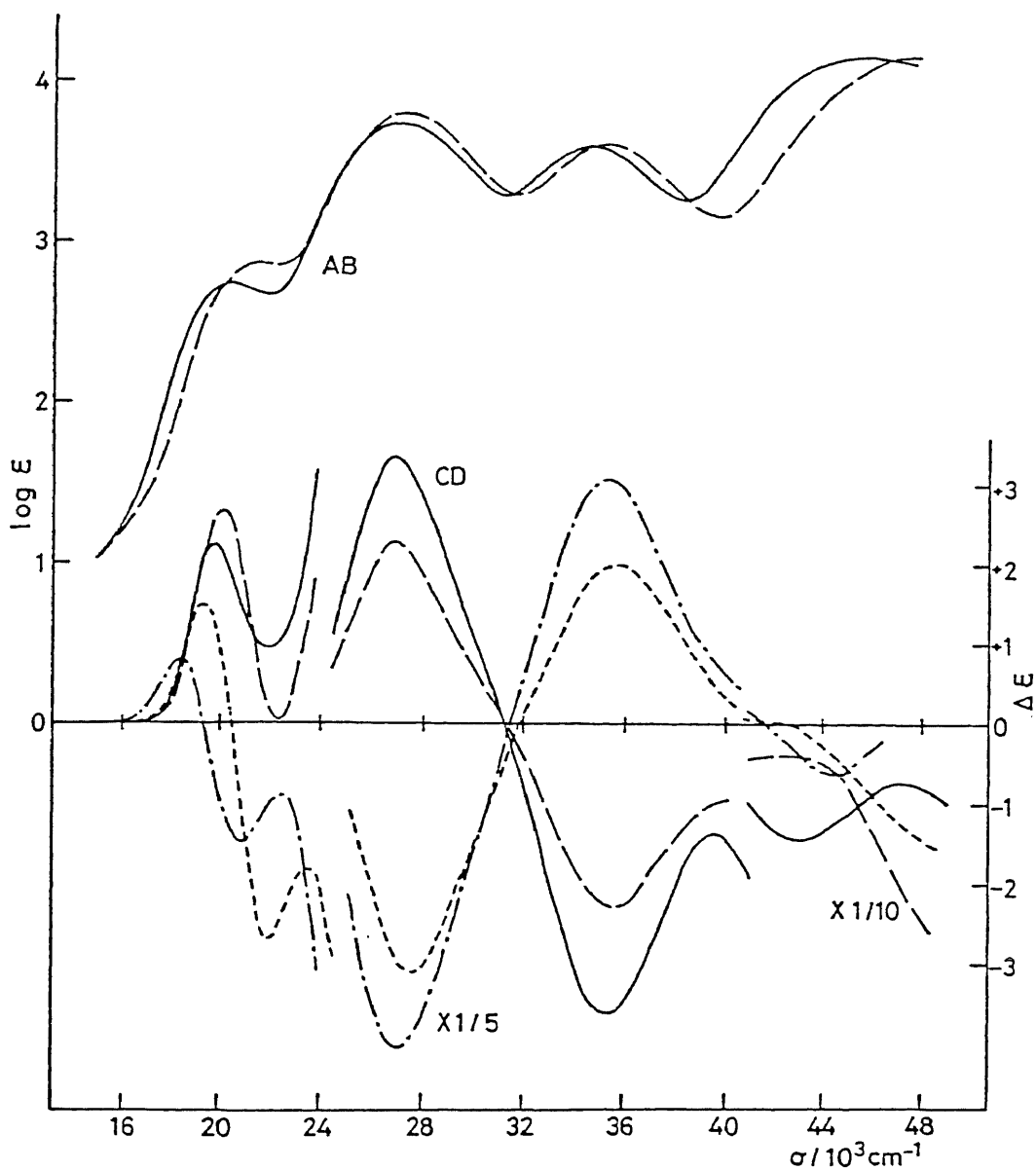
Figure 19. Absorption and CD spectra of $(+)_{550}^{CD} \cdot (+)_{370}^{CD} - [Co-(aese)(tn)_2]^{2+}$ (————), $(+)_{550}^{CD} \cdot (-)_{370}^{CD} - [Co(aese)-(tn)_2]^{2+}$ (—·—·—), $\Lambda - (S) - [Co(aese)(en)_2]^{2+}$ (————), and $\Lambda - (R) - [Co(aese)(en)_2]^{2+}$ (————).
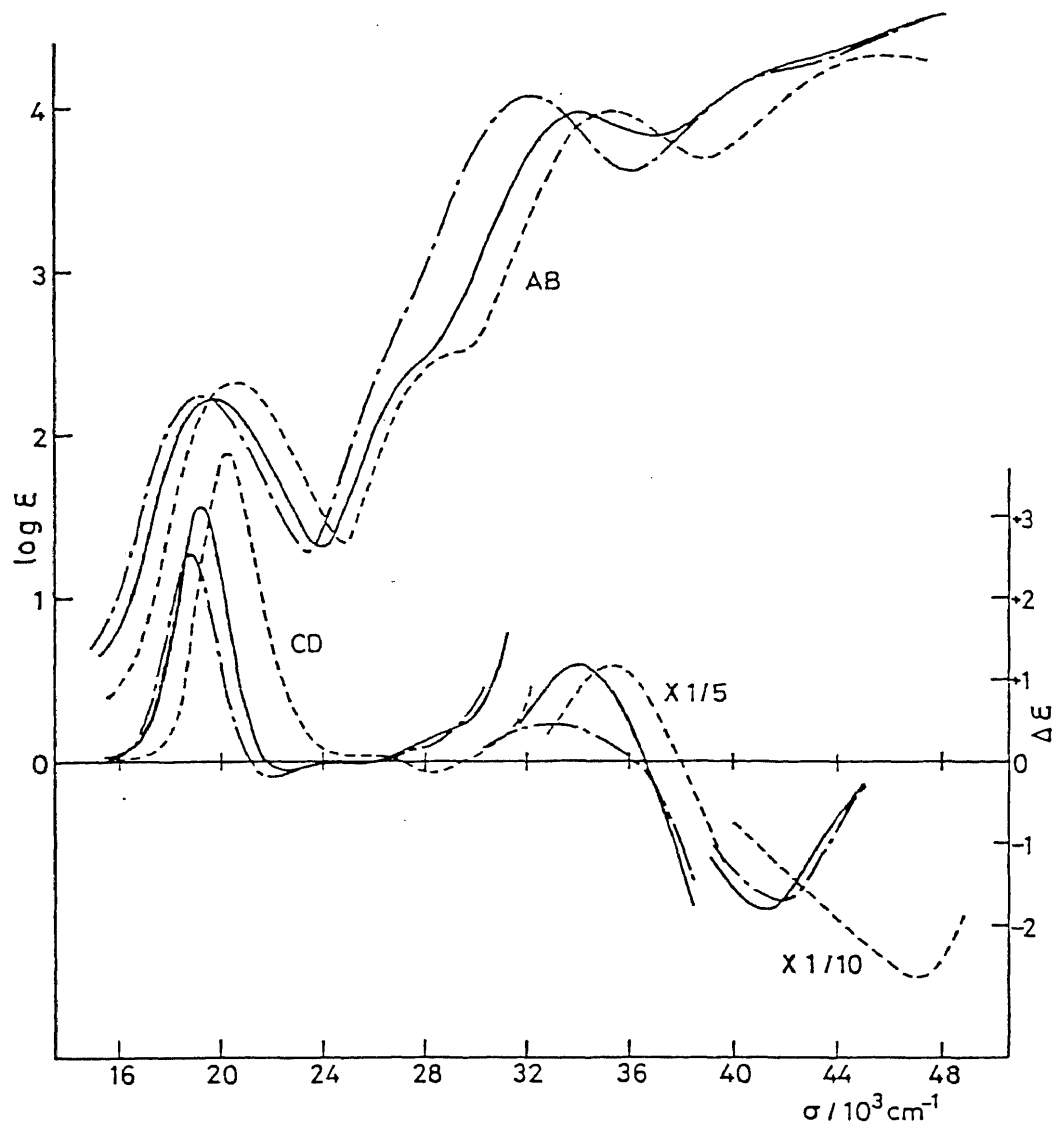
Figure 20. Absorption and CD spectra of $(+)^{CD}_{550}$-[Co(mea)-
(tn)$_2$]$^{3+}$ (————), $(+)^{CD}_{550}$-[Co(mseea)(tn)$_2$]$^{3+}$ (—·—·—),
and Λ-(R)-[Co(mea)(en)$_2$]$^{3+}$ (—————).
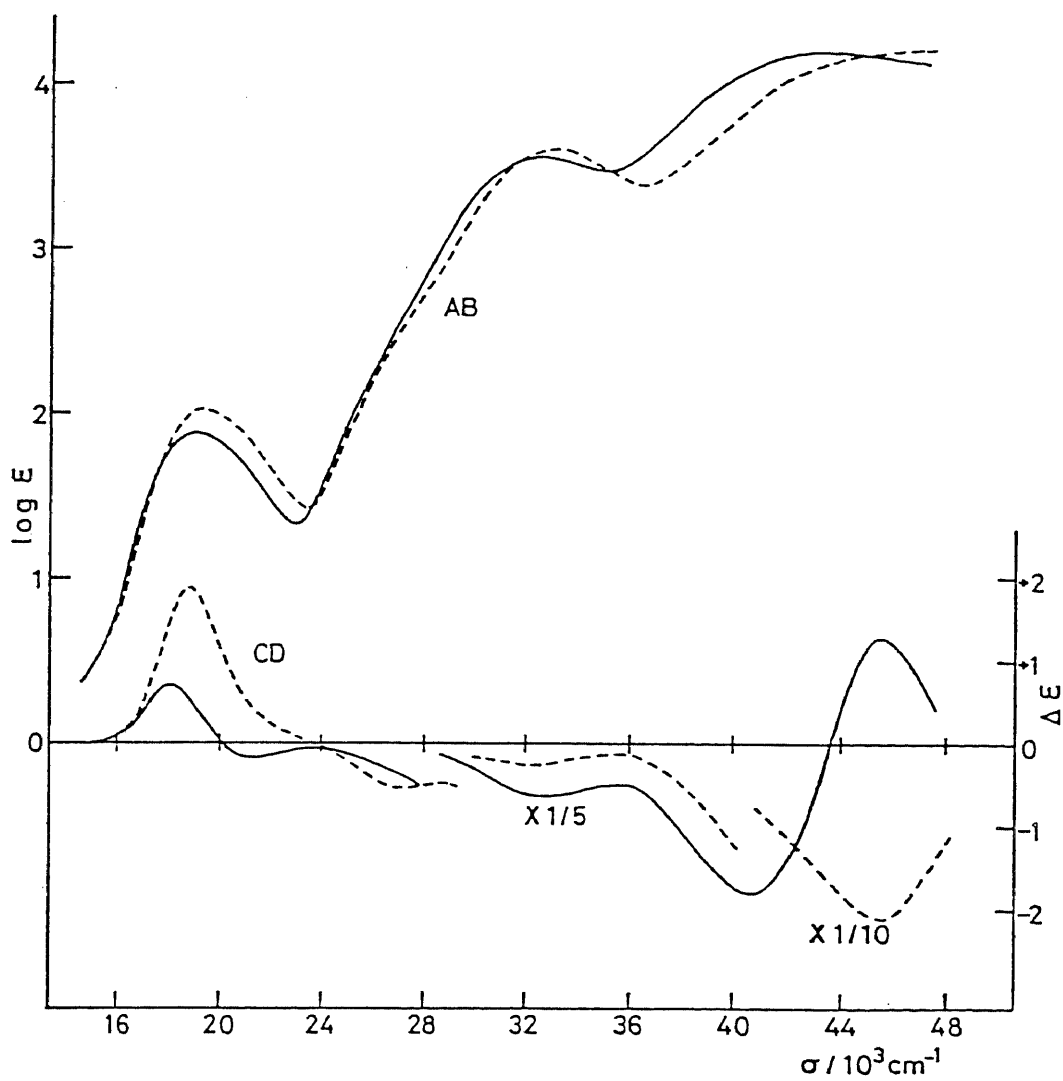
Figure 21. Absorption and CD spectra of $(+)^{CD}_{550}$-[Co(aesei)-(tn)$_2$]$^{2+}$ and Λ-$(+)^{CD}_{500}$-[Co(aesei-N,O)(en)$_2$]$^{2+}$ (-----).

Table 18. Absorption data of bis(trimethylenediamine)cobalt(III) complexes.

Complex	First band	Second band	Charge transfer band
$(+)_{600}^{CD}$-[Co(aet)(tn)$_2$]$^{2+}$	16.9 (1.61sh) 19.92 (2.11)	27.3 (2.51sh)	34.13 (4.12) 45.35 (4.20)
$(+)_{600}^{CD}$-[Co(aes)(tn)$_2$]$^{2+}$	16.0 (1.64 sh) 19.70 (2.21)		32.36 (4.16) 46.30 (4.16)
$(+)_{550}^{CD}$·$(+)_{370}^{CD}$-[Co(aese)(tn)$_2$]$^{2+}$	20.20 (2.73)		26.88 (3.74) 34.42 (3.61) 45.15 (4.19)
$(+)_{550}^{CD}$·$(-)_{370}^{CD}$-[Co(aese)(tn)$_2$]$^{2+}$	20.68 (2.66)		26.96 (3.81) 34.48 (3.62) 44.15 (4.63)
$(+)_{500}^{CD}$-[Co(aesi-N,S)(tn)$_2$]$^{2+}$	22.15 (2.36)		33.67 (4.12) 44.64 (4.17)
$(+)_{550}^{CD}$-[Co(aesei-N,O)(tn)$_2$]$^{2+}$	19.01 (1.87)		32.47 (3.55) 43.48 (4.20)
$(+)_{550}^{CD}$-[Co(mea)(tn)$_2$]$^{3+}$	19.67 (2.22)	28.3 (2.52sh)	34.07 (3.97) 43.9 (4.33sh) 49.02 (4.60)
$(+)_{550}^{CD}$-[Co(mseea)(tn)$_2$]$^{3+}$	19.16 (2.24)		32.15 (4.07) 43.1 (4.28sh) 48.78 (4.57)

Table 18. Continued

Wave numbers and log ε values (in parentheses) are given in 10^3 cm^{-1} and mol^{-1} dm^3 cm^{-1}, respectively. Sh denotes a shoulder.

energy than those of the corresponding thiolato and thioether complexes, $[Co(aet)(tn)_2]^{2+}$ and $[Co(mea)(tn)_2]^{3+}$, respectively. This is consistent with the conclusion that the ligand field strength is S > Se in the bis(ethylenediamine)cobalt(III) complexes (Chapter V-B-1).

As shown in Fig. 21, the absorption spectral behavior of $[Co(aesei)(tn)_2]^{2+}$ is agree well with that of $[Co(aesei-N,O)(en)_2]^{2+}$, showing a first absorption band at 19.01×10^3 cm^{-1} with a vague shoulder on higher energy and a weak charge transfer band at 32.47×10^3 cm^{-1}. This suggests that linkage isomerization occured during the oxidation process with excess hydrogen peroxide and the O-bonded seleninato complex was obtained as in the case of the bis(ethylenediamine)cobalt(III) complex.

V-C. Circular Dichroism (CD) Spectra.

V-C-1. Bis(ethylenediamine)cobalt(III) Complexes.

The CD spectra of the bis(ethylenediamine)cobalt(III) complexes with a selenium- or sulfur-containing ligand are shown in Figs. 11-16 and their data are summarized in Table 19.

The Δ and Λ isomers are possible for $[Co(aes)(en)_2]^{2+}$, $[Co(aet)(en)_2]^{2+}$, and $[Co(aesi)(en)_2]^{2+}$. As shown in Fig. 11, the CD spectrum of $(+)^{CD}_{500}-[Co(aes)(en)_2]^{2+}$ agrees with that of $(+)^{CD}_{500}-[Co(aet)(en)_2]^{2+}$ in the whole region, showing three CD bands, (+), (+), and (-), from lower energy in the first absorption band region. The $(+)^{CD}_{500}$ aet isomer has been assigned to the Λ configuration on the basis of the CD sign of the two lower energy bands (the split components of the $^1A_1 \rightarrow {}^1E_1$ transition).[4] Therefore, the $(+)^{CD}_{500}$ aes isomer is also assignable to the Λ configuration. The $(+)^{CD}_{500}$ aesi isomer, which is the oxidation product of $\Lambda-(+)^{CD}_{500}-[Co(aet)(en)_2]^{2+}$, shows a major positive CD band at lower energy in the first absorption band region (Fig. 16), and then can be assigned to the Λ configuration.

Taking the asymmetric chalcogen donor atom, (R) and (S), into consideration, four isomers, $\Delta-(R)$, $\Delta-(S)$, $\Lambda-(R)$, and $\Lambda-(S)$, are possible for the selenenato, sulfenato, selenoether, and thioether complexes (Chapter II-A-3). The oxidation of $\Lambda-(+)^{CD}_{500}-[Co(aet)(en)_2]^{2+}$ produced the two sulfenato isomers, $(+)^{CD}_{500} \cdot (+)^{CD}_{360}-$ and $(+)^{CD}_{500} \cdot (-)^{CD}_{360}-[Co(aese)(en)_2]^{2+}$. Both

Table 19. CD data of bis(ethylenediamine)cobalt(III) complexes.

Complex	First band	Second band	Charge transfer band
$(+)_{500}^{CD}$-[Co(aet)(en)$_2$]$^{2+}$	17.5 (+1.00sh) 19.27 (+1.37) 22.08 (-0.29)	26.67 (-0.71)	35.34 (-4.62) 45.5 (-11.1)
$(+)_{500}^{CD}$-[Co(aes)(en)$_2$]$^{2+}$	16.6 (+0.75sh) 19.01 (+1.35) 22.2 (-0.47sh)	24.45 (-0.61) 28.17 (+0.18)	33.44 (-4.26)
$(+)_{500}^{CD}$·$(+)_{360}^{CD}$-[Co(aese)(en)$_2$]$^{2+}$	19.96 (+2.72)		26.88 (+11.56) 35.59 (-11.29) 40.5 (-4.28sh)
$(+)_{500}^{CD}$·$(-)_{360}^{CD}$-[Co(aese)(en)$_2$]$^{2+}$	19.27 (+1.53) 21.83 (-2.65)		27.55 (-15.39) 35.59 (+10.24) 41.7 (+0.64sh) 48.8 (-15.8)
$(+)_{500}^{CD}$·$(-)_{360}^{CD}$-[Co(aesee)(en)$_2$]$^{2+}$	19.23 (2.04) 22.12 (-2.25)		27.78 (-15.04) 33.56 (+7.80) 38.5 (+2.95sh) 47.62 (-16.9)
$(+)_{500}^{CD}$-[Co(aesi-N,S)(en)$_2$]$^{2+}$	21.05 (+1.46) 24.21 (-0.48)	28.65 (+0.39)	34.97 (- 4.18) 47.2 (-22.0)
$(+)_{500}^{CD}$-[Co(aesei-N,O)(en)$_2$]$^{2+}$	17.15 (+1.90)	27.17 (-0.52)	32.26 (-1.25) 45.5 (-21.8)

Table 19. Continued

Compound			
$(+)^{CD}_{500}$-[Co(mea)(en)$_2$]$^{3+}$	20.20 (+3.82)	28.41 (-0.15)	35.46 (+5.92) 47.1 (-27.5)
$(+)^{CD}_{500}$-[Co(eea)(en)$_2$]$^{3+}$	20.20 (+3.08)	28.17 (-0.10)	35.46 (+6.90) 45.9 (-23.1)
$(+)^{CD}_{500}$-[Co(bea)(en)$_2$]$^{3+}$	20.04 (+2.54) 23.53 (-0.02)		35.09 (+5.57) 47.2 (-37.6)
$(+)^{CD}_{500}$-[Co(mseea)(en)$_2$]$^{3+}$	19.80 (+3.55)	25.97 (+0.10)	33.90 (+3.98) 46.3 (-20.8)
$(+)^{CD}_{500}$-[Co(eseea)(en)$_2$]$^{3+}$	19.76 (+2.87)	25.97 (+0.08)	33.90 (+3.05) 45.7 (-16.8)
$(+)^{CD}_{500}$-[Co(bseea)(en)$_2$]$^{3+}$	19.61 (+2.15) 22.47 (-0.15)	26.32 (+0.07)	33.56 (+2.85) 46.3 (-37.2)

Wave numbers and $\Delta\varepsilon$ values (in parentheses) are given 10^3 cm^{-1} and mol^{-1} dm^3 cm^{-1}, respectively. Sh denotes a shoulder.

isomers show a positive CD band at lower energy in the first absorption band region, while in the sulfenato charge transfer band region (ca. 27×10^3 cm^{-1}), the $(+)_{500}^{CD} \cdot (+)_{360}^{CD}$ isomer shows a positive CD band and the $(+)_{500}^{CD} \cdot (-)_{360}^{CD}$ isomer a negative one (Fig. 12). This CD spectral behavior is consistent with that of the Λ-(S)- and Λ-(R)-[Co(L-cysteinesulfenato-N,S)(en)$_2$]$^{2+}$,[2b) and then the $(+)_{500}^{CD} \cdot (+)_{360}^{CD}$ and $(+)_{500}^{CD} \cdot (-)_{360}^{CD}$ aese isomers can be assigned to the Λ-(S) and Λ-(R) configuration, respectively. In contrast to the fact that the two isomers, Λ-(R) and Λ-(S), were formed for [Co(aese)(en)$_2$]$^{2+}$ (Λ-(R) : Λ-(S) = 3 : 1), $(+)_{500}^{CD} \cdot (-)_{360}^{CD}$-[Co(aesee)(en)$_2$]$^{2+}$ was selectively formed by the oxidation reaction of Λ-$(+)_{500}^{CD}$-[Co(aes)(en)$_2$]$^{2+}$. The $(+)_{500}^{CD} \cdot (-)_{360}^{CD}$ aesee isomer shows a quite similar CD spectrum to that of the Λ-(R) aese isomer (Fig. 12). Therefore, it is suggested that the $(+)_{500}^{CD} \cdot (-)_{360}^{CD}$ aesee isomer takes the Λ-(R) configuration. This stereoselectivity suggests that there is an intramolecular hydrogen bond between the selenenato or sulfenato oxygen atom and the adjacent amine proton in Λ-(R)-[Co(aesee or aese)(en)$_2$]$^{2+}$ and its hydrogen bond stabilizes the Λ-(R) configuration. The hydrogen bond is more favorable for the Λ-(R) aesee isomer than the Λ-(R) aese one, because the bond lengths of Co-Se and Se-O are longer than those of Co-S and S-O, respectively, as mentioned in Chapter V-A.

The $(+)_{500}^{CD}$ mseea, eseea, and bseea isomers, which were derived from Λ-$(+)_{500}^{CD}$-[Co(aes)(en)$_2$]$^{2+}$, show a positive CD band (ca. 19.7×10^3 cm^{-1}), whose intensity decreases with the

order of the mseea, eseea, and bseea isomers, though the bseea
isomer shows a weak negative CD band at the higher energy side
in the first absorption band region (Figs. 14). A similar CD
spectral behavior is observed for a series of the corresponding
$(+)_{500}^{CD}$ thioether isomers (Fig. 15). Taking these facts and
the assignment of the $(+)_{500}^{CD}$ mea and eea isomers[4] into
consideration, the $(+)_{500}^{CD}$ mseea, eseea, bseea, and bea isomers
are assigned to the Λ configuration. The ^{1}H NMR spectrum of
the $(+)_{500}^{CD}$ mseea isomer exhibits a single peak in the methyl
protons region (2.26 ppm from DSS) and that of the $(+)_{500}^{CD}$ eseea
isomer one set of triplet peaks (centered at 1.57 ppm). The
$(+)_{500}^{CD}$ bseea isomer shows a single peak due to the aromatic
protons (7.52 ppm). The ^{1}H NMR spectral behavior of the
selenoether isomers is in line with that of the corresponding
thioether isomers.[4,5] Molecular model constructions of the
selenoether and thioether complexes reveal that the (R)
configuration is preferable for the Λ isomer, because the Se-
or S-alkyl group in the Λ-(S) configuration have a nonbonding
interaction with the adjacent ethylenediamine chelate ring.
Moreover, the X-ray structural analysis indicates that the
$(+)_{500}^{CD}$ mseea isomer takes the Λ-(R) configuration (Chapter V-
A-2). Based on these results, it is suggested that all of the
$(+)_{500}^{CD}$ selenoether and thioether isomers take selectively the
Λ-(R) configuration in solution. In the charge transfer band
region, the Λ-(R) selenoether and thioether isomers show one
positive CD band, while Λ-[Co(aes)(en)$_2$]$^{2+}$, Λ-[Co(aet)(en)$_2$]$^{2+}$,

and Λ-[Co(aesi)(en)$_2$]$^{2+}$, which has no chirality due to the chalcogen donor atoms show a negative one (Figs. 11 and 13-16). This fact suggests that the CD band in this region is contributed by not only the configurational chirality due to the skew pair of chelate rings but also the chirality of the asymmetric selenium or sulfur donor atom.

As shown in Fig. 16, the O-bonded seleninato isomer, $(+)_{500}^{CD}$-[Co(aesei-N,O)(en)$_2$]$^{2+}$, which is the oxidation product of Λ-$(+)_{500}^{CD}$-[Co(aes)(en)$_2$]$^{2+}$, shows a positive CD band in the first absorption band region. This CD spectrum is enantiometric to that of the spontaniously resolved Λ-$(-)_{500}^{CD}$ aesei-N,O isomer, whose absolute configuration was determined by X-ray analytical study (Chapter V-A-1). These facts suggest that no isomeriza-tion occured during the oxidation procedure and the $(+)_{500}^{CD}$ aesei-N,O isomer takes the Λ configuration. The ^{13}C NMR spectrum of Λ-$(+)_{500}^{CD}$-[Co(aesei-N,O)(en)$_2$]$^{2+}$ exhibits ten peaks for the six carbon atoms of the complex (Fig. 22 and Table 20). Only recently, Yamanari et al. reported the separation of the two diastereomers, Λ-(R) and Λ-(S), for the corresponding O-bonded sulfinato complex , [Co(aesi-N,O)(en)$_2$]$^{2+}$, by use of a SP-Sephadex column, and each of the two diastereomers showed five ^{13}C NMR signals (Table 20).[13] The ^{13}C NMR spectral behavior of the Λ-$(+)_{500}^{CD}$ aesei-N,O isomer is in good agreement with that of a mixture of the Λ-(R) and Λ-(S) aesi-N,O isomers. Therefore, the Λ-$(+)_{500}^{CD}$ aesei-N,O isomer is assigned to take a mixture of the (R) and (S) configurations in solution. It is
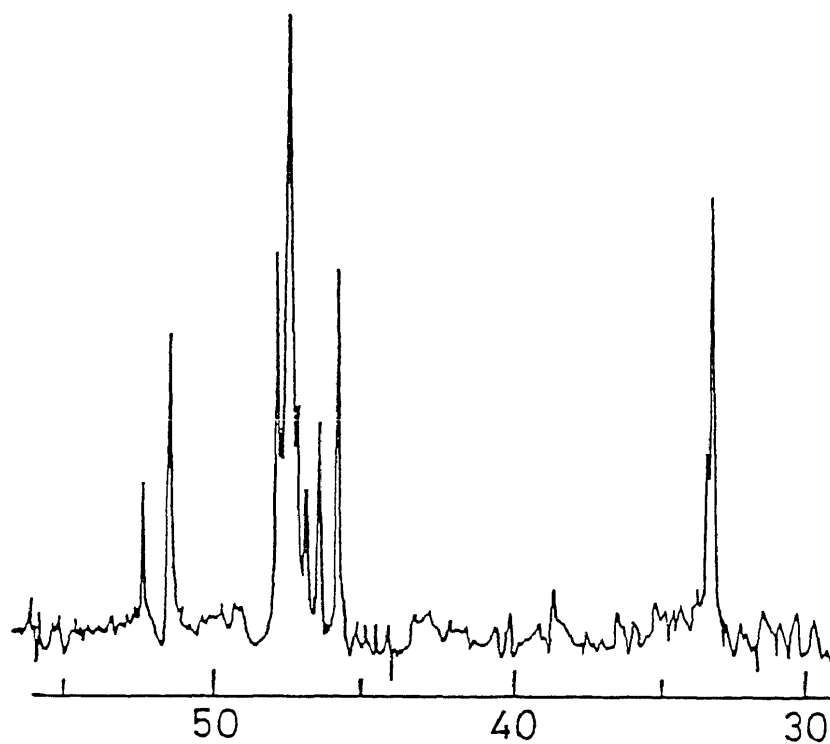
Figure 22. ^{13}C NMR spectrum of Λ-(+)$_{500}^{CD}$-[Co(aesei-N,O)(en)$_2$]$^{2+}$.

Table 20. ^{13}C NMR datum of $\Lambda-(+)_{500}^{CD}-[Co(aesei-N,O)(en)_2]^{2+}$.

Complex	δ from DSS
$\Lambda-(+)_{500}^{CD}-[Co(aesei-N,O)(en)_2]^{2+}$	32.94(2)
	33.10(1)
	45.45(2)
	46.10(1)
	46.53(1)
	46.86(2)
	47.08(4)
	47.51(2)
	51.09(2)
	51.95(1)
$\Lambda-(R)-[Co(aesi-N,O)(en)_2]^{2+}$ a)	28.53(1)
	43.83(1)
	45.51(2)
	45.87(1)
	51.77(1)
$\Lambda-(S)-[Co(aesi-N,O)(en)_2]^{2+}$ a)	28.78(1)
	44.48(1)
	44.97(1)
	45.62(2)
	52.20(1)

a) Ref. 13(δ from Me_4Si). The values in parentheses show the relative intensity.

probable that the $\Lambda-(+)^{CD}_{500}$ aesei-N,O isomer prefers to the (R) configuration, because there is an intramolecular hydrogen bond between the pendant oxygen atom and the adjacent amine proton in this configuration. This is supported by the fact that the spontaniously resolved $\Delta-(-)^{CD}_{500}-[Co(aesei-N,O)(en)_2]^{2+}$ takes the (S) configuration in crystal (Chapter V-A-1). Taking these facts and the peak hight of the ^{13}C NMR spectrum of the $\Lambda-(+)^{CD}_{500}$ aesei-N,O isomer into consideration, it is suggested that the ratio of the two isomers, $\Lambda-(R)$: $\Lambda-(S)$, is about 2 : 1 in solution. However the two aesei-N,O isomers, $\Lambda-(R)$ and $\Lambda-(S)$, could not be separated by use of a SP-Sephadex column, in contrast to the case of the corresponding aesi-N,O isomers. Furthermore, the spontaniously resolved $(+)^{CD}_{500}$ aesei-N,O isomer showed a decrease in CD intensity (ca. 12 %) with time in a short period (ca. 10 min), during which time no change in the absorption spectrum was noticed. These facts suggest that the inversion at selenium in $[Co(aesei-N,O)(en)_2]^{2+}$ occurs much faster than that at sulfur in $[Co(aesi-N,O)-(en)_2]^{2+}$.[13)]

V-C-2. Bis(trimethylenediamine)cobalt(III) Complexes.

The CD spectra of the bis(trimethylenediamine)cobalt(III) complexes with a selenium- or sulfur-containing ligand are shown in Figs. 17-21, together with those of the corresponding bis(ethylenediamine) complexes. Their data are summarized in Table 21.

Table 21. CD data of bis(trimethylenediamine)cobalt(III) complexes.

Complex	First band	Second band	Charge transfer band
$(+)^{CD}_{600}$-[Co(aet)(tn)$_2$]$^{2+}$	16.67 (+0.70) 19.23 (-0.46) 22.08 (+1.13)	30.21 (-1.30)	34.42 (-8.72) 43.1 (-7.0)
$(+)^{CD}_{600}$-[Co(aes)(tn)$_2$]$^{2+}$	15.70 (+0.43) 18.45 (-0.36) 20.79 (+0.76)	24.41 (-0.89)	32.68 (-7.56) 45.5 (-6.6)
$(+)^{CD}_{550}\cdot(+)^{CD}_{370}$-[Co(aese)(tn)$_2$]$^{2+}$	19.67 (+2.25)		26.81 (+16.71) 35.34 (-17.95) 44.76 (-14.2)
$(+)^{CD}_{550}\cdot(-)^{CD}_{370}$-[Co(aese)(tn)$_2$]$^{2+}$	18.38 (+0.85) 20.70 (-1.48)		27.03 (-20.18) 35.27 (+15.26) 44.3 (-6.1)
$(+)^{CD}_{500}$-[Co(aesi-N,S)(tn)$_2$]$^{2+}$	21.51 (+0.33)		33.56 (-5.45) 41.67 (-6.6)
$(+)^{CD}_{550}$-[Co(aesei-N,O)(tn)$_2$]$^{2+}$	18.15 (+0.69) 21.23 (-0.18)		32.47 (-3.12) 40.49 (-9.14) 45.7 (+6.4)
$(+)^{CD}_{550}$-[Co(mea)(tn)$_2$]$^{3+}$	19.23 (+3.14) 22.47 (-0.11)	29.4 (-0.43sh)	34.13 (+5.68) 41.32 (-18.4)
$(+)^{CD}_{550}$-[Co(mseea)(tn)$_2$]$^{3+}$	18.80 (+2.57) 21.98 (-0.18)		32.15 (+2.31) 41.59 (-17.2)

Table 21. Continued

Wave numbers and $\Delta\varepsilon$ values (in parentheses) are given in 10^3 cm^{-1} and mol^{-1} dm^3 cm^{-1}, respectively. Sh denotes a shoulder.

The Δ and Λ isomers are possible for each of [Co(aet)-(tn)$_2$]$^{2+}$, [Co(aes)(tn)$_2$]$^{2+}$, and [Co(aesi)(tn)$_2$]$^{2+}$. As shown in Fig. 17, the CD spectrum of $(+)_{600}^{CD}$-[Co(aet)(tn)$_2$]$^{2+}$ agrees well with that of Λ-[Co(aet)(en)$_2$]$^{2+}$, except for the two bands at higher energy in the first absorption band region (ca. 19 and 22 x 10^3 cm^{-1}). Furthermore, the stoichiometric oxidation of $(+)_{600}^{CD}$-[Co(aet)(tn)$_2$]$^{2+}$ generated Λ-(R)- and Λ-(S)-[Co(aese)-(tn)$_2$]$^{2+}$ (vide infra), as in the oxidation reaction of Λ-[Co-(aet)(en)$_2$]$^{2+}$ (Chapter V-C-1). These facts suggest that the starting thiolato complex, $(+)_{600}^{CD}$-[Co(aet)(tn)$_2$]$^{2+}$, takes the Λ configuration. As shown in Fig. 17, $(+)_{600}^{CD}$-[Co(aes)(tn)$_2$]$^{2+}$ exhibits a CD spectrum quite similar to that of Λ-$(+)_{600}^{CD}$-[Co-(aet)(tn)$_2$]$^{2+}$ over the whole region, and then can be assigned to the Λ configuration. The $(+)_{500}^{CD}$ aesi isomer, which is the oxidation product of Λ-$(+)_{600}^{CD}$-[Co(aet)(tn)$_2$]$^{2+}$, shows a positive CD band in the first absorption band region (Fig. 18), being also assigned to the Λ configuration. These facts indicate that the oxidation reaction for the starting thiolato complex proceeded with retention of its absolute configuration, as in the case for the bis(ethylenediamine)cobalt(III) complexes (Chapter V-C-1). In the present bis(trimethylenediamine)-cobalt(III) complexes, Λ-[Co(aet)(tn)$_2$]$^{2+}$, Λ-[Co(aes)(tn)$_2$]$^{2+}$, and Λ-[Co(aesi)(tn)$_2$]$^{2+}$, which has no chirality due to the coordinated chalcogen atom, commonly show a negative CD band in the chalcogen-to-metal charge transfer band region, similar to that of the corresponding bis(ethylenediamine) complexes,

though the CD spectra in the first absorption band region are different from one another (Fig. 17 and 18). This may suggest that the configurational chirality due to the skew pair of chelate ring can be deduced from the CD sign in the chalcogen-to-metal charge transfer band region as for the bis(diamine)-cobalt(III) complexes with the aet, aes, or aesi ligand.

Taking the asymmetric chalcogen donor atom, (R) and (S), into consideration, four isomers, Δ-(R), Δ-(S), Λ-(R), and Λ-(S), are possible for each of $[Co(aese)(tn)_2]^{2+}$, $[Co(mea)-(tn)_2]^{3+}$, and $[Co(mseea)(tn)_2]^{3+}$. The two isomers, $(+)_{550}^{CD} \cdot (+)_{370}^{CD}$- and $(+)_{550}^{CD} \cdot (-)_{370}^{CD}$-$[Co(aese)(tn)_2]^{2+}$, which are formed by the stoichiometric oxidation reaction of $(+)_{600}^{CD}$-$[Co(aet)-(tn)_2]^{2+}$ with aqueous H_2O_2, show the CD spectra quite similar to those of Λ-(S)- and Λ-(R)-$[Co(aese)(en)_2]^{2+}$, respectively, over the whole region (Fig. 19). This fact suggests that the $(+)_{550}^{CD} \cdot (+)_{370}^{CD}$ and $(+)_{550}^{CD} \cdot (-)_{370}^{CD}$ aese isomers take the Λ-(S) and Λ-(R) configurations, respectively. This assignment is confirmed by comparing the vicinal CD due to the asymmetric sulfur atom and the configurational CD due to the skew pair of chelate rings for $[Co(aese)(tn)_2]^{2+}$ with those for $[Co(aese)-(en)_2]^{2+}$. Figure 23 shows the (S) vicinal and the Λ configurational CD curves calculated from the observed CD curves of Λ-(R) and Λ-(S)-$[Co(aese)(tn)_2]^{2+}$, together with those calculated from Λ-(R)- and Λ-(S)-$[Co(aese)(en)_2]^{2+}$. The (S) vicinal CD curves for $[Co(aese)(tn)_2]^{2+}$ is quite similar to that for $[Co(aese)(en)_2]^{2+}$, showing two bands, (-)
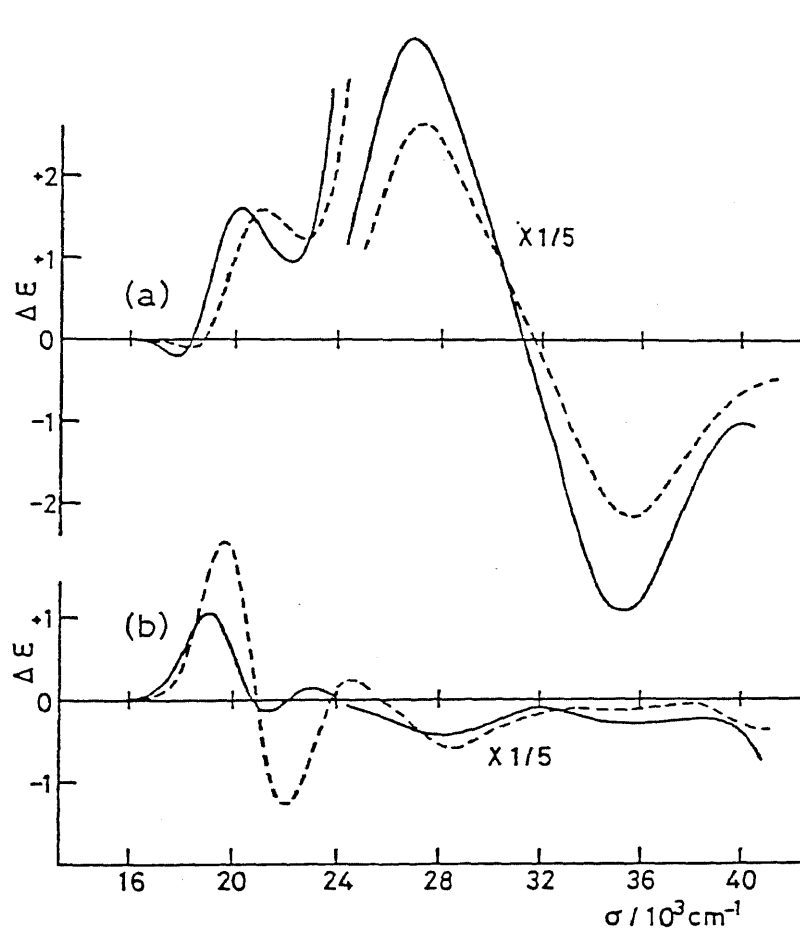
Figure 23. (a): Vicinal CD curves ($\Delta\varepsilon[(S)] = 1/2\{\Delta\varepsilon[\Lambda-(S)] - \Delta\varepsilon[\Lambda-(R)]\}$) of [Co(aese)(tn)$_2$]$^{2+}$ (———) and [Co-(aese)(en)$_2$]$^{2+}$ (-----). (b): Configurational CD curves ($\Delta\varepsilon[\Lambda] = 1/2\{\Delta\varepsilon[\Lambda-(S)] + \Delta\varepsilon[\Lambda-(R)]\}$) of [Co-(aese)(tn)$_2$]$^{2+}$ (———) and [Co(aese)(en)$_2$]$^{2+}$ (-----).

and (+), from lower energy in the first absorption band region, and two intense band, (+) and (-), from lower energy in the sulfur-to-metal charge transfer band region. A similar relation is also observed for the Λ configurational CD curves; the dominant positive CD band is observed at the lower energy side of the first absorption band region and a negative band in the sulfenato charge transfer band region (ca. 28×10^3 cm^{-1}), though the CD intensity for $[Co(aese)(tn)_2]^{2+}$ is weaker than that for $[Co(aese)(en)_2]^{2+}$ in the first absorption band region. The formation ratio of the two isomers, $\Lambda-(R) : \Lambda-(S)$, is about 5 : 6 for $[Co(aese)(tn)_2]^{2+}$, and this ratio is in contrast to the case for $[Co(aese)(en)_2]^{2+}$ ($\Lambda-(R) : \Lambda-(S) =$ 3 : 1). This may be due to the absence of the effective intramolecular hydrogen bond between the sulfenato oxygen atom and the adjacent amine proton in $[Co(aese)(tn)_2]^{2+}$, because of the flexibility of the six-membered trimethylene-diamine chelate ring.

Each of $(+)^{CD}_{550}-[Co(mea)(tn)_2]^{3+}$ and $(+)^{CD}_{550}-[Co(mseea)-(tn)_2]^{3+}$, which is the methylation product of $\Lambda-[Co(aet)-(tn)_2]^{2+}$ and $\Lambda-[Co(aes)(tn)_2]^{2+}$, respectively, shows a major positive CD band in the first absorption band region, as well as $\Lambda-(+)^{CD}_{500}-[Co(mea)(en)_2]^{3+}$ and $\Lambda-(+)^{CD}_{500}-[Co(mseea)(en)_2]^{3+}$ (Figs. 13 and 20). Therefore, it is suggested that no isomerization occurs during the methylation procedure and the $(+)^{CD}_{550}$ mea and mseea isomers take the Λ configuration. As shown in Fig. 24, the ^1H NMR spectrum of $\Lambda-(+)^{CD}_{550}-[Co(mea)-$
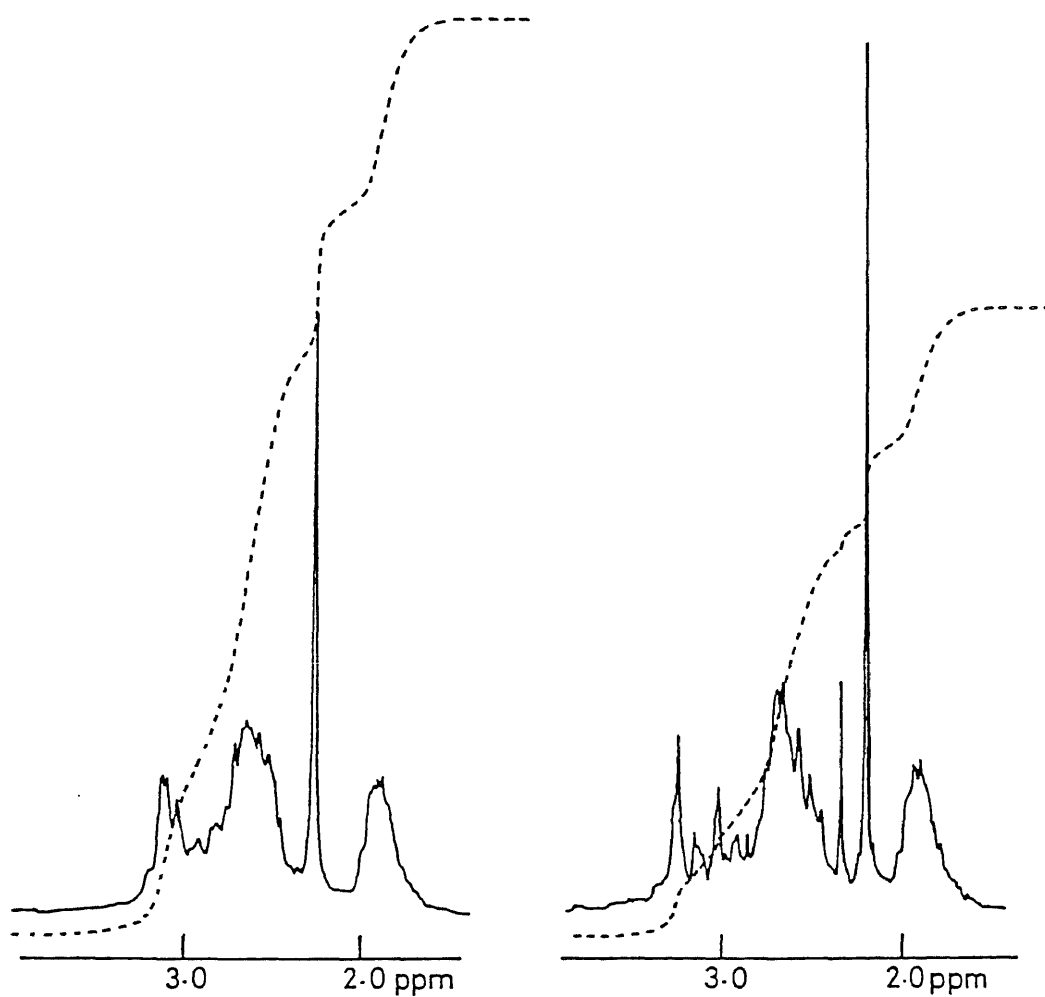
Figure 24. ^1H NMR spectra of $\Lambda-(+)\frac{CD}{550}-[Co(mea)(tn)_2]^{3+}$ (left) and $\Lambda-(+)\frac{CD}{550}-[Co(mseea)(tn)_2]^{3+}$ (right).

$(tn)_2]^{3+}$ exhibits a single peak in the methyl protons region (2.26 ppm from DSS), suggesting that the $\Lambda-(+)\frac{CD}{550}$ mea isomer takes either the (R) or (S) configuration in solution. It is probable that the $\Lambda-(+)\frac{CD}{550}$ mea isomer prefers to the (R) configuration as $\Lambda-(+)\frac{CD}{500}-[Co(mea)(en)_2]^{3+}$ (Chapter V-C-1), because there is a nonbonded interaction between the methyl group and the adjacent diamine chelate ring when $\Lambda-[Co(mea)-(tn)_2]^{3+}$ takes the (S) configuration. In the sulfur-to-metal charge transfer band region, $\Lambda-(+)\frac{CD}{550}-[Co(mea)(tn)_2]^{3+}$ shows a positive CD band similar to that of $\Lambda-(R)-[Co(mea)(en)_2]^{2+}$ (Fig. 20). The CD sign in this region is closely related to the chirality due to the chalcogen donor atom as mentioned in Chapter V-C-1. From these facts, it is suggested that $(+)\frac{CD}{550}-[Co(mea)(tn)_2]^{3+}$ takes selectively the $\Lambda-(R)$ configuration in solution. For $\Lambda-(+)\frac{CD}{550}-[Co(mseea)(tn)_2]^{3+}$, the ^1H NMR spectrum shows two peaks in the methyl protons region (2.19 and 2.32 ppm, in the ratio 4 : 1)(Fig. 24). This indicates that the $\Lambda-(+)\frac{CD}{550}$ mseea isomer takes a mixture of the $\Lambda-(R)$ and $\Lambda-(S)$ configurations in solution, contrary to the case of $\Lambda-(+)\frac{CD}{550}-[Co(mea)(tn)_2]^{3+}$, although the (R) configuration seems to be dominant for the $\Lambda-(+)\frac{CD}{550}$ mseea isomer. It is considered that the nonbonded interaction between the methyl group and the adjacent diamine chelate ring in $\Lambda-(S)-[Co(mseea)(tn)_2]^{3+}$ is not so conspicuous as that in $\Lambda-(S)-[Co(mea)(tn)_2]^{3+}$, because of the longer bond lengths of Co-Se and Se-C than those of Co-S and S-C (Chapter

V-A-2). The CD spectrum of Λ-(+)$_{550}^{CD}$-[Co(mseea)(tn)$_2$]$^{3+}$ shows

a positive band in the chalcogen-to-metal charge transfer band

region (ca. 32 x 10^3 cm^{-1}) as well as Λ-(R)-[Co(mea)(tn)$_2$]$^{3+}$,

though the CD intensity of the former is weaker than that of

the latter (Fig. 20). This supports that the Λ-(+)$_{550}^{CD}$ mseea

isomer has dominantly the (R) configuration, because a negative

CD band will appear in the chalcogen-to-metal charge transfer

band region if not so (Chapter V-C-3). The Λ-(+)$_{550}^{CD}$ mseea

isomer chromatographed on SP-Sephadex column gave only one

adsorbed band and all of its fractions showed the same CD

spectra in the whole region. This suggests that the inversion

at selenium in Λ-(+)$_{550}^{CD}$-[Co(mseea)(tn)$_2$]$^{3+}$ occurs as in the

case for thioether and selenoether cobalt(III) complexes.[1c,36]

As shown in Fig. 21, the (+)$_{550}^{CD}$ aesei-N,O isomer, which

is the oxidation product of Λ-(+)$_{600}^{CD}$-[Co(aes)(tn)$_2$]$^{2+}$, shows

a major positive CD band in the first absorption band region,

though a weak negative CD band appears at higher energy in

this region. This CD spectral behavior is quite similar to

that of Λ-[Co(gly)(tn)$_2$]$^{2+}$.[35b] These facts suggest that no

isomerization occured during the oxidation procedure as in the

case of the bis(ethylenediamine)cobalt(III) complexes and the

(+)$_{550}^{CD}$ aesei isomer takes the Λ configuration. In the O-bonded

seleninato charge transfer band region (ca. 32 x 10^3 cm^{-1}), the

Λ-(+)$_{550}^{CD}$ aesei-N,O isomer exhibits a negative CD band similar to

that of Λ-(+)$_{500}^{CD}$-[Co(aesei-N,O)(en)$_2$]$^{2+}$. This may suggest

that the Λ-(+)$_{550}^{CD}$ aesei-N,O isomer takes a mixture of the (R)

and (S) configuration in solution as well as $\Lambda-(+)_{500}^{CD}$-[Co-(aesei-N,O)(en)$_2$]$^{2+}$ (Chapter V-C-1).

V-D. Protonation Equilibria.

V-D-1. Protonation Equilibrium of the Selenenato Complex.

The selenenato complex, $[Co(aesee)(en)_2]^{2+}$, shows the instantaneous and reversible absorption spectral change with pH change of the solution and an isosbestic point is observed at 328 nm. The intensity of the characteristic selenenato charge transfer band at 27.55×10^3 cm^{-1} decreases with the increasing acid concentration $(HClO_4)$, as in the case of the corresponding sulfenato complex, $[Co(aese)(en)_2]^{2+}$.[6,11] Accordingly, the Se-bonded selenenate ligand seems to be protonated on the pendant oxygen atom. The value of the protonation constant (pKa) at 25°C, $\mu = 1.0$ mol dm^{-3} $(NaClO_4)$, is calculated from the following equation:

$$pKa = - \log \gamma_H + pH_{meas} - \log\{(A_{HL} - A) / (A - A_{L^-})\}$$

where A_{HL} and A_{L^-} are the absorbances of acid and base, respectively, and A is the absorbance containing both of them. The γ_H is the activity coefficient of hydrogen ion and the value, $- \log \gamma_H = 0.13$, is calculated by the Debye-Hückel equation.[37] The value of pH_{meas} at $- \log\{(A_{HL} - A)/(A - A_{L^-})\}$ = 0 is determined to 3.36 ± 0.07 by least-squares treatment from Fig. 25. As a result, the value of pKa can be determined to be 3.49 ± 0.07. This value indicates that the selenenate ligand of $[Co(aesee)(en)_2]^{2+}$ is at least 10^3-fold more basic than the sulfenato ligand of $[Co(aese)(en)_2]^{2+}$ (pKa = 0.15 ± 0.07, at 25°C, $\mu = 4.0$ mol dm^{-3} $(LiClO_4)$).[6] Therefore, the
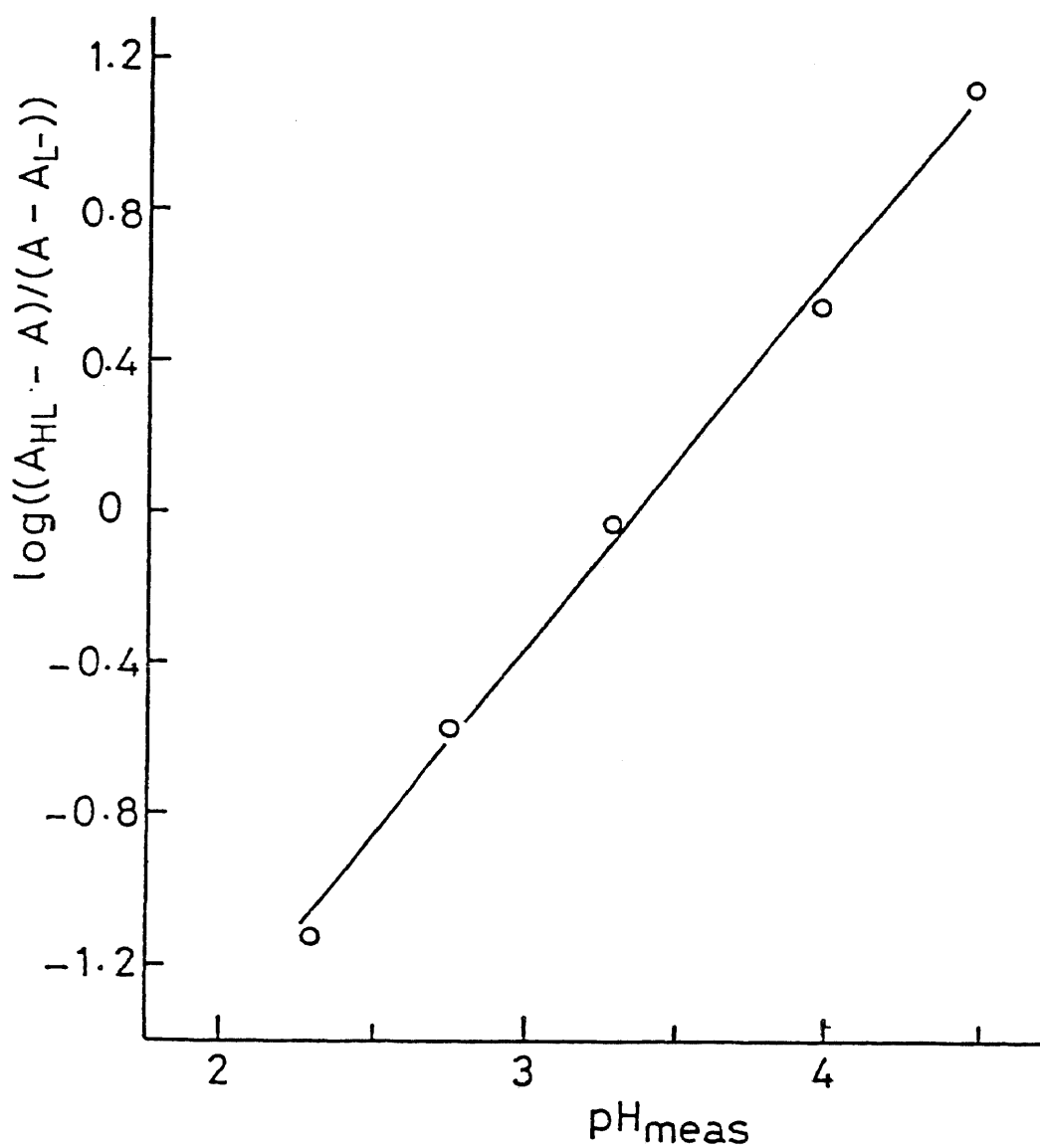
Figure 25. Relation between pH_{meas} and log $\{(A_{HL} - A)/(A - A_{L}-)\}$ of $[Co(aesee)(en)_2]^{2+}$ (absorbance at 305 nm).

aesee and aese complexes give the protonated complexes, [Co-(Haesee)(en)$_2$]$^{3+}$ and [Co(Haese)(en)$_2$]$^{3+}$, in 70 % HClO$_4$ solution, respectively.

The absorption and CD spectra of the Haesee and Haese complexes derived from Λ-(R)-[Co(aesee)(en)$_2$]$^{2+}$ and Λ-(R)- and Λ-(S)-[Co(aese)(en)$_2$]$^{2+}$, respectively, are shown in Fig. 26(a) and their data are summarized in Table 22. The charge transfer band at ca. 27.5 x 10^3 cm^{-1}, which is characteristic of the selenenato and sulfenato complexes, disappears in the protonated complexes. These complexes show the absorption spectra quite similar to those of the corresponding selenoether and thioether complexes, though the former complexes exhibit the first absorption bands at higher energy and the charge trnasfer bands at lower energy than the latter complexes (Figs. 13-15 and 26(a)).

The CD pattern for each of the Haese isomers derived from the Λ-(R) and Λ-(S) aese isomers coincides well with that of the parental aese isomers in the first absorption band region (Figs. 12 and 26(a)). Furthermore, the CD spectral change for each of the two aese isomers is instantaneous and reversible with pH change as well as the absorption spectral one. Therefore, no inversion occurs for the aese isomers during the protonation reaction, namely, the two Haese isomers take the same absolute configuration as the parental aese isomers. The Λ-(R) and Λ-(S) Haese isomers show almost enantiometric CD bands in the sulfur-to-metal charge transfer band region (ca.
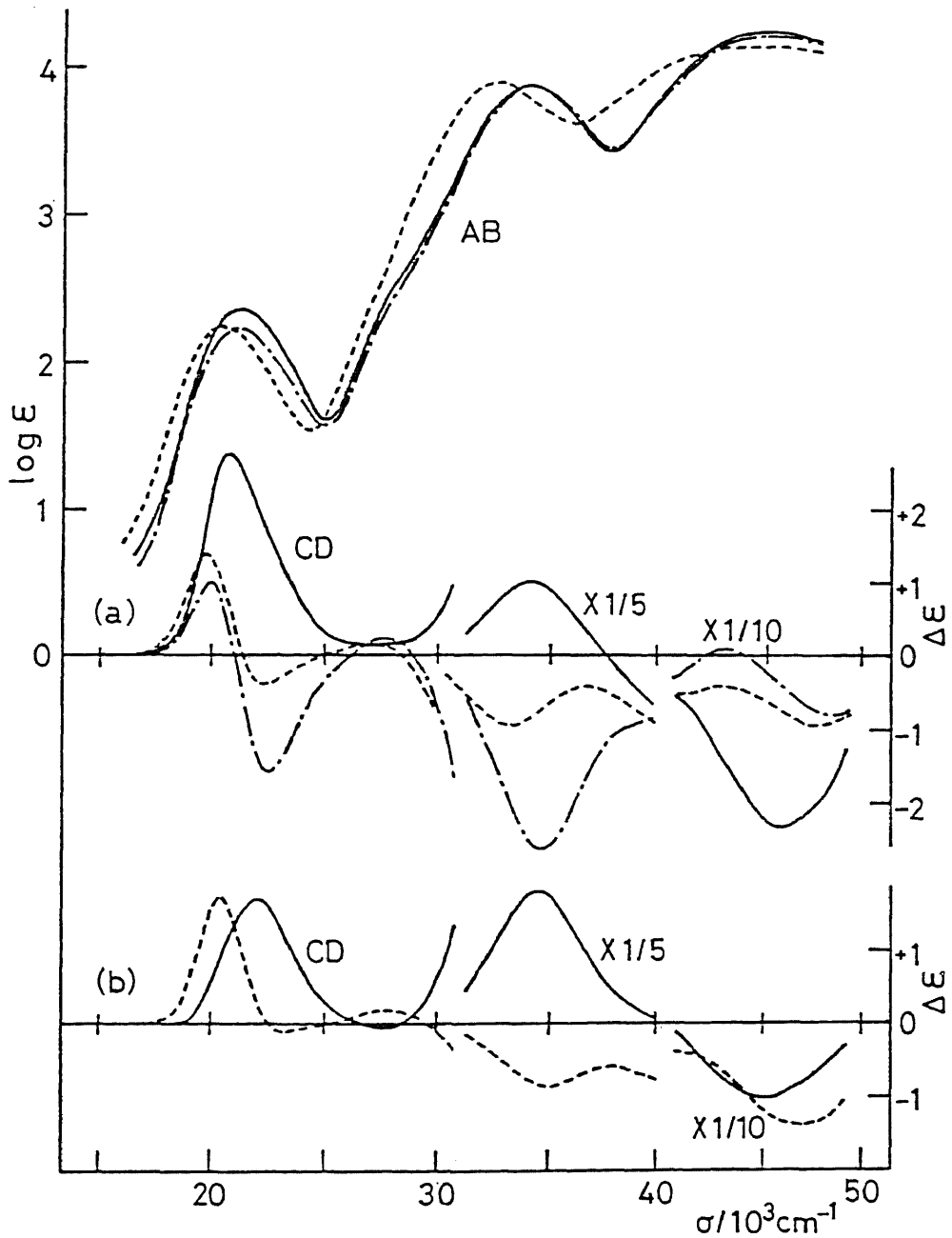
Figure 26. (a); Absorption and CD spectra of Λ-(S)-[Co(Haese)-

(en)$_2$]$^{3+}$ (————), Λ-(R)-[Co(Haese)(en)$_2$]$^{3+}$ (—·—·—),

and Λ-[Co(Haesee)(en)$_2$]$^{3+}$ (—————). (b); Vicinal CD

curve of (S)-sulfur (————) and Λ configurational CD

curve (—————) of [Co(Haese)(en)$_2$]$^{3+}$.

Table 22. Absorption and CD data of Λ-(R)- and Λ-(S)-[Co(Haese)(en)$_2$]$^{3+}$ and (+)$_{500}^{CD}$-[Co(Haesee)(en)$_2$]$^{3+}$.

Complex	Absorption maxima $\sigma/10^3$ cm^{-1} (logε/mol^{-1} dm^3 cm^{-1})		CD extrema $\sigma/10^3$ cm^{-1} ($\Delta\varepsilon$/mol^{-1} dm^3 cm^{-1})	
Λ-(S)-[Co(Haese)(en)$_2$]$^{3+}$	21.21	(2.37)	20.83	(+2.78)
	34.07	(3.88)	34.25	(+5.04)
	45.15	(4.27)	45.8	(-10.2)
Λ-(R)-[Co(Haese)(en)$_2$]$^{3+}$	21.16	(2.23)	19.96	(+1.01)
	34.25	(3.87)	22.52	(-1.60)
	45.35	(4.23)	27.62	(+0.24)
			34.72	(-13.19)
			39.5	(-4.4sh)
			43.1	(+1.0)
			47.2	(-8.2)
(+)$_{500}^{CD}$-[Co(Haesee)(en)$_2$]$^{3+}$	20.53	(2.24)	19.80	(+1.41)
	32.57	(3.90)	22.27	(-0.41)
	45.45	(4.16)	26.88	(+0.16)
			33.06	(-4.72)
			41.15	(-5.10)
			47.6	(-9.4)

Sh denotes a shoulder.

35×10^3 cm^{-1}), indicating that the chirality of the sulfur

donor atom dominate the CD sign in this region. This result

can be applied to the corresponding cobalt(III) complexes with

an asymmetric selenoether or thioether donor atom, because Λ-

(S)-[Co(Haese)(en)$_2$]$^{3+}$ exhibits a CD spectrum quite similar to

that of Λ-(R)-[Co(mseea or mea)(en)$_2$]$^{3+}$ (Figs. 13 and 26(a)),

although the (S)-sulfur atom in the former corresponds

configurationally to the (R)-selenium or -sulfur atom in the

latter. This is also supported from the fact that the vicinal

CD curve of the (S)-sulfur atom calculated from the observed

CD curves of Λ-(R)- and Λ-(S)-[Co(Haese)(en)$_2$]$^{3+}$ shows a

similar CD spectral pattern of trans(tertiary amine N,Se)-

[Co(mseea)(N(CH$_2$CH$_2$NH$_2$)$_3$)]$^{3+}$ whose CD contribution is due to

the (R)-selenium atom (Fig. 26(b)).[26]

Similar instantanious and reversible CD spectral change

is also observed for Λ-(R)-[Co(aesee)(en)$_2$]$^{2+}$. However, the

CD spectrum of the Haesee isomer derived from the Λ-(R) aesee

one differs significantly from that of Λ-(R)-[Co(Haese)(en)$_2$]$^{3+}$

(Fig. 26(a)), though the parental Λ-(R) aesee and Λ-(R) aese

isomers show quite similar CD spectra to each other (Fig. 12).

The CD spectrum of the Haesee isomer agrees well with the Λ

configurational CD curve calculated from the observed CD

curves of Λ-(R)- and Λ-(S)-[Co(Haese)(en)$_2$]$^{3+}$ (Fig. 26(b)),

and furthermore, with the CD spectrum of Λ-[Co(aesi)(en)$_2$]$^{2+}$

which has no chirality due to the sulfur donor atom (Fig. 16).

These facts suggest that the inversion at chiral selenium

occurs and the Haesee isomer takes a mixture of the Λ-(R) and

Λ-(S) configuration in $HClO_4$ solution, because of the abesence

of an intramolecular hydrogen bond which stabilizes the Λ-(R)

configuration (Chapter V-C-1).

V-D-2. Protonation Equilibrium of the Seleninato Complex.

The O-bonded seleninato complex, $[Co(aesei-N,O)(en)_2]^{2+}$,

shows the instantanious and reversible absorption spectral

change with pH change of the solution, as in the case of the

selenenato complex, $[Co(aesee)(en)_2]^{2+}$, and an isosbestic

point is observed at 287 nm. The intensity of the charge

transfer band at ca. 33×10^3 cm^{-1} decreases with the

increasing acid concentration ($HClO_4$), while the first

absorption band little changes. The value of the protonation

constant for $[Co(aesei-N,O)(en)_2]^{2+}$ at 25°C, $\mu = 1.0$ mol dm^{-3}

($NaClO_4$), is determined to be 1.91 ± 0.05 in the same manner

as that for $[Co(aesee)(en)_2]^{2+}$ (Fig. 27)(Chapter V-D-1). The

corresponding sulfinato complex, $[Co(aesi-N,O)(en)_2]^{2+}$, gave

a pKa of $- 0.7$ (8 mol dm^{-3} ($NaClO_4$) uncorrected H^+ activity

coefficient change).[7] This is consistent with the conclusion

that the selenenate ligand is more basic than that of the

sulfenate one, as mentioned in Chapter V-D-1.

The absorption and CD spectra of the Haesei-N,O complex

in 1 mol dm^{-3} $HClO_4$ solution are shown in Fig. 28 and their

data are summarized in Table 23, together with those of the

parental complex, Λ-(+)$_{500}^{CD}$-$[Co(aesei-N,O)(en)_2]^{2+}$. The charge
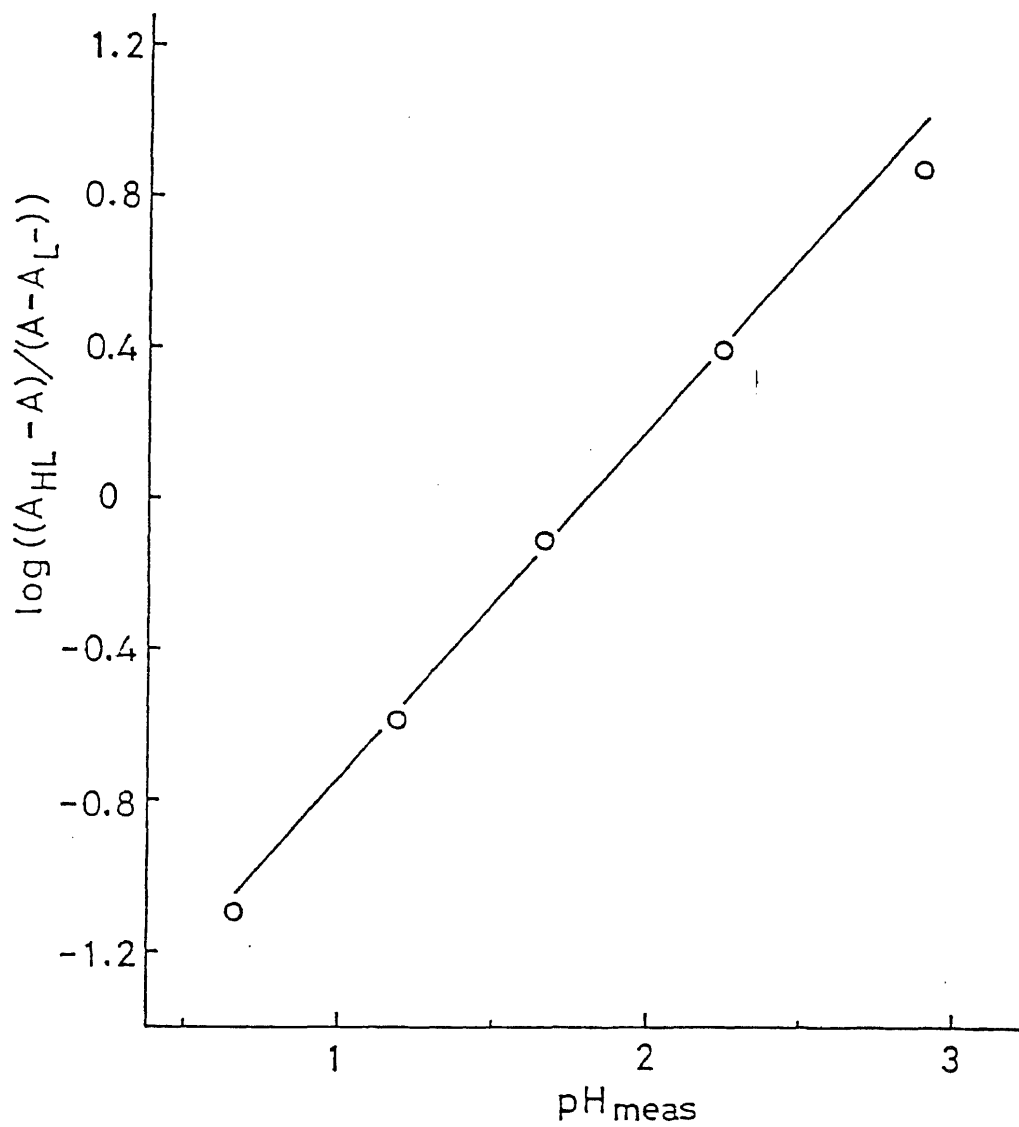
Figure 27. Relation between pH_{meas} and log {$(A_{HL} - A)/(A -$
$A_L-)$} of $[Co(aesei-N,O)(en)_2]^{2+}$ (absorbance at 304 nm).
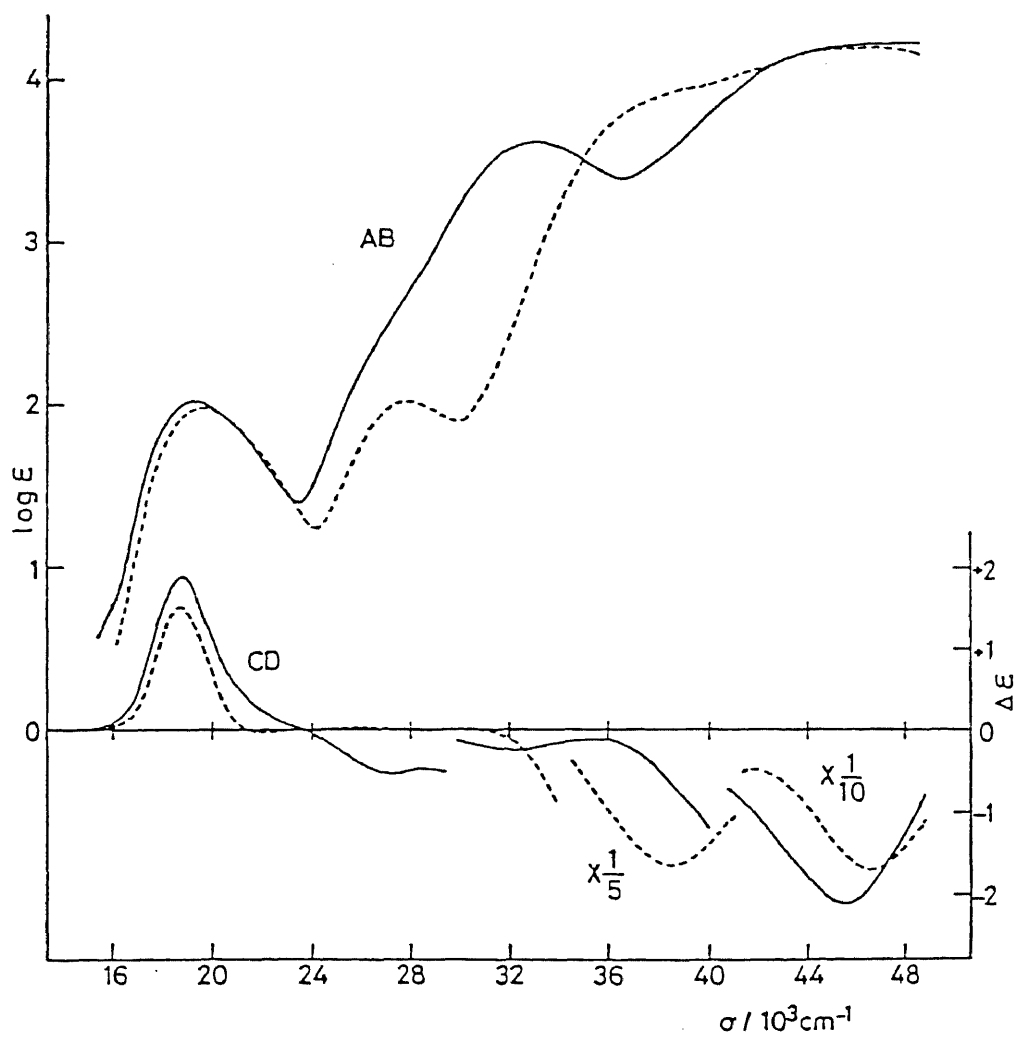
Figure 28. Absorption and CD spectra of $(+)^{CD}_{500}$-[Co(Haesei-

N,O)(en)$_2$]$^{3+}$ (------) and Λ-$(+)^{CD}_{500}$-[Co(aesei-N,O)-

(en)$_2$]$^{2+}$ (———).

Table 23. Absorption and CD data of $(+)_{500}^{CD}$-[Co(Haesei-N,O)(en)$_2$]$^{3+}$.

Complex	Absorption maxima $\sigma/10^3$ cm^{-1} ($\log\epsilon$/mol^{-1} dm^3 cm^{-1})	CD extrema $\sigma/10^3$ cm^{-1} ($\Delta\epsilon$/mol^{-1} dm^3 cm^{-1})
$(+)_{500}^{CD}$-[Co(Haesei)(en)$_2$]$^{3+}$	19.57 (1.98)	18.76 (+1.52)
	27.86 (2.02)	21.88 (-0.11)
	39.1 (3.93sh)	25.97 (+0.05)
	45.45 (4.18)	29.85 (+0.03)
		36.76 (-8.10)
		46.5 (-16.9)

Sh denotes a shoulder.

transfer band at ca. 33×10^3 cm^{-1} disappears in the protonated

complex, which causes the appearence of the second absorption

band at 27.86×10^3 cm^{-1}, and the complex show the new intense

shoulder at ca. 39×10^3 cm^{-1}. On the other hand, the first

absorption band of the protonated complex is quite similar to

that of the parental aesei-N,O complex. The absorption spectral

behavior of the Haesei-N,O complex is in agreement with that

of the O-bonded sulfoxide complex, $[Co(NH_2CH_2CH_2S(CH_3)O-N,O)$

$(en)_2]^{3+}$.[9] Taking these facts into consideration, it is

suggested that the protonation does not occur on the Co-bonded

oxygen atom but on the pendant oxygen one.

The Haesei-N,O isomer derived from $\Lambda-(+)_{500}^{CD}-[Co(aesei-$

N,O)(en)$_2]^{2+}$ shows a major positive CD band in the first

absorption band region and a negative one in the charge

transfer band region (ca. 38×10^3 cm^{-1}). This suggest that

the Haesei-N,O isomer takes the Λ configuration as the parental

$\Lambda-(+)_{500}^{CD}$ aesei-N,O isomer. Figure 29 shows the ^{13}C NMR spectra

of $\Lambda-(+)_{500}^{CD}-[Co(Haesei-N,O)(en)_2]^{3+}$. Nine peaks are observed

for the six carbon atoms of the complex, suggesting that the

$\Lambda-(+)_{500}^{CD}$ Haesei-N,O isomer takes a mixture of the $\Lambda-(R)$ and $\Lambda-$

(S) configurations in HClO$_4$ solution as well as the parental $\Lambda-$

$(+)_{500}^{CD}$ aesei-N,O isomer (Chapter V-C-1). However, the $\Lambda-(+)_{500}^{CD}$

Haesei-N,O isomer seems to have different ratio of the two configura-

tions from the parental isomer, because the relative peak hight

of pairs of ^{13}C peaks for the former is reversed as comparing

to that for the latter (Figs. 22 and 29). This may suggest
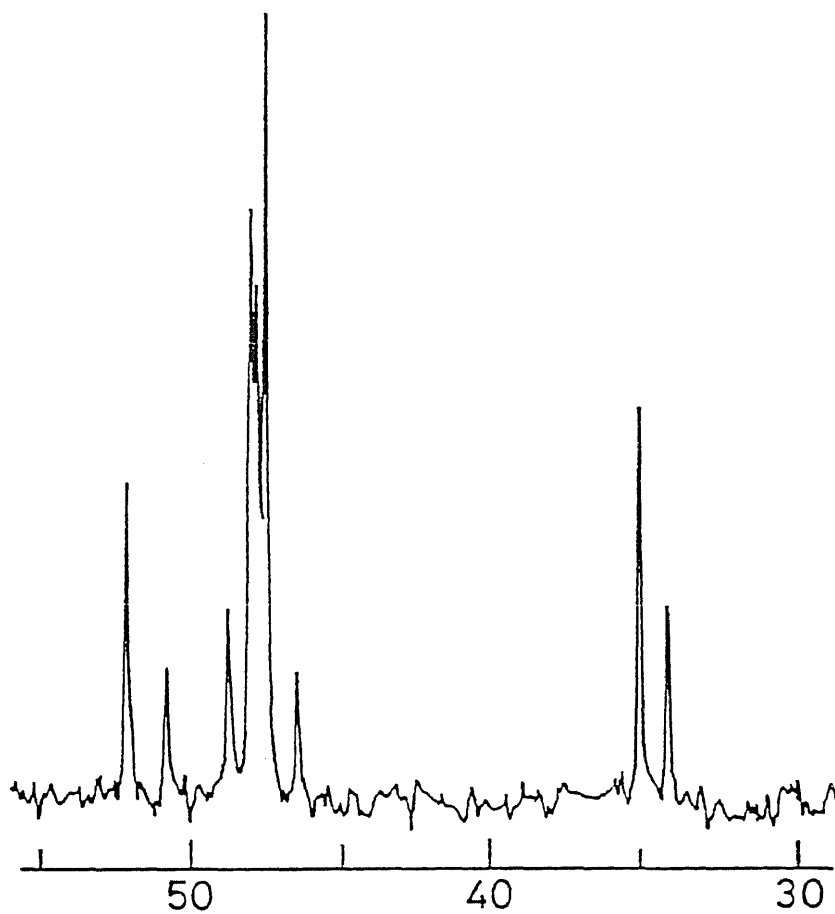
Figure 29. ^{13}C NMR spectrum of $\Lambda-(+)^{CD}_{500}-[Co(Haesei-N,O)(en)_2]^{3+}$.

Table 24. ^{13}C NMR datum of Λ-[Co(Haesei-N,O)(en)$_2$]$^{3+}$.

Complex	δ from DSS
Λ-(+)$_{500}^{CD}$-[Co(Haesei-N,O)(en)$_2$]$^{3+}$	33.91(1)
	34.83(2)
	46.27(1)
	47.35(4)
	47.62(3)
	47.84(3)
	48.59(1)
	50.65(1)
	52.01(2)

The values in parentheses show the relative intensity.

that the inversion at chiral selenium occurs during the protonation reaction and the hydroxyl group takes dominantly the more stable equatorial orientation, because of the absence of an intramolecular hydrogen bond which stabilizes the Λ-(R) configuration (Chapter V-C-1).

Concluding Remarks

(1)   Bis(ethylenediamine)- and bis(trimethylenediamine)-
cobalt(III) complexes with a selenium-containing ligand have
been prepared for the first time, together with corresponding
cobalt(III) complexes with a sulfur-containing ligand.   The
selenolato and thiolato complexes, $[Co(aes)(diamine)_2]^{2+}$ and
$[Co(aet)(diamine)_2]^{2+}$, have been prepared by the reduction of
organic diselenide and disulfide, respectively, with diamine-
cobalt(II) mixture solution, and then optically resolved by the
fractional crystallization of the diastereomers with $[Sb_2(d$-
$tart)_2]^{2-}$.   The other optically active cobalt(III) complexes
with a selenenate, seleninate, selenoether, sulfenate,
sulfinate, or thioether ligand have been derived from the
optically active selenolato or thiolato complexes by utilizing
the strong nucleophilic property of the selenolate or thiolate
ligand.   These complexes have been characterized from their
absorption, CD, and ^1H and ^{13}C NMR spectra.

(2)   Of the cobalt(III) complexes in the present work,
the molecular structures and absolute configurations of $(-)_{500}^{CD}$-
$[Co(aesei)(en)_2]^{2+}$, $(+)_{500}^{CD}$-$[Co(mseea)(en)_2]^{3+}$, and $(+)_{550}^{CD}$.
$(+)_{370}^{CD}$-$[Co(aese)(tn)_2]^{2+}$ have been determined by X-ray
diffraction methods.   The mean bond lengths of Co-Se, Se-C,
and Se-O were 2.386 A, 1.968 A, and 1.698 A, respectively,
and they are longer than those of corresponding Co-S, S-C, and
S-O (2.267 Å, 1.818 Å, and 1.466 Å).

(3) The alkylation and oxidation reactions of the

selenolato and thiolato complexes have proceeded with retention

of their absolute configurations. For the seleninato complexes,

$[Co(aesei)(diamine)_2]^{2+}$, only the O-bonded isomers have been

obtained by the oxidation reaction of the selenolato complexes

with excess hydrogen peroxide, while the S-bonded sulfinato

isomers, $[Co(aesi-N,S)(diamine)_2]^{2+}$, have been obtained by the

same oxidation reaction of the thiolato complexes. This

suggests that the treatment of the selenolato complexes with

excess hydrogen peroxide is accompanied by the produce of the

linkage isomerization.

(4) The chiral chalcogen atoms in the selenoether and

thioether complexes with the Λ configuration took selectively

the (R) configuration except for $\Lambda-(+)_{550}^{CD}-[Co(mseea)(tn)_2]^{3+}$

((R) : (S) = 4 : 1). This stereoselectivity could be attributed

to the nonbonded interaction between the alkyl group on the

chalcogen atom and the adjacent diamine chelate ring in the

$\Lambda-(S)$ configuration.

(5) The stereoselectivity was also observed for $[Co-(aesee)(en)_2]^{2+}$ (only $\Lambda-(R)$), $[Co(aese)(en)_2]^{2+}$ ($\Lambda-(R)$: $\Lambda-(S)$

= 3 : 1), and $[Co(aesei-N,O)(en)_2]^{2+}$ ($\Lambda-(R)$: $\Lambda-(S)$ = 2 : 1).

This suggests the intramolecular hydrogen bond between the

oxygen atom on the chalcogen atom and the adjacent amine proton

in the $\Lambda-(R)$ isomer. The hydrogen bond has stabilized the

$\Lambda-(R)$ isomer more effectively for the aesee and aesei-N,O

complexes than for the corresponding aese and aesi-N,O ones,

respectively, because of the longer bond lengths of Co-Se and Se-O than those of Co-S and S-O, respectively.

(6)   The absorption spectral behavior of cobalt(III) complexes with a selenium donor atom have been quite similar to that of the corresponding cobalt(III) complexes with a sulfur donor atom, though the first absorption bands and chalcogen-to-metal charge transfer bands of the former complexes commonly shifted to lower energy than those of the latter ones.   This indicates that the order of the ligand field strength is S > Se and the coordinated selenium is better reductant than the analogous coordinated sulfur.

(7)   From the first absorption spectral behavior of the complexes in this work, the order of the ligand field strength for the various selenium- or sulfur-containing ligands can be regarded as follows: $R\underline{SO}_2{}^- \gg$ (en) $> R\underline{S}OH \approx R\underline{S}O^- > R\underline{S}^- >$ $R\underline{Se}OH \gtrsim R\underline{S}R' \approx$ (gly) $\approx R\underline{Se}O^- \gtrsim R\underline{Se}^- > R\underline{Se}R' > R\underline{S}O_2{}^- > R\underline{Se}O_2{}^-$.

(8)   The CD spectral behavior of the cobalt(III) isomers with a selenium donor atom has been quite similar to that of the corresponding cobalt(III) isomers with a sulfur donor atom.

(9)   In the chalcogen-to-metal charge transfer band region, the Λ isomers of the bis(ethylenediamine)- and bis(trimethylenediamine)cobalt(III) complexes with a selenolate, thiolate, or sulfinate ligand, which have no chirality due to the asymmetric chalcogen atom, commonly showed a negative CD band, though the CD patterns in the first absorption band region

were different from one another. This suggests that the

configurational chirality due to the skew pair of chelate

rings can be deduced from the CD pattern in the chalcogen-to-

metal charge transfer band region as for these complexes.

(10) The vicinal CD due to the asymmetric sulfur donor

atom has been separated from the configurational CD due to the

skew pair of chelate rings for $[Co(aese)(en)_2]^{2+}$, $[Co(aese)-(tn)_2]^{2+}$, and $[Co(Haese)(en)_2]^{3+}$, and it was found that the

chirality of the sulfur donor atom dominates the CD sign in

the sulfur-to-metal charge transfer band region. This result

could be applied to the cobalt(III) complexes with a selenenato,

selenoether, or thioether donor atom , because the CD spectra

of the selenenato isomer and selenoether or thioether isomers

agreed well with those of the corresponding isomers of $[Co-(aese)(en)_2]^{2+}$ and $[Co(Haese)(en)_2]^{3+}$, respectively.

(11) From the CD and ^{1}H and ^{13}C NMR spectra of $\Lambda-(+)^{CD}_{500}-$$[Co(aesei-N,O)(en)_2]^{2+}$ and $\Lambda-(+)^{CD}_{500}-[Co(mseea)(tn)_2]^{3+}$, it

was found that these isomers take a mixture of the (R) and (S)

configurations in solution, because of the inversion at chiral

selenium.

(12) For the selenenato and seleninato complexes, $[Co-(aesee)(en)_2]^{2+}$ and $[Co(aesei-N,O)(en)_2]^{2+}$, the protonation

occured on the pendant oxygen atom to generate the complexes

with a coordinated selenenic or seleninic acid in acidic

solution, as in the case for the corresponding cobalt(III)

complexes with a sulfenate or sulfinate ligand. The values of the protonation constant of these complexes indicated that the selenenate and seleninate ligands are much more basic than the sulfenate and sulfinate ones, respectively. The CD and ^{13}C NMR spectra suggested that the inversion at chiral selenium occured during the protonation reaction for $[Co(aesee)(en)_2]^{2+}$ and $[Co(aesei-N,O)(en)_2]^{2+}$, because of the disappearance of the intramolecular hydrogen bond in the protonated complexes, $[Co(Haesee)(en)_2]^{3+}$ and $[Co(Haesei-N,O)(en)_2]^{3+}$.

References

1) a) R. C. Elder, L. R. Florian, R. E. Lake, and A. M. Yacynych, Inorg. Chem., 12, 2690 (1973).

b) R. H. Lane, F. A. Sedor, M. J. Gilroy, P. F. Eisenhardt, J. P. Bennett, Jr., R. X. Ewall, and L. E. Bennett, Inorg. Chem., 16, 93 (1977).

c) W. G. Jackson and A. M. Sargeson, Inorg. Chem., 17, 2165 (1978).

d) D. L. Nosco, R. C. Elder, and E. Deutsch, Inorg. Chem., 19, 2545 (1980).

e) K. Yamanari and Y. Shimura, Bull. Chem. Soc. Jpn., 53, 3605 (1980).

f) J. D. Lydon, R. C. Elder, and E. Deutsch, Inorg. Chem., 21, 3186 (1982).

g) L. Roecker, M. H. Dickman, D. L. Nosco, R. J. Doedens, and E. Deutsch, Inorg. Chem., 22, 3632 (1983).

h) M. S. Reynolds, J. O. Oliver, J. M. Cassel, D. L. Nosco, M. Noon, and E. Deutsch, Inorg. Chem., 22, 3632 (1983).

i) K. Yamanari and Y. Shimura, Bull. Chem. Soc. Jpn., 57, 1596 (1984).

2) a) C. P. Sloan and J. H. Krueger, Inorg. Chem., 14, 1481 (1975).

b) W. G. Jackson, A. M. Sargeson, and P. O. Whimp, J. C. S. Chem. Comm., 1976, 934.

c) D. L. Herting, C. P. Sloan, A. W. Cabral, and J. H. Krueger, Inorg. Chem., 17, 1649 (1978).

d) H. C. Freeman, C. J. Moore, W. G. Jackson, and A. M. Sargeson, Inorg. Chem., 17, 3513 (1978).

e) T. Isago, K. Igi, and J. Hidaka, Bull. Chem. Soc. Jpn., 52, 407 (1979).

f) K. Okamoto, T. Isago, M. Ohmasa, and J. Hidaka, Bull. Chem. Soc. Jpn., 55, 1077 (1982).

g) K. Okamoto, K. Yakayama, H. Einaga, and J. Hidaka, Bull.Chem. Soc. Jpn., 56, 165 (1983).

h) K. Wakayama, K. Okamoto, H. Einaga, and J. Hidaka, Bull. Chem. Soc. Jpn., 56, 1995 (1983).

i) T. Konno, K. Okamoto, and J. Hidaka, Bull. Chem. Soc. Jpn., 56, 2631 (1983).

j) K. Okamoto, M. Suzuki, H. Einaga, and J. Hidaka, Bull. Chem. Soc. Jpn., 56, 3513 (1983).

k) K. Okamoto, M. Kanesaka, M. Nomoto, and J. Hidaka, Chem. Lett., 1983, 1861.

3) B. A. Lange, K. Libson, E. Deutsch, and R. C. Elder, Inorg. Chem., 15, 2985 (1976).

4) K. Yamanari, J. Hidaka, and Y. Schimura, Bull.Chem. Soc. Jpn., 50, 2299 (1977).

5) R. C. Elder, G. J. Kennard, M. D. Payne, and E. Deutsch, Inorg. Chem., 17, 1296 (1978).

6) I. K. Adzamli, K. Libson, J. D. Lydon, R. C. Elder, and E. Deutsch, Inprg. Chem., 18, 303 (1979).

7) H. Mäcke, V. Holding, and A. M. Adamson, J. Am. Chem. Soc., 102, 6889 (1980).

8) V. H. Houlding, H. Mäcke, and A. W. Adamson, Inorg. Chem., 20, 4279 (1981).

9) G. J. Gainsford, W. G. Jackson, and A. M. Sargeson, J. Am. Chem. Soc., 104, 137 (1982).

10) M. Kita, K. Yamanari, and Y. Shimura, Bull. Chem. Soc. Jpn., 55, 2873 (1982).

11) J. D. Lydon and E. Deutsch, Inorg. Chem., 21, 3180 (1982).

12) M. Kojima and J. Fujita, Bull. Chem. Soc. Jpn., 56, 139 (1983).

13) K. Yamanari and Y. Shimura, Chem. Lett., 1984, 761.

14) C. A. Stein, P. E. Ellis, Jr., R. C. Elder, and E. Deutsch, Inorg. Chem. 15, 1618 (1976).

15) The IUPAC rules, Inorg. Chem., 9, 1 (1970).

16) R. S. Cahn, C. K. Ingold, and V. Prelog, Angew. Chem. Intern. Ed. Engl., 5, 385 (1966).

17) F. A. Cotton and G. Wilkinson,"Advanced Inorganic Chemistry," Jhon Wiley & Sons, New York, 1967.

18) F. A. Cotton,"Chemical Application of Group Theory," Interscience Publishers, New York, 1964, Chap. 8.

19) L. E. Orgel, J. Chem. Soc., 4756 (1952).

20) H. Yamatera, Bull. Chem. Soc. Jpn., 31, 95 (1958).

21) R. Tsuchida, Bull. Chem. Soc. Jpn., 13, 388, 436 (1938).

22) K. Fajans, Naturwissenschaften, 11, 165 (1923).

23) C. K. Jφrgensen, " Modern Aspects of Ligand Field Theory,"

North-Holland Pub. Co. (1971), p. 345-347.

24) T. M. Dunn, D. S. McClure, and R. G. Pearson,"Some Aspects of Crystal Field Theory," Haper and Row, New York, 1965.

25) C. J. Hawkins,"Absolute Configuration of Metal Complexes," John-Wiley $ Sons, New York (1971).

26) V. P. Wystrach and F. C. Schaefer, J. Am. Chem. Soc., 77, 5915 (1955).

27) D. L. Klayman, J. Org. Chem., 30, 2454 (1965).

28) "International Tables for X-ray Crystallography," The Kynoch Press, Birmingham (1974), Vol. IV.

29) W. C. Hamilton, Acta Crystallogr., 12, 609 (1959).

30) K. Okamoto, T. Tsukihara, J. Hidaka, and Y. Schimura, Bull. Chem. Soc. Jpn., 51, 3534 (1978).

31) B. E. Douglas, D. H. McDaniel, and J. J. Alexander, "Consepts and Models of Inorganic Chemistry," 2nd ed, John-Wiley & Sons, New York (1983).

32) T. Makino, S. Yano, and S. Yoshikawa, Inorg. Chem., 18, 1048 (1979).

33) a) T. Nomura, F. Marumo, and Y. Saito, Bull. Chem. Soc. Jpn., 42, 1016 (1969).

b) H. U. F. S. Jensen, Acta. Chem. Scand., 26, 3421 (1972).

c) K. Matsumoto, H. Kawaguchi, H. Kuroya, and S. Kawaguchi, Bull. Chem. Soc. Jpn., 46, 2424 (1973).

d) K. Matsumoto, S. Ooi, H. Kawaguchi, M. Nakano, and S. Kawaguchi, Bull. Chem. Soc. Jpn., 55, 1840 (1982).

34) a) C. T. Liu and B. E. Douglas, Inorg. Chem., 3, 1356 (1964).

b) D. A. Buckingham, S. F. Mason, A. M. Sargesom, and K. R. Turnbull, Inorg. Chem., 5, 1649 (1966).

c) M. Saburi, M. Honma, and S. Yoshikawa, Inorg. Chem., 8, 367 (1969).

35) a) G. R. Brubaker and D. P. Schaefer, Inorg. Chem., 10, 968 (1971).

b) G. R. Brubaker and D. P. Schaefer, Inorg. Chem., 10, 2170 (1971).

36) K. Nakajima, M. Kojima, and J. Fujita, Chem. Lett., 1982, 925.

37) H. L. Schläfer, "Komplexbildung in Lösung," Springer-Verlag, Berlin (1965).

Acknowledgement.